NASA CR- 139045

TRACKING AND DATA RELAY SATELLITE SYSTEM USER IMPACT AND NETWORK COMPATIBILITY STUDY — FINAL REPORT

HUGHES AIRCRAFT COMPANY
Space and Communications Group
El Segundo, California 90009

19 JUNE 1973
FINAL REPORT

HUGHES

HUGHES AIRCRAFT COMPANY
SPACE AND COMMUNICATIONS GROUP

Prepared For
GODDARD SPACE FLIGHT CENTER
Greenbelt, Maryland 20771

1. Report No.	2. Government Accession No.	3. Recipient's Catalog No.
4. Title and Subtitle Tracking and Data Relay Satellite System User Impact and Network Compatibility Study - Final Report		5. Report Date 19 June 1973
		6. Performing Organization Code
7. Author(s)		8. Performing Organization Report No.
9. Performing Organization Name and Address Hughes Aircraft Company, Space and Comm. Group, NASA Systems Division, 909 North Sepulveda Boulevard El Segundo, California		10. Work Unit No.
		11. Contract or Grant No. NAS 5-20357
12. Sponsoring Agency Name and Address National Aeronautics and Space Administration Goddard Space Flight Center Greenbelt, Maryland 20771 F. Shelton, Code 860.3		13. Type of Report and Period Covered Final Report 19 June 1972 to 19 June 1973
		14. Sponsoring Agency Code

15. Supplementary Notes

16. Abstract

The report contains data on antenna configurations for the low data rate users of the TDRSS. It treats the coverage and mutual visibility considerations between the user satellites and the relay satellites and relates these considerations to requirements of antenna beamwidth and fractional user orbital coverage. A final section includes user/T-DRS telecommunication link budgets and forward and return link data rate tradeoffs.

17. Key Words (Selected by Author(s)) TDRSS USER IMPACT STUDY	18. Distribution Statement		
19. Security Classif. (of this report) Unclassified	20. Security Classif. (of this page) Unclassified	21. No. of Pages 119	22. Price

CONTENTS

CONTENTS (cont'd)

ILLUSTRATIONS

ILLUSTRATIONS (cont'd)

TABLES

1. INTRODUCTION

This report presents the results of the Tracking and Data Relay
Satellite System (TDRSS) User Impact and Network Compatibility Study
conducted by Hughes Aircraft Company, Space and Communications Group
for the National Aeronautics and Space Administration, Goddard Space
Flight Center, under Contract NAS 5-20357. This study was to identify
and examine antennas for the user spacecraft which satisfy TT & C
data rates and have minimum impact on the user. The intended scope of
the study also originally included considerations of compatibility
with the NASA network ground stations and significant effort on
antenna configurations which reject or protect from earth generated
radio frequency interference (RFI).

Upon notification that the frequency bands of operation for the
telecommunication links between the TDRS and the users had been changed
from VHF/UHF to S-band, this contractor redirected the remaining effort
to concentrate on S-band user antennas, specifically those for which
reliable hardward implementation data was available.

Accordingly, applicable experience from past and current commercial
and military space programs has been utilized to arrive at a number of
antennas which can be considered suitable candidates for user spacecraft
missions. Notwithstanding the elimination of VHF and UHF for the links,
the preliminary data gathered on antennas for these bands is nevertheless
included in this report at the end of Section 4, User Antenna Study.

2. SUMMARY

2.1 General TDRSS Concept

The TDRSS concept employs two synchronous altitude geostationary satellites deployed in order to provide telecommunication links between multiple earth-orbiting satellites and a centrally located ground station[1]. The benefits of employing a data relay satellite system are:

(1) Increased user real-time data capability

(2) A possible reduction of user satellite on-board data storage

(3) A possible reduction of the geographic extent and complexity of the NASA ground tracking and data network.

Figure 2.1 shows the general configuration of the overall system. TDRS E is stationed above the Atlantic and TDRS W is above the Pacific Ocean. The communication links from the ground station to the user are defined as forward links, while the links from the user spacecraft to the ground station are defined as return links.

Although the overall system concept embraces three categories of user, that is, high, medium, and low data rate types, the category exclusively dealt with in this study is the low data rate (LDR) type.[*] For this service both the forward and return links are implemented with broad coverage (26 degree field of view) antennas aboard the TDRS.

To put this report into proper perspective, it is of value to discuss the characteristics of two major interacting constituents of the system: the TDRS itself and the user satellites.

_____

[*]Although the nomenclature for this service has been recently changed to the Multi-Access Service (MAS), the term LDR will be used throughout the remainder of this report.
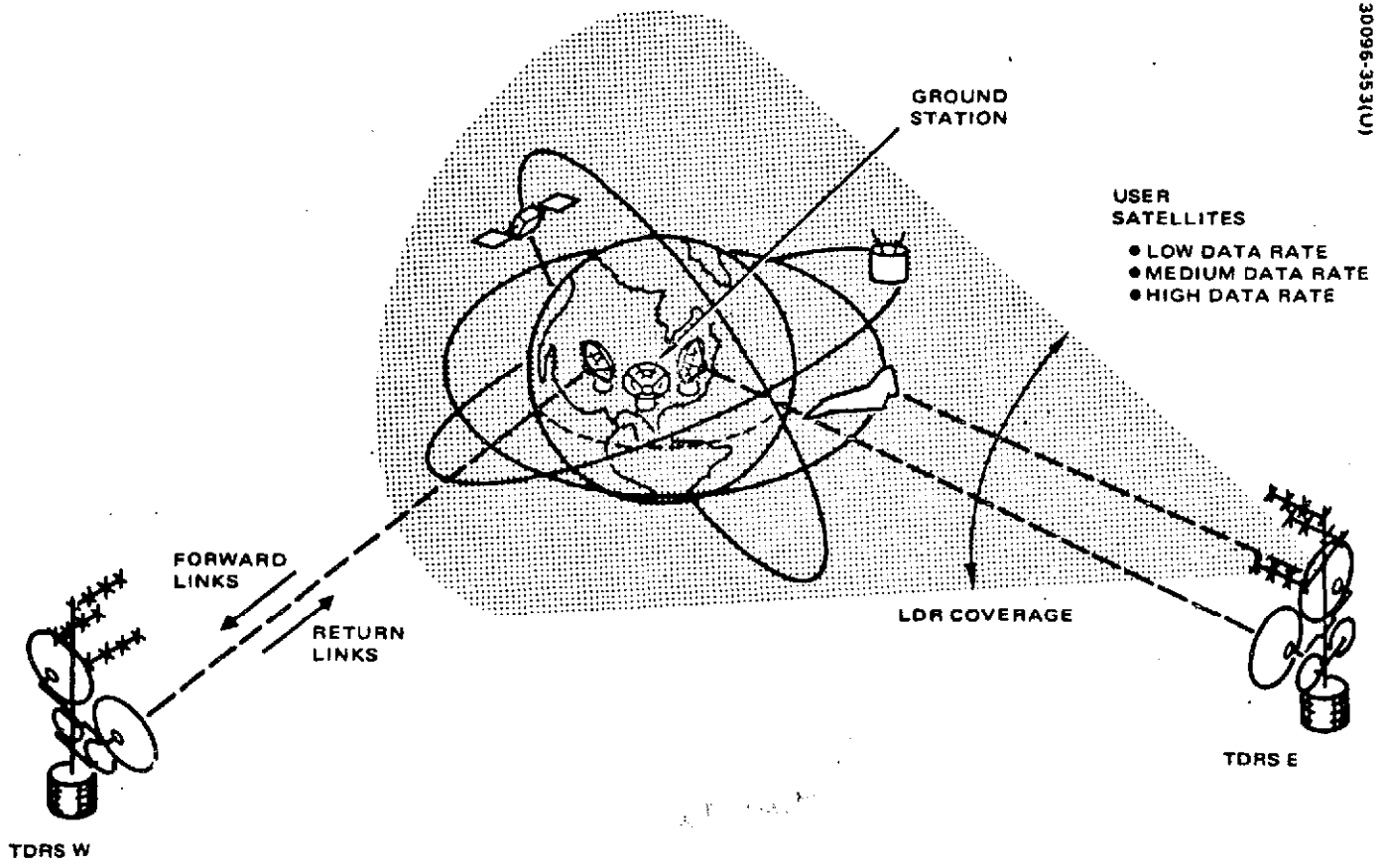
Figure 2.1.   TDRS System Concept

2.2   User and TDRS Characteristics

The LDR links between a TDRS and user spacecraft employ broad coverage TDRS antennas, accommodating user spacecraft with orbital altitudes up to 3300 km. Examination of the NASA '78, '79, and '80 Mission Models in Appendix A* shows the majority of users to be orbiting at 300 to 1000 km, which is well within the range of the field of view of the TDRS antennas. To give some idea of the distribution of the users, Figure 2.2 shows a mission model summary derived from Appendix A, in the form of a density profile. Each dot in the figure represents a different user mission. Also shown is a profile of the user orbital inclinations which shows the distribution tends to bunch at around 30° and polar orbit inclinations.

The forward link was defined by the contract Statement of Work[2] to operate at UHF and was subsequently changed[3] to S-band (in the 2025 to 2120 MHz range). The range of forward link bit rates to be considered is 100 to 1024 bits per second. Effective system noise temperature of the user at S-band is defined as 1500 K.

The return link from the user, originally at VHF and subsequently also changed to S-band (in the 2200 to 2300 MHz range) is to provide a range of bit rates of 1 to 10 kilobits per second.

The relevant TDRS characteristics include a 25 dBW equivalent isotropically radiated power (EIRP) at the edge of the field of view; a receiver antenna gain of 28 dB over the field of view; and an effective system noise temperature of 540 K. These figures are consistent with the latest Hughes TDRS baseline[1].

A summary of these parameters and characteristics which will be used throughout the remainder of this report is shown in Table 2.1.

---

*Received from the Study Project Office on 18 July 1972. The following were eliminated from the models: Deep Space, Geosynchronous, Elliptical Orbit Users, and Medium and High Data Rate Users.
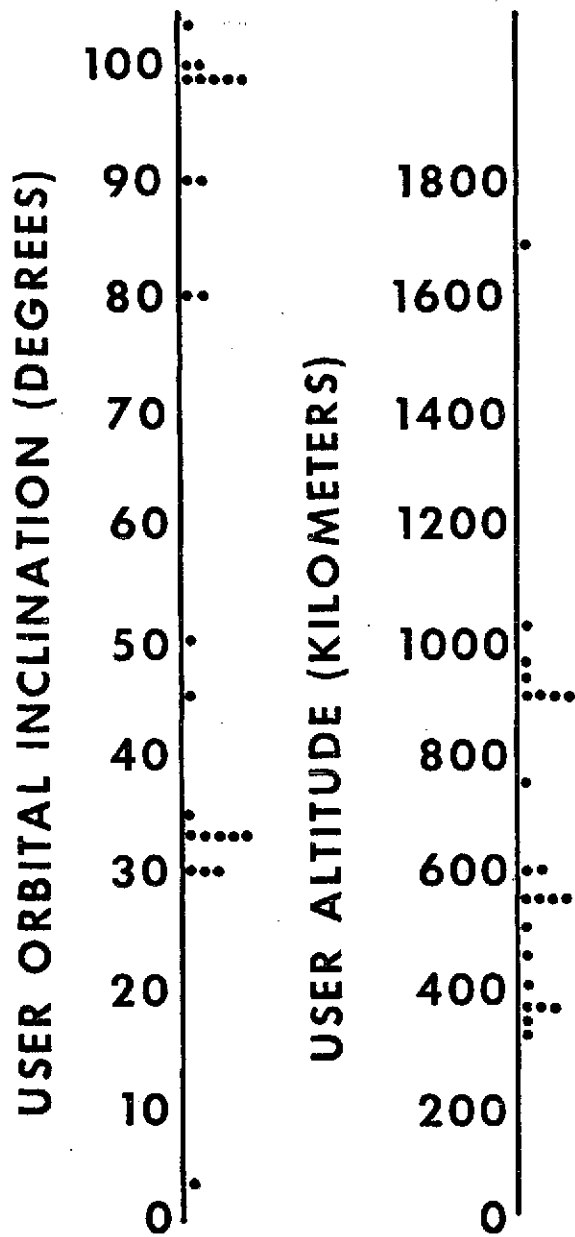
Figure 2.2. User Mission Model Summary

20717-2666

Table 2.1 Link Parameters

Forward Link

Frequency Range	2025 - 2120 MHz
Bit Rates	100 - 1024 bps
TDRS EIRP	25 dBW
User Noise Temperature	1500 K

Return Link

Frequency Range	2200 - 2300 MHz
Bit Rates	1 - 10 kbps
TDRS Receive Antenna Gain	28 dB
TDRS Noise Temperature	540 K

Figure 2.3 INFLUENCE OF USER ANTENNA GAIN ON LDR

LINK RATE

USER ANTENNA GAIN - DECIBELS
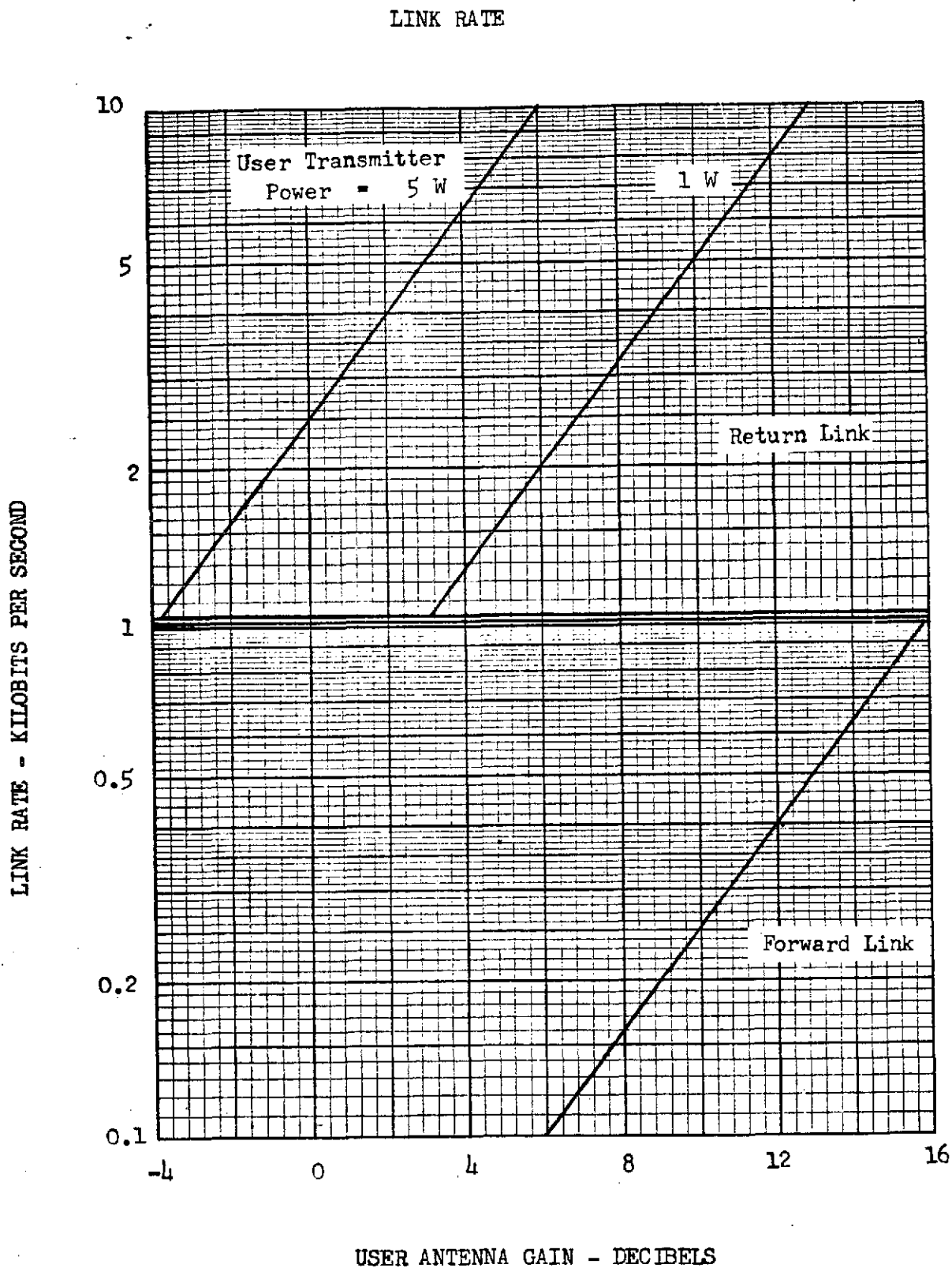
2.3   TDRSS Performance Summary

Figure 2.3 shows the results of the telecommunications link performance calculations which are developed in Section 5 of this report. It is seen that for the return link performance specified by the Statement of Work for the Study, the data rate requirements of 1 - 10 kilobits per second can be satisfied by user antenna gains of between 3 and 13 dB. This condition holds for the 1 watt user RF power originally specified. It is further seen that, given the capability to generate 5 watts of RF power, the user's antenna gain requirements are significantly reduced in that the same data rate performance can be achieved by much more modest antennas with gains of between -4 and 6 dB.

In order to obtain the specified forward link data rates of 100 bps to 1024 bps, Figure 2.3 shows that the user antenna gains should be between 6 and 16 dB. For the lower part of this range of say 100-200 bps, the 6 - 9 dB of antenna gain required is shown in Section 4 to be achievable with modest antennas such as spirals of helices. However, above 200 bps the antenna gain requirements on the user become more difficult to achieve with simple antennas.

Two methods of easing the user's antenna gain requirements on the forward link are an increase in TDRS EIRP and a decrease in the user's receiving system noise temperature. With respect to the latter, the current Hughes baseline for the TDRS itself employs bipolar silicon transistors which provide a system noise temperature of 540 K. A reduction in the user's effective noise temperature to this value from the currently estimated 1500 K produces a decrease in antenna gain of almost 4.5 dB. Thus, it is believed that some combination of increased TDRS EIRP and reduced user noise temperature is needed to permit the use of relatively modest user antennas to achieve the full range of specified forward link rates.

2.4   Analysis Summary

Calculations are performed in Section 3 in which visibility
time, expressed as a percentage of the user's orbital period, is determined
as a function of the beamwidth of the user antenna. Visibility is
assumed to exist when a TDRS falls within the user's antenna beam. Cases
are examined for the two orbital inclinations (33 and 99°) which dominate
the mission model and for antennas which are either fixed, partially
gimballed, or capable of being fully gimballed. The resulting data,
plotted in a series of curves, will aid in preliminary determination of
the gimballing and beamwidth constraints for each user depending on the
fraction of the orbital period over which communication via the TDRS is
desired.

Section 4 consists of a comparative examination of candidate
antennas for the user spacecraft. The alternatives presented include low
gain antennas which are usually fixed rather than gimballed, and medium
gain antennas which require either gimballing or switching between separate
antennas for optimum telecommunication visibility with the TDRS's.
Presented for consideration also in this section is a series of spacecraft
antennas for which actual hardware experience has been accumulated. These
include antennas from such early space programs as Surveyor and SYNCOM
to the most recent such as the Canadian domestic communications satellite,
Anik, and proposed missions such as the HS-507 Pioneer Venus spacecraft.

3. USER/TDRS COVERAGE AND MUTUAL VISIBILITY STUDY

3.1 Methodology and Ground Rules

The purpose of this section is to determine the maximum and minimum
periods of mutual visibility between a typical user spacecraft and <u>at
least one</u> of two TDRS's. It is assumed that mutual visibility exists when
a TDRS falls within the antenna beam of the user satellite. The TDRS space-
craft have been taken to be in geosynchronous orbits. The coverage and
visibility analysis in this section is valid regardless of actual TDRS
longitudinal position as long as a constant separation between the two
TDRS's is maintained. For purposes of this analysis, a separation of
116° has been assumed.

Analysis of the NASA '78, '79, '80 mission models (Appendix A) shows
that the TDRSS users have predominately low altitude circular orbits with
inclinations of 33° and 99°. Beamwidths ranging from 30° to 100° have been
used in the analysis, which is consistent with the frequencies and antenna
sizes considered here.

Three cases have been investigated:
1) No gimballing of the antenna
2) $\pm 90^{\circ}$ gimballing of the antenna about an axis parallel to the
   orbit normal direction
3) Gimballing of the antenna through the maximum possible gimbal
   angle $\pm\alpha$ as defined in Figure 3.1.

For each case noted the task can be described as follows: For a
particular user orbital inclination, altitude and antenna beamwidth,
calculate the maximum and minimum communication time between the user and
one or both TDRS for a revolution of the user's orbit. The duration
of communication is then defined as the sum of all periods of mutual
visibility taking place within the span of one orbital period of the user
spacecraft. Several revolutions of the user's orbit are examined to
determine the true maximum and minimum values of total visibility time.
For convenience the results are expressed in terms of a percentage of
the orbital period.
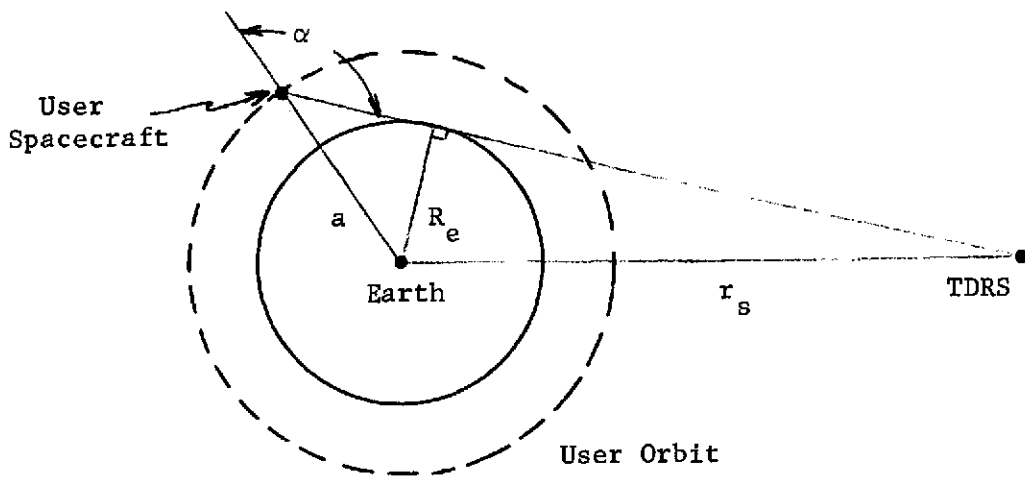
Figure 3.1.   Maximum User Antenna
Gimbal Angle α

3.2 Mathematical Model[(4)]

The approach taken is to determine the radius vector to the user as a function of time in an earth fixed coordinate system and to compare this vector with the constant radius vectors to each TDRS. By comparing these two vectors and rejecting the orbital period times when the earth intervenes between them, mutual visibility as defined above is determined.

For a circular orbit the anomalistic mean motion $\bar{n}$ can be written as

$$\bar{n} = n_o \left[1 + \frac{3}{2} J_2 \frac{R_e^2}{a^2} \left(1 - \frac{3}{2} \sin^2 i \right) \right],$$

where

n_o = Keplerian mean motion = $\sqrt{\mu / a^3}$

J_2 = coefficient of first zonal harmonic of earth's potential

R_e = earth's equatorial radius

a = circular orbit radius

i = orbital inclination

μ = earth's gravitational parameter

Refering to Figure 3.2, at any time t the true anomaly ν is simply

$$\nu = \bar{n} \, t,$$
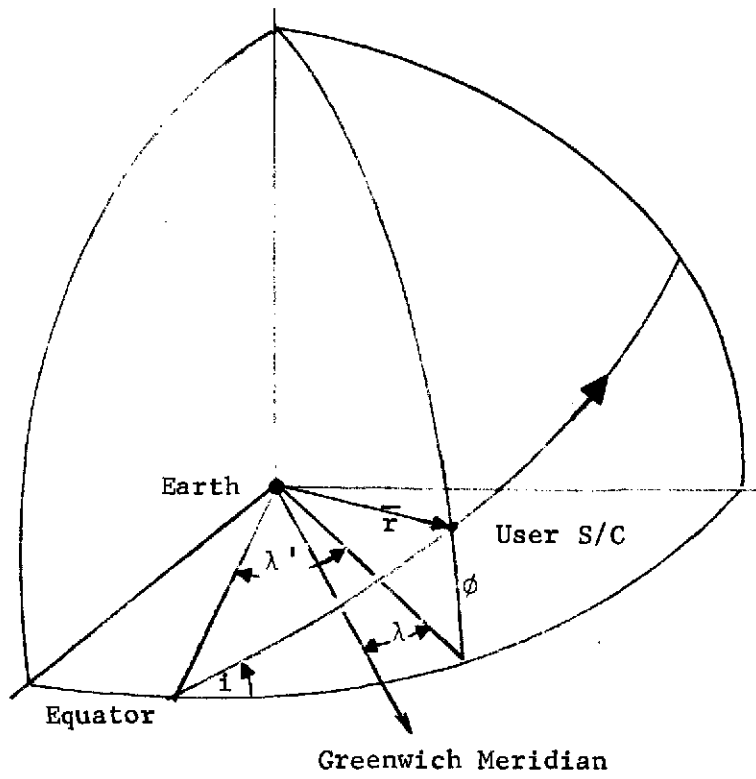
Figure 3.2. User Orbit Plane Geometry

and the latitude ϕ and longitude λ of the subsatellite point can be computed from

$$\sin \phi = \sin i \sin \nu$$

$$\cos \lambda' = \cos \nu / \cos \phi$$

$$\sin \lambda' = \tan \phi / \tan i$$

$$= \lambda' - \omega_e t ,$$

where

$$\omega_e = \text{earth's rotation rate.}$$

Thus, the radius vector $\bar{r}$ to the user spacecraft in the earth fixed system is described as

$$r_1 = a \cos \phi \cos \lambda$$

$$r_2 = a \cos \phi \sin \lambda$$

$$r_3 = a \sin \phi,$$

while the radius vector $\bar{R}$ to a particular TDRS is just

$$R_1 = r_s \cos \lambda_o$$

$$R_2 = r_s \sin \lambda_o$$

$$R_3 = 0,$$

where,

$$r_s = \text{synchronous radius}$$

$$\lambda_o = \text{TDRS operating longitude}$$
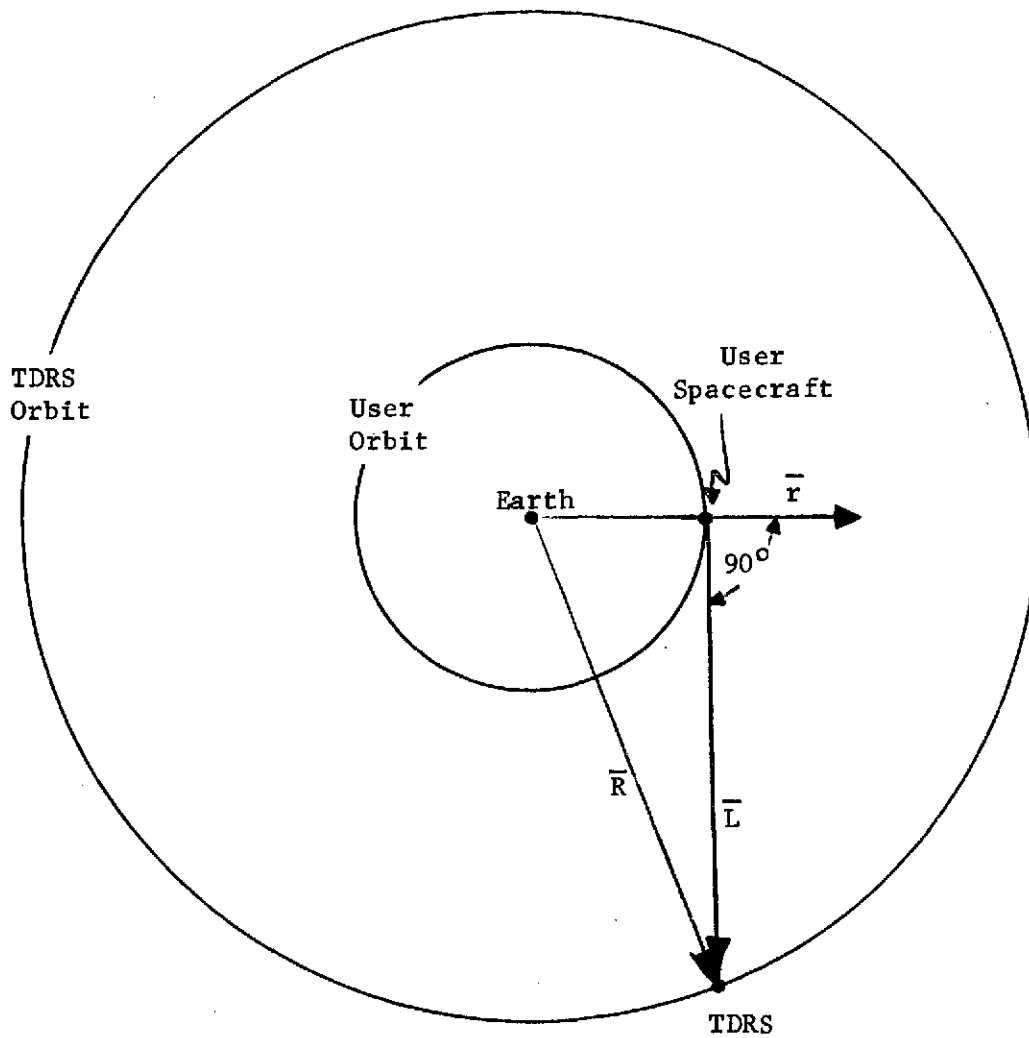
Figure 3.3. User/TDRS Line-of-Sight Geometry

If $\bar{L}$ is allowed to represent the line-of-sight direction from the user to the TDRS, then

$$\bar{L} = \bar{R} - \bar{r} ,$$

and, since the user's antenna for Case 1 (no gimballing) is assumed to point outwards along the satellite radius vector, visibility exists if

$$\frac{\bar{r} \cdot \bar{L}}{a |L|} < \cos \frac{\Theta}{2} ,$$

where

Θ = user antenna beamwidth

For Case 2 ($\pm 90°$ gimballing) two conditions must be met for communications to be possible. First, the line-of-sight vector $\bar{L}$ must be within $90°$ of the radius vector (see Figure 3.3), i.e., the following must hold:

$$\bar{r} \cdot \bar{L} > 0.$$

Secondly, allowing movement of the antenna through $\pm 90°$ about an axis parallel to the orbit normal and letting the unit vector $\bar{P}$ represent the antenna pointing direction anywhere along the $180°$ sweep, in order for visibility to exist, the following condition must hold:

$$\frac{\bar{P} \cdot \bar{L}}{|L|} \geq \cos \frac{\Theta}{2}$$

For Case 3 ($\pm \alpha$ gimballing), the conditions that must be met are the same as for Case 2 except that the first inequality is replaced by

$$\frac{\bar{r} \cdot \bar{L}}{a |L|} \geq \cos \alpha$$

Figure 3.4. Maximum and Minimum Visibility Times as a Function of User Antenna Beam-Width (θ) for case 1 (No Gimballing)

(a) • User Inclination = 33°
    • User Altitude: 300 - 1000 km

Percent of User Orbital Period

Maximum Visibility

Minimum Visibility

User Antenna Beamwidth - Degrees

(b) • User Inclination = 99°
    • User Altitude: 300 - 1000 km
    • Minimum Visibility Time = 0. min.

Percent of User Orbital Period

Maximum Visibility

User Antenna Beamwidth - Degrees

3.3 Coverage and Visibility Study Results

The results of the study are presented in Figures 3.4-3.9 and, with the exception of Figure 3.5, these curves show visibility time as a function of beamwidth (Θ). For Cases 1 and 2 analysis indicates that communication time is essentially independent of user orbital altitude for 300 km $\leq$ h $\leq$ 1000 km, and thus altitude does not appear as a parameter in the results for these cases. Figure 3.4 shows the maximum and minimum visibility times that will be experienced between the user and at least one TDRS for Case 1 (no gimballing). The visibility times are expressed as a percentage of the user's orbital period and as a function of user antenna beamwidth. Figure 3.4a is for a user orbital inclination of 33° and Figure 3.4b is for i = 99°. As can be seen from the first curve a minimum of zero communication time exists for beamwidths of 65° or less. This means that for this antenna size there will be some revolutions of the user orbit for which no communication is possible with the TDRSs. A similar condition exists for user orbits inclined at 99° for $30^{\circ} \leq \Theta \leq 100^{\circ}$ (Figure 3.4b). Figure 3.4 also shows that the maximum visibility time for i = 99° is consistently less than that for i = 33° when compared at the same beamwidth. This is to be expected since in the latter orientation the TDRS is never as far out of the user orbit plane as for the polar type orbits, and it is this out-of-plane distance that determines visibility time.

Figure 3.5 presents an example of the geographic extent of the visibility regions for each TDRS when viewing a low altitude 33° inclined user orbit. For illustrative purposes, the TDRS's are assumed to be stationed at 19° W and 135° W longitude. A user antenna beamwidth of 90° is assumed for the case of no antenna gimballing. Communications with a particular TDRS is possible only when the user subsatellite point falls in the TDRS visibility region. Jointly, the two regions depicted in Figure 3.5 will allow the user spacecraft to communicate with one TDRS or the other from 25% to 42% of the time (Figure 3.4a). Similar curves could be generated for the other cases.

Figure 3.5. Visibility Regions for TDRS Located at 19°W and 135°W for Low Altitude 33° Inclined User Orbits for Case 1 (No Gimballing)

. $\theta = 90°$

4P60 OC 901

Figure 3.6 shows maximum and minimum visibility times for the case of $\pm$ 90° gimballing. As can be seen from the curve a minimum value of zero exists for user antenna beamwidths less than 57°, and increases to 76% at θ = 100°. Maximum visibility time increases rapidly from 48% for a 30° beam to a constant upper bound of 85% at θ = 40°. The upper bound is the same for all beamwidths since for Case 2 it is required that $\bar{r} \cdot \bar{L} > 0$, i.e., $\not{\prec} (\bar{r}, \bar{L}) < 90°$.

Figure 3.7 describes the maximum visibility times for a user orbital inclination of 99°. As with Case 1 the minimum communication time is zero for all beamwidths considered. The maximum remains constant at 46% for beamwidths less than about 55%. At this point, the curve rises sharply to 87% for $\theta \geq 70°$. This seemingly strange behavior can be explained by noting that for small beamwidhts only one TDRS at a time can fall near enough to the orbit plane of the user for communications to be possible. Thus, the lower level of the maximum visibility curve (46%) represents communications with just one TDRS. When the beamwidth is sufficiently large to allow communication with either TDRS at the same place in the user's orbit*, then the upper level of the maximum curve results.

For the case of gimballing the user antenna through the angle $\pm \alpha$, the results are presented in Figures 3.8 and 3.9. The curves are similar to those described earlier with two exceptions. First, since α is a function of altitude**, the maximum and minimum visibility times become a function of altitude as well, and the results are shown

* For a 90° polar orbit this requirement amounts to
$$\theta \geq 180° - | \lambda_{TDRS_1} - \lambda_{TDRS_2} | .$$
** $\alpha = \pi - \sin^{-1}\left(\dfrac{R_e}{a}\right)$ (Figure 3.1).

Figure 3.6. Maximum and Minimum Visibility Times as a Function of User Antenna Beamwidth (θ) for Case 2 (± 90° Gimballing).

- User Inclination = 33°
- User Altitude: 300 - 1000 km

Maximum Visibility

Minimum Visibility

Percent of User Orbital Period

User Antenna Beamwidth - Degrees
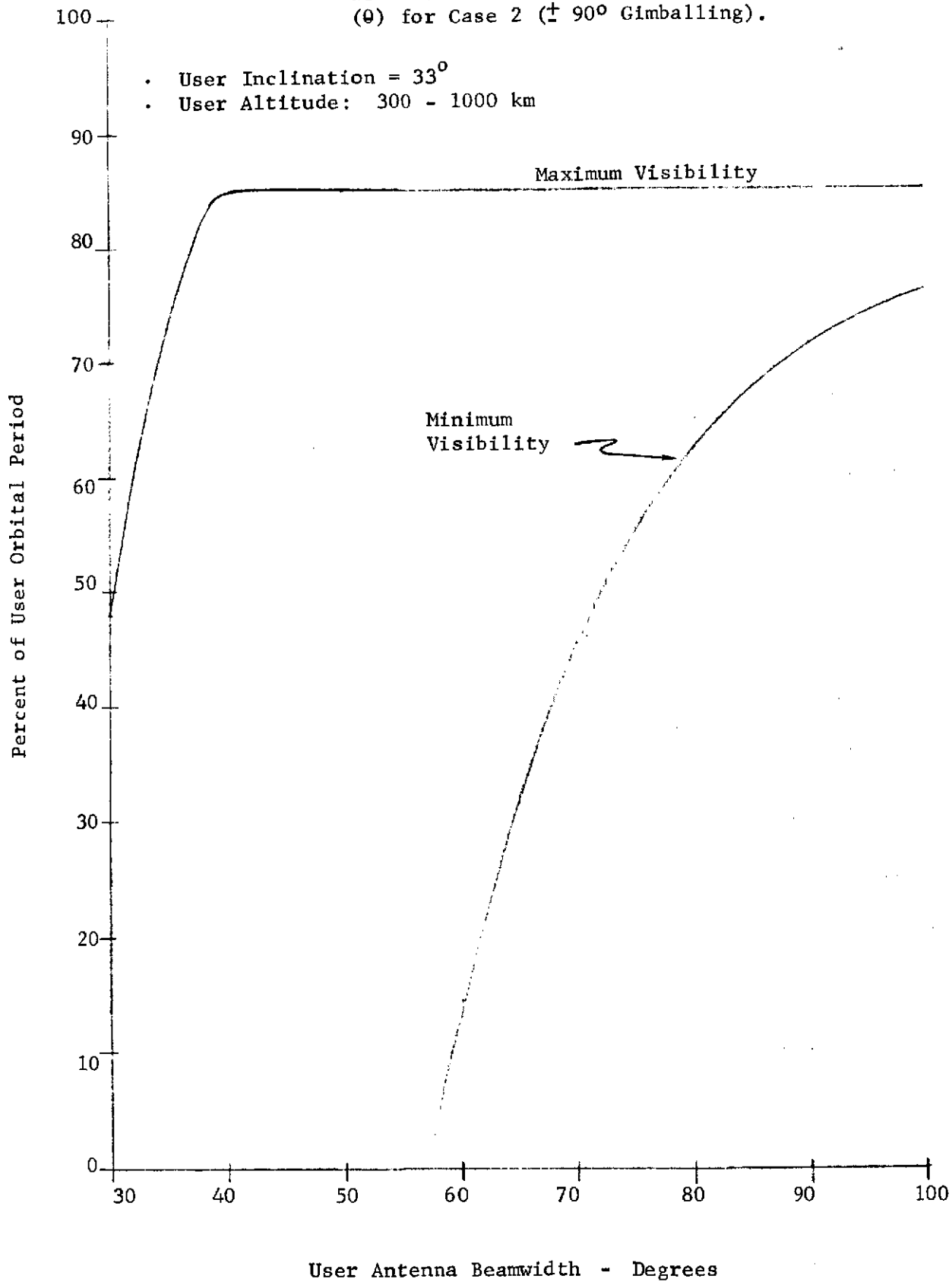
Figure 3.7. Maximum Visibility Times as a Function of User Antenna Beamwidth (θ) for Case 2 (± 90° Gimballing)

- User Inclination = 99°
- User Altitude: 300 - 1000 km
- Minimum Visibility Time = 0. min.

Percent of User Orbital Period

User Antenna Beamwidth - Degrees
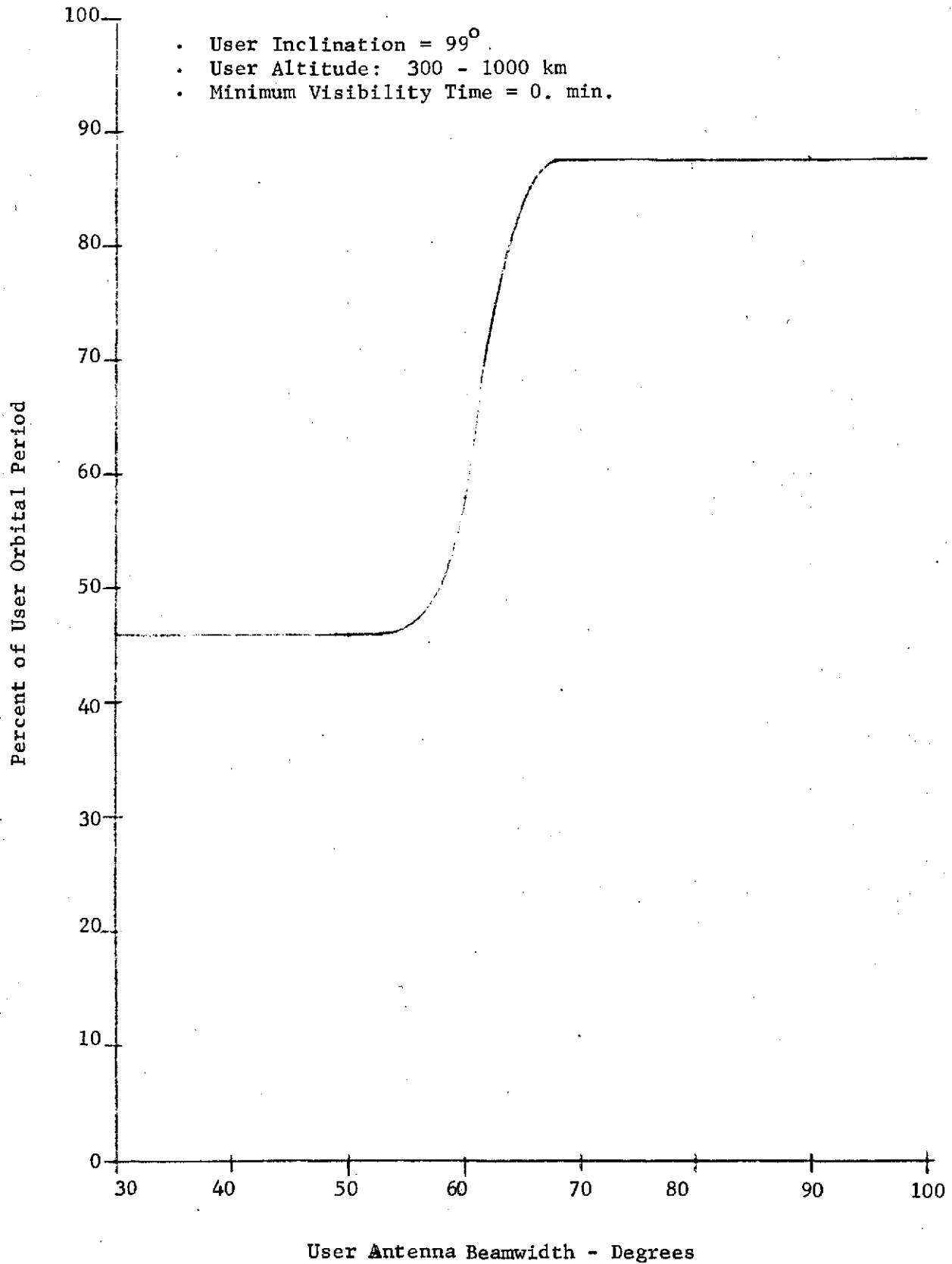
Figure 3.8. Maximum and Minimum Visibility Times as a Function of User Antenna Beamwidth (θ) for Case 3 ($\pm \alpha$ Gimballing)

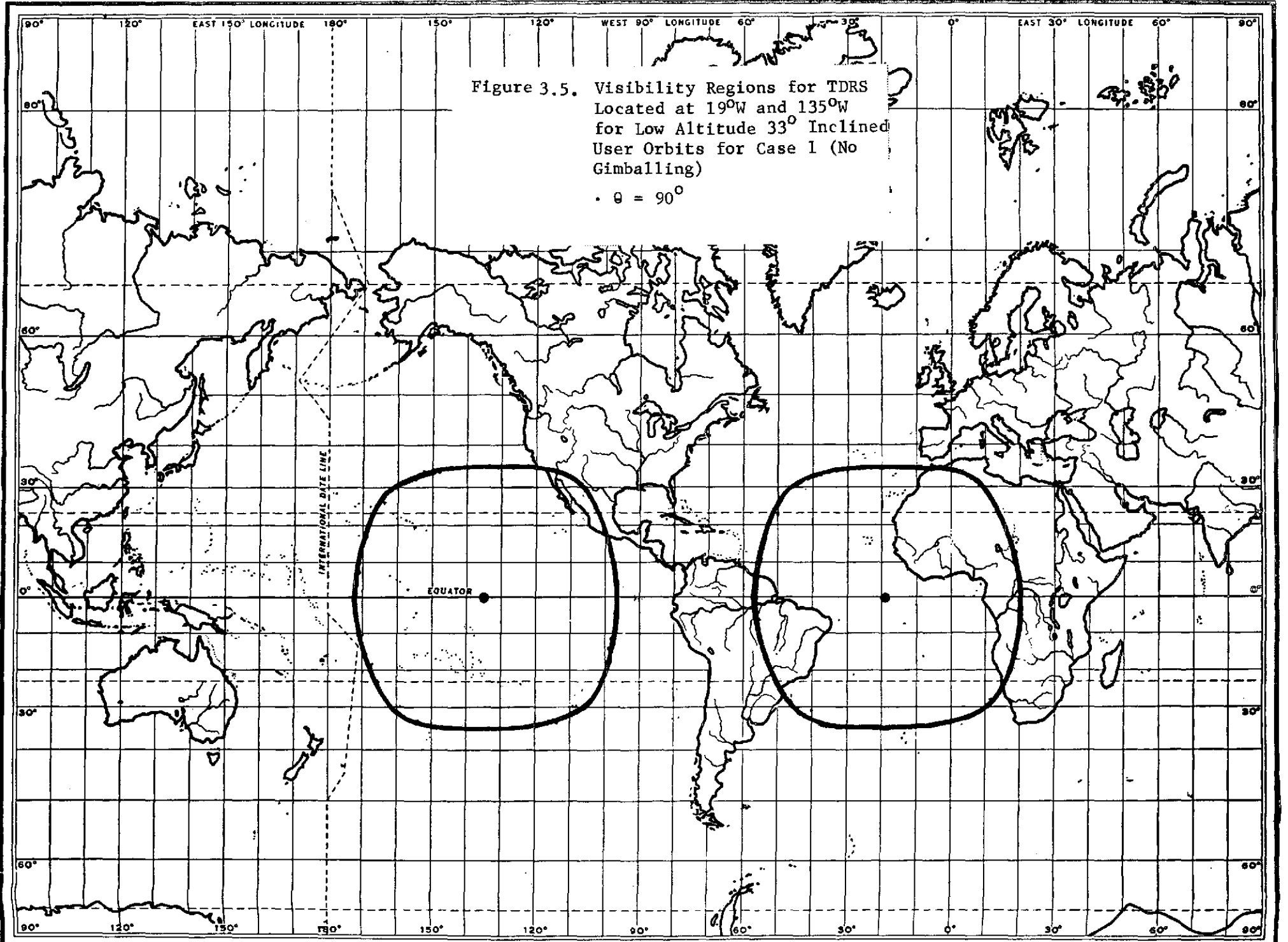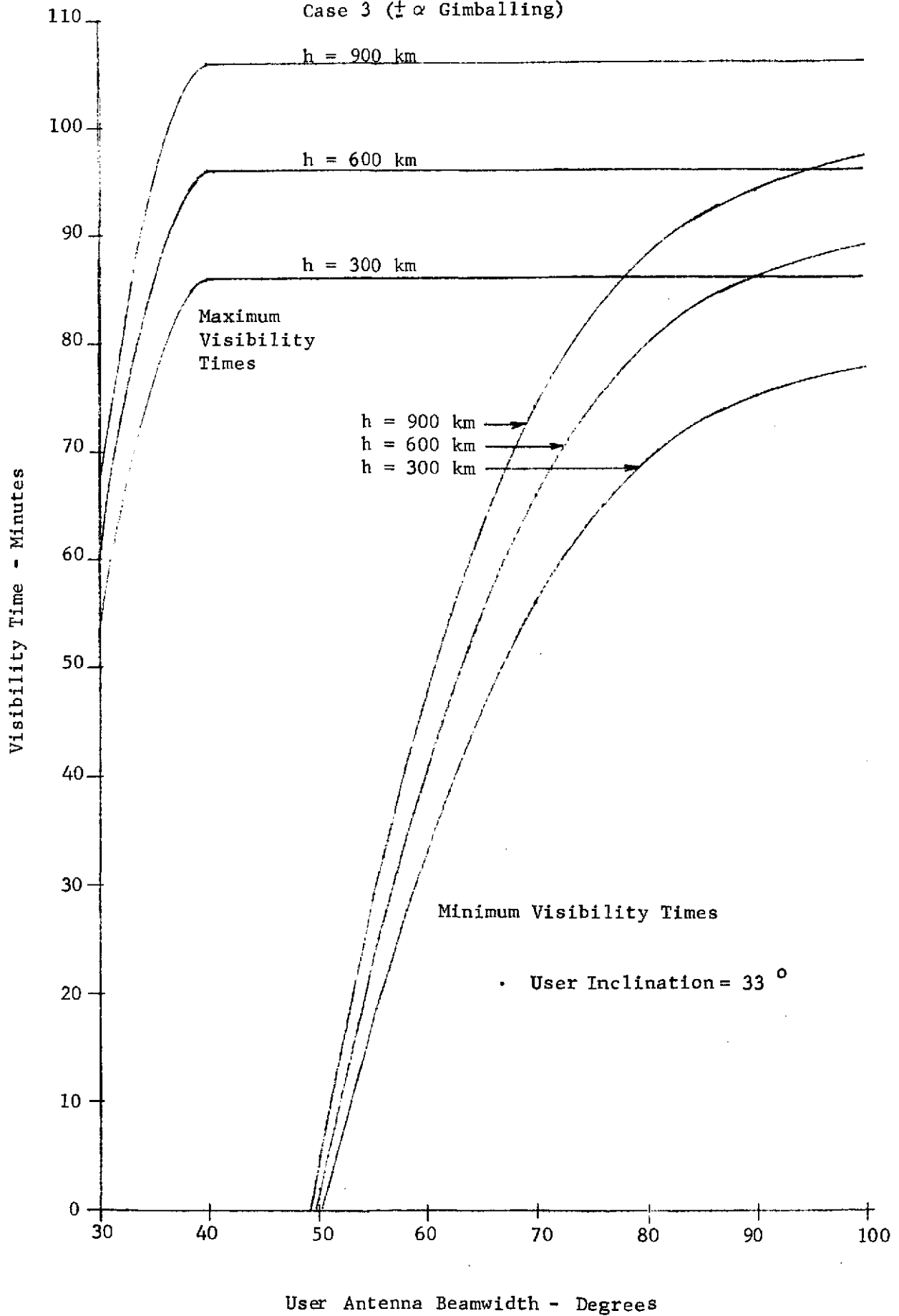Figure 3.9. Maximum Visibility Times as a
Function of User Antenna Beam-
width (Θ) for Case 3 ($\pm\alpha$
Gimballing)

· User Inclination = 99°

· Minimum Visibility Time = 0. min.

h = 900 km

h = 600 km

h = 300 km

Visibility Time - Minutes

User Antenna Beamwidth - Degrees
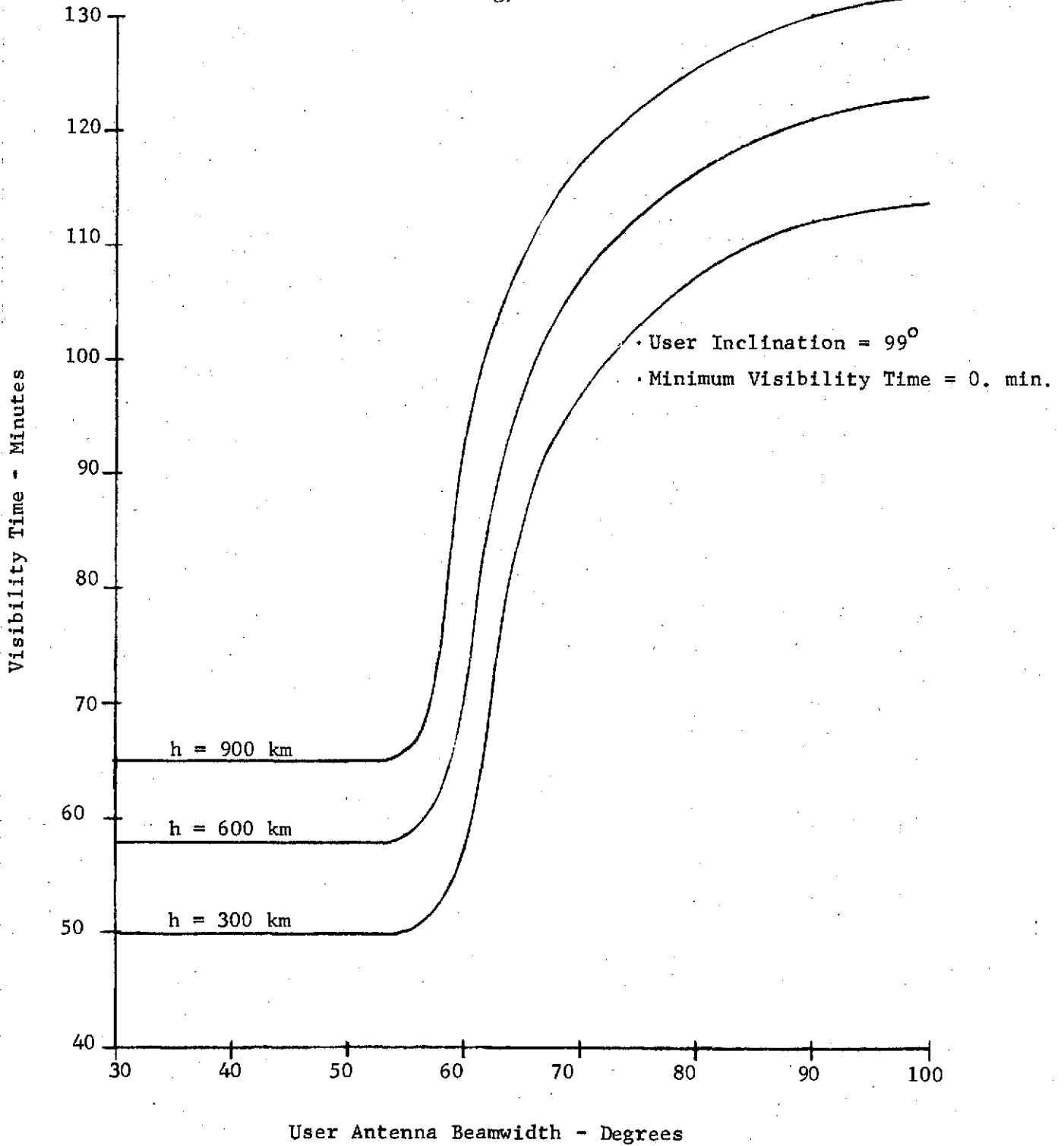
for altitudes of 300, 600 and 900 km. Secondly, since $107^O \leq \alpha \leq$ 120° for 300 km $\leq$ h $\leq$ 1000 km, α is sufficiently large so as to allow continuous communications with one or more TDRS for periods exceeding one revolution of the user orbit. Thus rather than describe visibility times in terms of a percentage of the user orbital period, they are simply shown in minutes. As can be seen from Figure 3.8 the same kind of behavior is displayed by the visibility curves as was seen in Figure 3.6 ($\pm$ 90° gimballing, i = 33°). Since $\alpha > 90^O$, increased communication time is expected, and in fact, both the maximum and minimum curves in Figure 3.8 do represent greater periods of visibility than those of Figure 3.6.

Figure 3.9 presents the maximum visibility times for a user inclination of 99° for Case 3. As before, near polar orbits result in a zero minimum visibility time for all beamwidths. And, as in the case of $\pm90^O$ gimballing, a rapid increase in communication time occurs in the vicinity of $\theta = 60^O$, essentially doubling visibility time for the larger beamwidths.

3.4 Conclusions and Recommendations

It has been the intent of this section to provide potential users of the TDRSS with sufficient data to allow preliminary determination of the constraints imposed upon the user antenna design as a result of user communication requirements. If a minimum value can be set on communication time, than for a particular orbital geometry, the data presented herein allows the user to determine both the optimum antenna beamwidth and the antenna gimballing scheme.

It is recommended that subsequent visibility studies be performed to investigate the impact of: (1) pointing the antenna along the orbit normal direction or along the velocity vector; (2) gimballing the antenna about an axis other than the orbit normal, e.g., the velocity vector, etc.; and (3) allowing two degrees of freedom in antenna gimballing. Furthermore, a small number of spacecraft are not referenced to the earth, but are either inertially oriented or are oriented with respect to the sun. An example of the latter is the Orbiting Solar Observatory (OSO). For these cases, similar visibility studies can be performed.

4. USER ANTENNA STUDY

4.1 Introduction

The antenna on the user spacecraft is one of the most critical elements in the telecommunications link with the TDRS. An antenna has mass, requires space, usually protrudes from the spacecraft body and often imposes attitude control, gimballing, and deployment constraints. Unlike conventional satellite-to-ground telemetry and command antennas, those on the user are required to exhibit some directivity toward the synchronous altitude TDRS. The higher the achievable gain, the better, since each additional dB of gain in the link is directly translatable to a higher supportable user bit rate.

A major factor limiting the telecommunications link performance is terrestrially generated radio frequency interference (RFI). The basic geometry of this RFI problem is shown in Figure 4.1. Each TDRS sees more than 40 percent of the earth's surface, and the LDR return link antenna collects noise power from all emitters in the visible region. The RFI noise level seen by each TDRS will vary slowly, since each TDRS always views the same large region. A low altitude user spacecraft views a considerably smaller portion of the earth's surface, and therefore is affected by a lesser number of RFI emitters, but is much closer to these emitters, effectively receiving higher power per emitter than the TDRS. A user, orbiting over high and low RFI emitting regions, experiences a wide range of RFI variations.

The most detailed estimate of the RFI that can be experienced by synchronous satellites in the frequency ranges previously allocated to the LDR service has been made by ESL, Inc. in a 1972 study for NASA[5]. These estimates were based on an emitter library containing the location, antenna pattern, transmitter power, etc., of about 45,000 RFI sources.
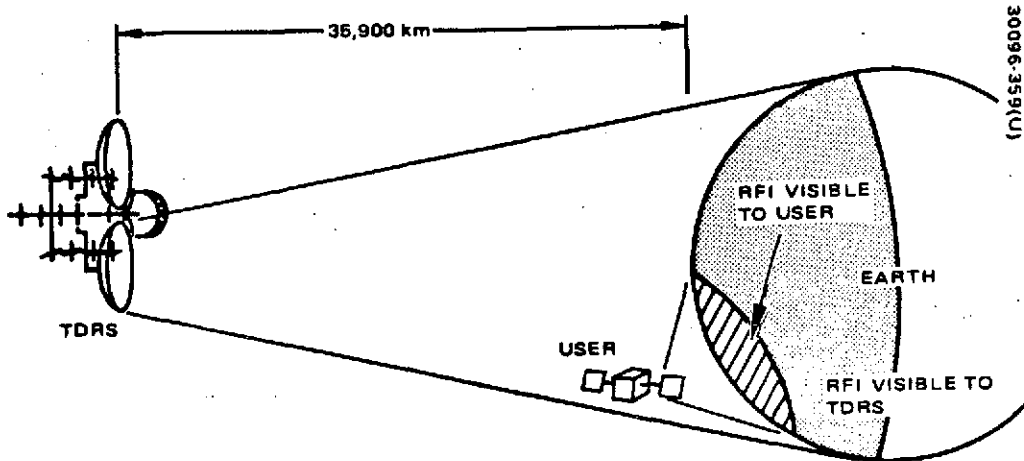
Figure 4.1. RFI Geometry

In view of the foregoing, a number of requirements must be imposed on the user spacecraft antenna design. To achieve maximum bit rates, the user receiving antenna should attain its maximum gain in the direction of the TDRS and at the same time achieve minimum gain towards the sources of RFI via the antenna side and back lobes. For the return link, the only available method on the user satellite of attempting to overcome the RFI problem is to achieve as high an EIRP in the direction of the TDRS as possible without regard to the side and back lobes.

The recent shift in link frequencies from VHF/UHF to S-band (2.25 GHz) eased the requirements on the user in a number of respects. The primary factor is that terrestrially generated RFI no longer appears to be the dominating influence on the user antenna. This fact is evident for two reasons. First, the number of terrestrial transmitters at 2 GHz is far less than the profuse numbers which exist globally at VHF and low UHF. An allocation of a small slot of frequency spectrum needed for the LDR service is probably much easier to obtain relatively interference-free at S-band than in the lower bands.

Furthermore, whereas the almost 3-to-1 frequency difference between the UHF and VHF links precluded the use of a single antenna for both links, that possibility can now be considered at S-band. Also, at S-band the aperture becomes smaller and the radiation pattern interaction between the antenna elements and the spacecraft structure becomes less severe.

Despite the fact that VHF and UHF have been deleted, the preliminary data gathered on antennas for these frequency ranges are included in this section for the purpose of completeness.

During the study effort, discussion with the GSFC User Impact Study program office[3] led to a request for this contractor to submit data on antennas which have been designed in-house. That is, emphasis is to be on hardware experience with data points extrapolated where necessary to the proper S-band frequency. These antennas, which are identified in Section 4.3, represent viable candidates for the user spacecraft since their weights and functions are more in line with anticipated user missions. Primarily because the data collected on S-band antennas has assumed a greater significance, this information is presented in Section 4.3, whereas the data on VHF and UHF antennas (plus scaled information for S-band) is held off until Section 4.4.

4.2 Technical Considerations

Antennas performing over the three distinct bands of VHF, UHF and S-band have been considered in this study. For these bands the same antenna types are applicable; the only differences being a scaling of size and weight. Tables 4.1 and 4.2 are based on data presented in Section 4.4. Not all configurations of the same generic type of antenna are included. For example, only a disc-on-rod antenna is included for endfire type antennas, although there are many others -- helix, polyrod, yagi, etc.

Typical families of antennas representative of different types are summarized in Section 4.4. This collection although not exhaustive serves as a basis of comparison of different generic types by categorizations according to gain, size, weight, etc.

4.2.1 Antenna Environments and Antenna/Spacecraft Interaction

The immediate area in the vicinity of the antenna elements is considered the antenna "environment." The detailed constituencies and characteristics of this environment have a profound effect on the shape of the resulting antenna radiation pattern. As frequencies become higher and consequently wavelengths smaller, the interacting effect between the antenna elements and the surrounding environment begins to decrease thus allowing the radiation pattern to become more purely the result of the antenna elements themselves. [6]

Thus, the effects of booms, other antennas, protruding equipment, supporting structures, and even the basic spacecraft structure itself present a variety of critical interacting influences. For the most part ascertaining these effects analytically is difficult and experimental techniques must be resorted to by the spacecraft designer.

Table 4.1 Classification of Omnidirectional Antennas

	Gain (dB)	Average Level of Back Radiation (dB)	Weight (kg)			Interaction with Spacecraft (Qualitative)*	Stowage and Deployment Requirement	Polarization		
			VHF	UHF	S-Band			Linear	Circular	Both
Unfurlable Turnstile	2	5	2.7	1.0	0.2	Large	Stored + Energy			X
Conical Spiral	2	14	3.4	1.1	1.0	Medium	None		X	
Slotted Dipole Cone	2	5	3.4	1.1	0.2	Large	None			X
Stripline Turnstile	2.5	20	2.7	1.0	0.2	Medium	None		X	
Cavity Fed Slot	2.5	20	3.4	1.1	0.2	Medium	None			X
Discone	3	17	4.1	1.4	0.26	Large	Stored + Energy	X		
Cup Dipole	3	23	4.1	1.4	0.26	Medium	Stored + Energy			X

*Largely dependent on spacecraft size in wavelengths.

+At S-band antenna size is small, alleviating deployment requirements in all but remote applications.

Table 4.2   Classification of Medium Gain Antennas

	Gain (dB)	Average Level of Back Radiation (dB)	Weight (kg)			Interaction with Spacecraft (Qualitative)*	Stowage and Deployment Requirement +	Polarization		
			VHF	UHF	S-Band			Linear	Circular	Both
Circularly Polarized Dipole Array	8	15	13.6	4.5	0.83	Medium	Stored Energy		X	
Linear Dipole Array	8	15	10.9	3.6	0.67	Medium	Stored Energy	X		
Dipole Planar Array	8	25	16.3	5.4	1.0	Small	Stored or External Energy			X
Disc-On-Rod	9	25	6.8	2.3	0.43	Small	Stored or External Energy			X
Prime Focus Reflector	10.5	22	20.0	6.8	1.2	Small	External Energy			X

*Largely dependent on spacecraft size in wavelengths

+Little, if at all, applicable to S-band implementation because size of element is small.
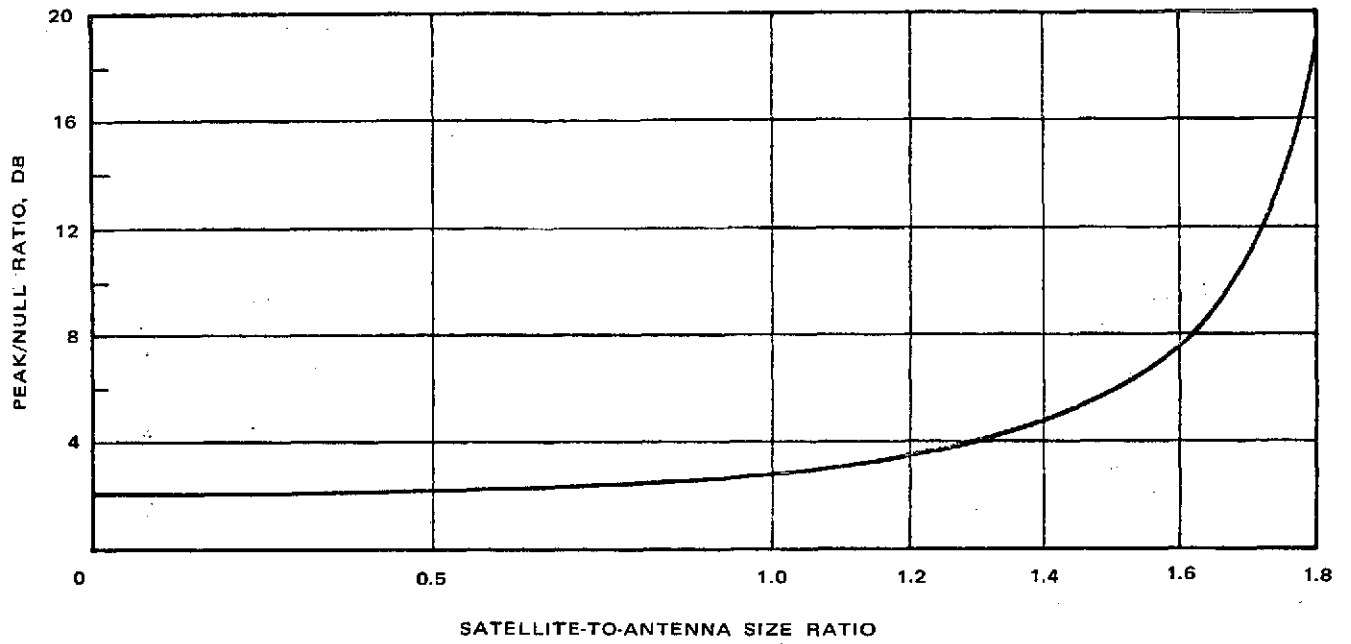
Figure 4.2   Typical Low Gain Antenna/Spacecraft Interaction

One more factor affecting this interaction is the gain of the antenna itself. The higher the gain, the less the interacting effect.

Generally speaking, antennas available to the user spacecraft designer can be separated into two distinct categories, that is, medium and low gain designs. The associated design problems and required system trades are in many respects different and can be discussed separately for these two separate classes of antennas.

The medium gain antennas, ranging in gains of about 10-15 dB, must usually be mechanically steered in order to keep the beam pointed at the TDRS because they have narrow beamwidths. In these ranges of antenna gain, there is a lower tendency for the pattern to be affected by the spacecraft structure as compared to the lower gain antennas.

For the lower gain antennas, falling in the range of gains of 2-5 dB, generally the opposite is true. Because of their relatively broad beamwidths, it may not be necessary to steer the elements continuously to keep the beam pointed toward the TDRS. Along with this advantage, however, comes the disadvantage of having lower discriminating protection against unwanted RFI arriving via the antenna radiation pattern side and back lobes. Furthermore, the structural integration of their elements into an overall spacecraft structural design is rendered difficult because of the aforementioned effect of basic pattern interaction with the structure.

When a low gain antenna is put on a satellite structure several variables modify the basic antenna radiation pattern (the intrinsic pattern in absence of the satellite body). The two most signfiicant variables are the antenna size versus the satellite structure size. The curve illustrated in Figure 4.2 shows a typical test result from NRL test analysis[6] of spacecraft interaction effects with satellite structures. In this test, a $\frac{\lambda}{4}$ turnstile antenna was mounted on a spherical spacecraft body. For varying spacecraft to antenna size, various degrees of pattern differences were observed. Generally speaking, as the satellite size is increased more numerous and deeper null appear as part of the

composite antenna/spacecraft characteristic. Besides spacecraft size, there are other factors affecting the antenna design; among the more important are geometry, element type and its location. Material properties have, at least for the turnstile design, been found to effect changes in performance.

Because of the numerous variables involved in the specification of the ultimate radiation characteristics of a low gain antenna, the antenna system integration problem is extremely difficult. Generally speaking before a system engineer can objectively select an appropriate design for his mission he is required to understand the impact of all spacecraft structural effects on all antennas from which he is making a selection so that he may choose the design which is more optimum for his application. This type of required data, unfortunately, is not readily available. It could however be determined partially through a systematic investigation.

In order to establish which low gain antenna design is most appropriate to a particular spacecraft geometry, it is valuable to conduct either a survey or a numerical and experimental investigation. The experimental approach involves the fabrication of various spacecraft structures and testing them in conjunction with different antenna configurations. A similar, however, for the same cost, more complete evaluation could be conducted analytically. A hybrid approach using methods in unison produces the best results when applied during the actual hardware development stage after which the antenna selection has already been completed. During this stage the numerical analysis could be used to provide initial insight with final design being verified by experiment.

Of the three methods of studying the spacecraft antenna interaction problem, it is believed the analytical approach is by far the most promising. It gives the capability by which a more complete set of parametric data can be derived; it lends itself more readily to changes, and it is particularly useful to assessing performance effects which are subject to design perturbations.

The available numerical techniques for analysis of structural interferences on antenna radiation characteristics can be divided into three different formulation methods. These methods are the most important ones available to date and utilize the following techniques:

    a)   Electromagnetic integral equation formulation

    b)   Wire-grid modeling

    c)   Geometrical diffraction theory

Each method has its range of applicability, accuracy and complexity.

The geometrical theory of diffraction[7,8,9] is best suited for the analysis of scattering problems where the interfering structures are large compared to a wavelength. Generally speaking the larger the structure the better the accuracy of the model. The technique is analogous conceptually to that of ray tracing.

The wire-grid modeling technique[10,11] is based on the premise that a solid conducting body may be substituted by a grid of thin wires configured to correspond to the geometry of the scatterer. Using this grid the unknown currents excited by the incident field may be determined by a system of simultaneous equations. Satisfactory application of this technique requires sufficiently short wire grid segments about 0.1 wavelengths. Once the currents on the grids are established, the corresponding reradiated fields can be calculated and then added to the primary field resulting in the total field of the antenna.

The technique using the magnetic field integral equation[12,13] is similar to that of the wire mesh. The advantages of this method are that it is theoretically more exact (neglecting mutual coupling), it imposes no restrictions on the materials of the medium, and it provides polarization insight because of its utilization of field vector formulation.

Although use of this latter technique has shown that individual deviation between the theoretical and experimental pattern of an antenna obstructed by a spacecraft can differ by as much as 5 dB, on the average the agreement is considerably better.

One particular advantage of the integral equation formulation is that it is sufficiently general with respect to the primary sources and consequently any source antenna may be used as an input to the analysis. In addition, once the matrix describing the scattering surface has been generated, it can be reused at relatively little additional expense in terms of computer utilization to determine the antenna location for an optimal combined radiation pattern.

Clearly, studies of this form are beyond the scope of this study. They have been highlighted in order to point out that valuable further studies in this field may be performed to aid the user spacecraft designer in determining the type and location of an antenna for use with the TDRSS.

4.2.2 Mounting and Deployment

Antenna location is generally a compromise between field-of-view requirements and the availability of space and payload mass for the satellite system. Omnidirectional antennas are often the most difficult to locate as their spherical field of view requirement is most difficult to achieve. Omnidirectional antennas are accordingly mounted on booms and masts to achieve a wide angle field of view.

Data return from satellites at low bit rates can be achieved with low EIRP. This provides an opportunity to use broadbeam, low gain antennas which do not require steering or tracking. For example, a slotted dipole cone type antenna will provide 2 dB gain over a hemispherical field of view. This antenna could be mounted on a short mast located away from the earth and nearly complete orbital coverage provided with a two satellite relay system. Care would need to be exercised to avoid interference with solar cell arrays or other movable equipments.

Satellite telecommunication subsystem designs for higher data rates, which require higher EIRP for reliable transmission may require a balance between antennas, transmitters and power supply in order to minimize overall equipment mass. Minimum mass configurations generally occur at that design point where the mass required for the antenna with its installation is approximately equal to the sum of the mass of the transmitter, its installation and power supply allocation. Thus a switched beam or electrically steered beam may be an appropriate design for the higher data rate users. In this case an unobstructed field of view is required for the installation of any element in a switched beam configuration and a complete unobstructed field of view is required for all elements in an electrically steered beam configuration. Mechanical gimbals may also be employed for high gain antennas where the mass of a phased array antenna would be prohibitive. It is judged that antennas 1 meter or more in diameter should use mechanical beam steering. Such an antenna would have a peak gain of 25 dB at 2.25 GHz. It may then be concluded that mechanical beam steering would not be appropriate for the low data rate class of user satellites.

4.2.3   Antenna Polarization

Terrestrially-generated RFI is assumed to consist of all polarizations of equal power; that is to say, if one were to measure the power level of the RFI with a linear polarized antenna, or a right-hand circularly polarized antenna, etc., the power level in each case would be the same. Therefore, there is no advantage in designing an antenna with any particular polarization in an attempt to reduce the level of the RFI. However, the receive signal level can be increased by adjusting the polarization of the transmitting antenna to the receive antenna or vice versa.

4.2.4   Low Gain Semi-Omnidirectional Antennas

Antennas on the order of a half wavelength are low gain (2-4 dB) and radiate nearly uniformly over large sectors. They have the advantages of being lightweight, can be easily stowed and deployed, and usually require no gimballing. They have the disadvantages of large interaction with the spacecraft and unwanted gain in the direction of the RFI. These latter effects can be minimized by placing them above a ground plane or inside a cup. Doing so reduces the back radiation with a corresponding decrease in radiated coverage. The degree to which the back radiation can be reduced depends on the size of the ground plane. One-half wavelength diameter ground planes are effective when the desired radiation is perpendicular to the ground plane. However, when maximum radiation is desired parallel to the ground plane, multiple wavelength sizes are required to reduce the radiation past the edge of the ground plane. Chokes placed at the edge of a ground plane effectively make it appear larger. The judicious use of the spacecraft structure can also act as a ground plane to partially shield from RFI sources.

Needless to say, directivity improvement by judicious use of ground plane characteristics can best be implemented at the higher frequencies. Here the wavelengths are relatively small and consequently insignificant structural difficulties arise.

In Table 4.1, these antennas have been classified according to back radiation, weight, interaction with the spacecraft, stowage and deployment requirements and polarization characteristics.

4.2.5   Multiple Wavelength Antennas

Multiple wavelength antennas can consist of continuous apertures or arrays of discrete elements. They are normally medium or high gain and radiate a pencil beam, fan beams or other special beam shapes. Continuous apertures include horns, parabolic and spherical reflectors, corner reflectors and lenses. They have the advantage of small interaction with the spacecraft and low back and sidelobes. They have the disadvantages of greater weight, usually require stowage and deployment and require mechanical steerability at the lower frequencies.

Array antennas consists of discrete radiators, either directly or parasitically excited. By varying the phase and amplitude of the fed radiating elements, these arrays can radiate anywhere from normal to the array (broadside) to parallel to it (endfire). Endfire arrays, although physically small in the plane orthogonal to the direction of maximum radiation, suffer from the fact that the gain increases only as t the square root of the length. Array type antenna have the advantage of small interaction with the spacecraft, and electronic steerability in some cases.*

For all of the configurations summarized in Section 4.4, the S-band designs pose fewer structural problems which allows for greater flexibility in the electrical design. Table 4.2 categorizes these antennas according to back radiation, weight, interaction with spacecraft, polarization and stowage and development characteristics.

*In all array designs the interaction between the spacecraft structure and the overall pattern is to a significant extent dependent upon the gain of the individual array elements themselves.

4.2.6 Antenna Switching

Two or more half wavelength antennas which have reduced coverage and lower back and sidelobes can be placed at different locations on the spacecraft and energized electrically to provide the required coverage.

Since continuous aperture antennas require mechanical steering to provide greater coverage, additional antennas could be placed on the spacecraft and switched in and out eliminating the need for steering. Although an array type antenna can be electronically scanned, the gain degrades as a function of the scan angle.[14] It may, therefore, be advantageous to provide more than one array and switch between them depending on the look angle required. As pointed out previously, the tradeoff between using more than one array and providing higher RF transmitter power depends on the point where minimum user spacecraft mass is achieved. Minimum mass configurations have been shown to occur at that point where the mass of the antenna is equal to the sum of the mass of the transmitter and its power supply.[15]

4.2.7 Feed Networks

The antennas discussed here may be fed by balanced transmission lines or by coax and a balun (balance-to-unbalance transformer), and in some cases by waveguide. Care must be taken to insure that the feed lines provide satisfactory isolation. Shielded balanced transmission lines offer the best guard against this since any currents induced on the shield or spacecraft excite equal currents on the two lines and are therefore RF grounded. When using coax lines the outer shield and the spacecraft structure itself must present zero resistance to the unwanted induced currents. Waveguide line becomes increasingly attractive from a loss standpoint with increasing frequency. However, even at S-band physical bulk and weight disadvantages still generally outweigh the electrical advantages. The recommended practice, therefore, is to use coaxial cable feed lines.

4.2.8   Antenna Weights

The antenna weights given in the Tables 4.1 and 4.2 include
both the radiating elements and the feed network and represent
construction techniques which make use of modern spacecraft
antenna structural and materials technology.   Techniques
of construction such as electroforming resulting in wall thickness
of .013 cm, etching on copper clad polyguide and metal forming has
substantially reduced the weight of antennas.   Choices of lightweight
materials such as honeycomb and metal sprayed plastics have become
more available.   Radiating surfaces, whether directly or parasitically
excited, can be perforated with holes up to a half wavelength at the
operating frequency without serious degradation of performance.   In
addition, surfaces can be formed by half wavelength resonant structures
eliminating the need for solid surfaces.   Feed networks have been
developed in air stripline with reduced weight and power loss.

The weights of the Hughes antennas for past space missions
reflect the materials and structural technology in existence at the
time they were designed. Thus, the weights for similar antennas
to those given in Section 4.3 could be considerably lower in most
cases if up to date antenna technology were utilized.
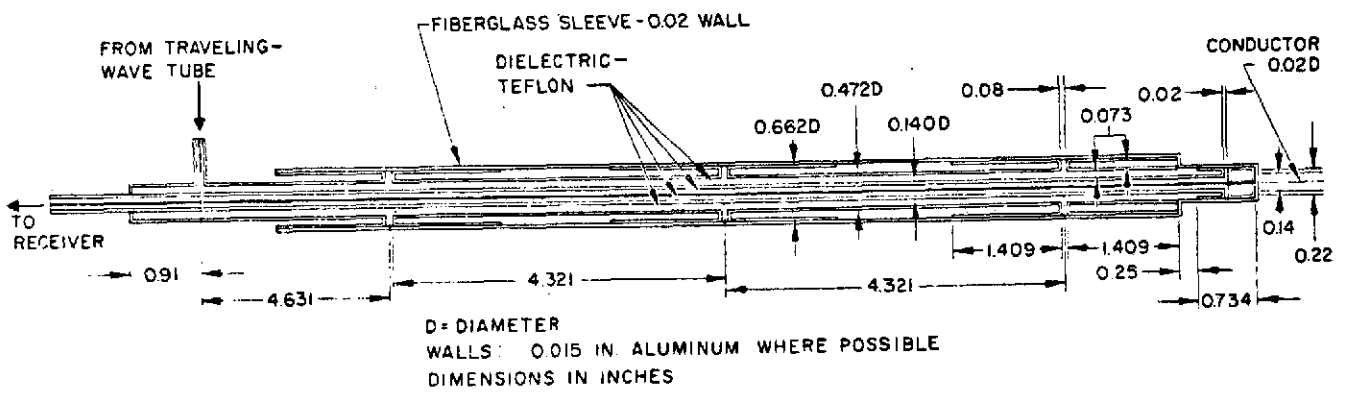
Figure 4.3.   SYNCOM Antenna Configuration

4.3   S-Band Antenna Studies

In order to obtain practical satellite S-band antenna hardware
data, this contractor was requested to specifically examine and report
on actual satellite antenna designs. This section presents electrical
and mechanical performance data for various Hughes satellite antennas,
either actual or proposed hardware designs. Where data for the proposed
TDRS S-band frequency was not available, the actual designs were extra-
polated in terms of mass and dimensions from their operating frequencies.

4.3.1   SYNCOM [16]

The SYNCOM antenna required an omnidirectional pattern in a plane
perpendicular to the axis of satellite rotation and a directional or
flattened "pancake" pattern in the plane containing the axis. This was
achieved by an array of three collinear skirted dipoles mounted on and
extending from the axis of rotation. Figure 4.3 shows the configuration
of the SYNCOM antenna. The dipoles are center-fed by annular slots in a
coaxial transmission line. A single skirted receiving dipole (for operation
at 8 GHz) is shown at the right-hand tip of the antenna structure.

The measured antenna radiation patterns provided by the SYNCOM
antenna are shown in Figure 4.4 for both azimuth and elevation cuts. It
is noted that the SYNCOM antenna operated at 1.8 GHz, however, scaling the
dimensions to 2.25 GHz for TDRS has negligible effect on the overall antenna
weight, which at 1.8 GHz was 2 kilograms. The overall antenna performance
and characteristics are given in Table 4.3.

Table 4.3   SYNCOM Antenna Characteristics

Antenna type	Skirted collinear dipoles
Peak gain	6 dB
Beamwidth	24 degrees
Dimensions	40 centimeters long
Weight	2 kg including support and deployment mechanism
Mounting	Skirts mounted on rod concentric with spin axis
Materials	Aluminum, fiberglass, Teflon
Polarization	Circular
Comments	Pancake beam; spring-actuated unfolding deployment mechanism

4.3.2   Surveyor [17]

The high gain Surveyor antenna was a mechanically steerable circularly polarized slot planar array. The antenna, shown mounted on the spacecraft opposite the solar panel in Figure 4.5, was constructed of thin-walled waveguide and used copper clad sheeting etched to form a modified Franklin array. A more detailed view of the array itself and measured radiation patterns are shown in Figure 4.6. The peak gain achieved at 2 GHz was 27 dB. Characteristics of the Surveyor planar array are given in Table 4.4.

Table 4.4   Surveyor Antenna Characteristics

Antenna type	Planar array
Peak gain	27 dB
Beamwidth	7 degrees
Dimensions	90 by 105 centimeters
Weight	17.7 kg
Polarization	Right-hand circular
Mounting	Antenna/solar panel positioner
Materials	Aluminum, foam, fiberglass
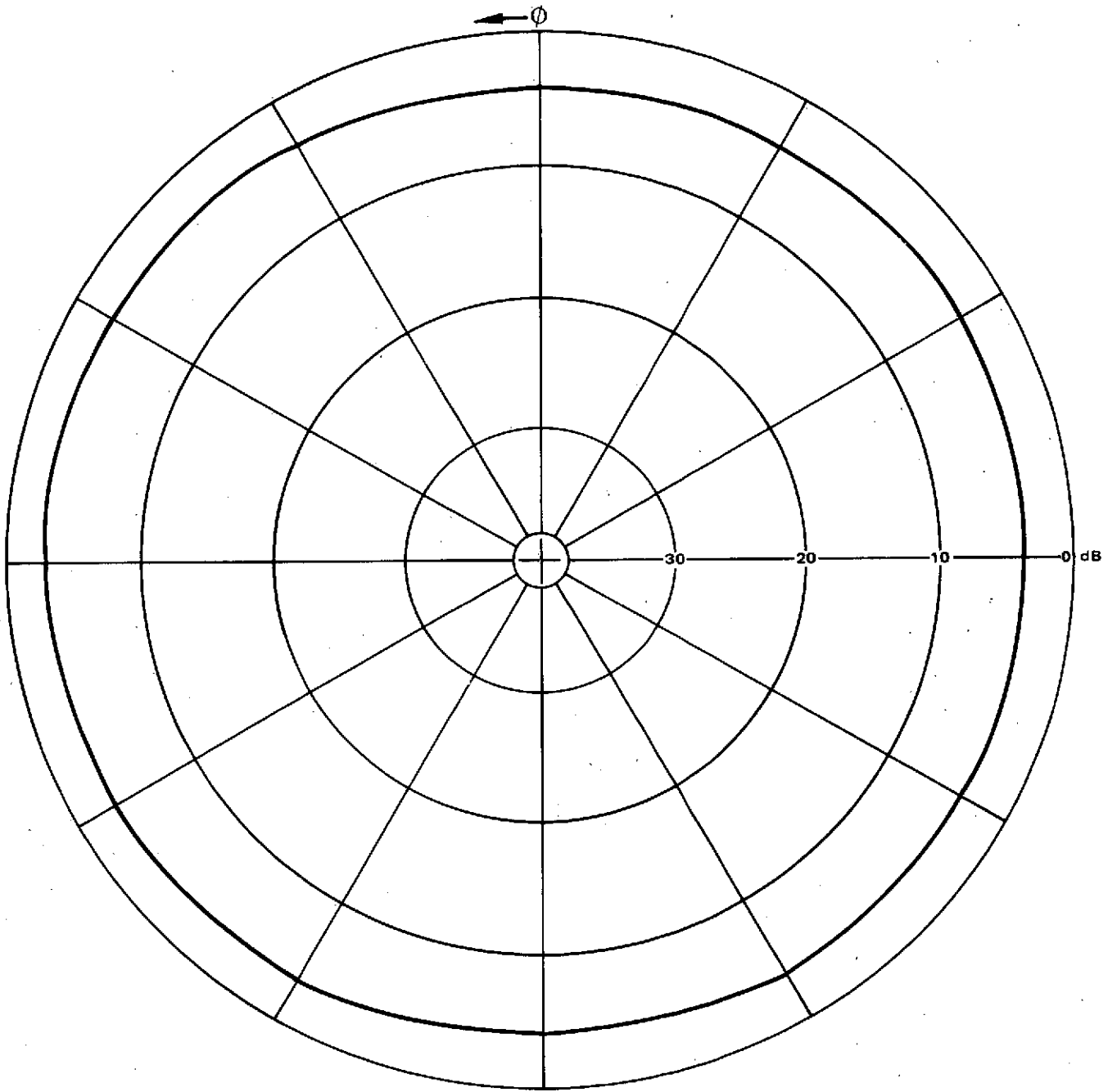
Figure 4.4. SYNCOM Antenna Radiation Pattern – Azimuth Cut
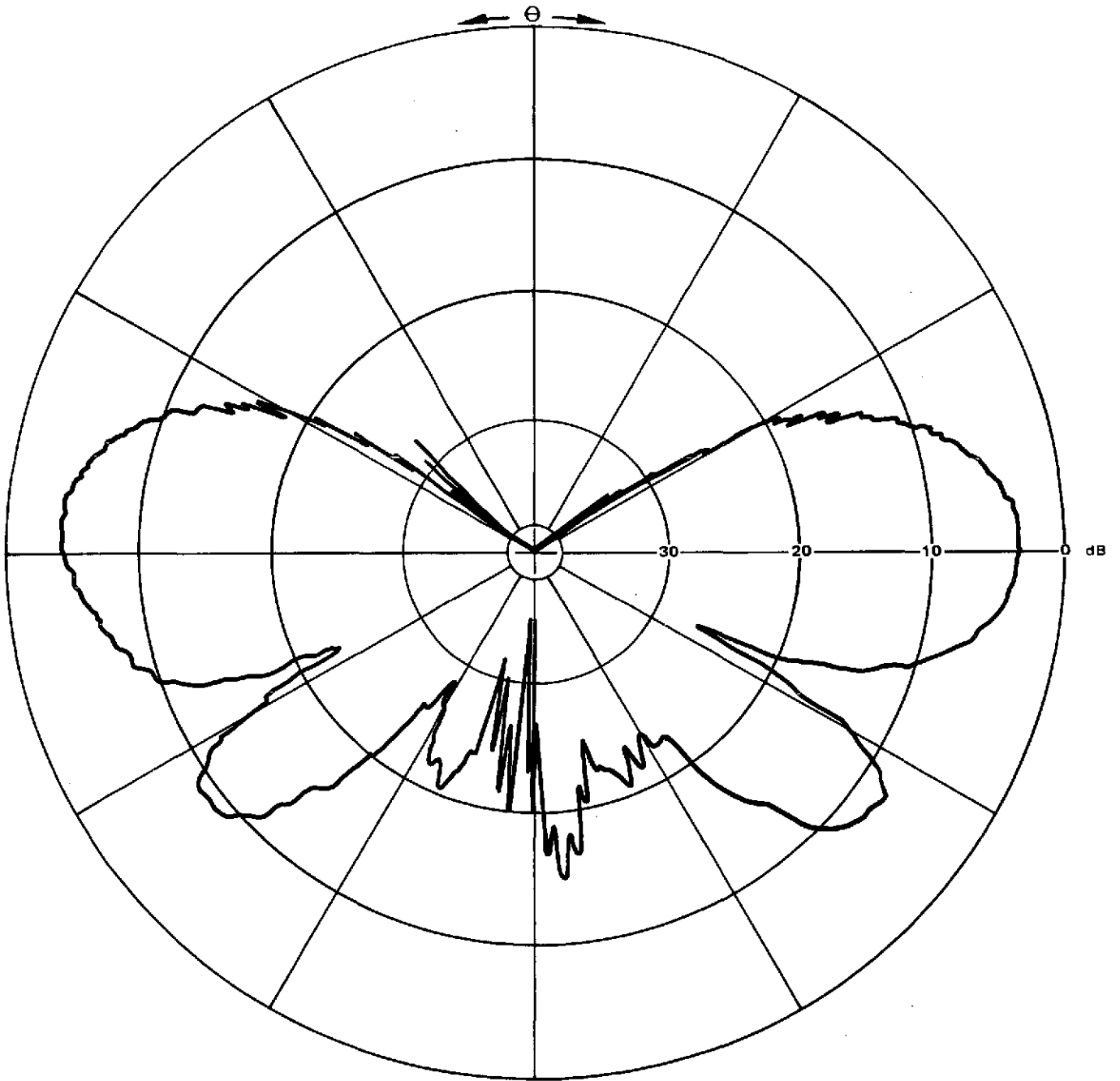
Figure 4.4. SYNCOM Antenna Radiation Pattern –
Elevation Cut
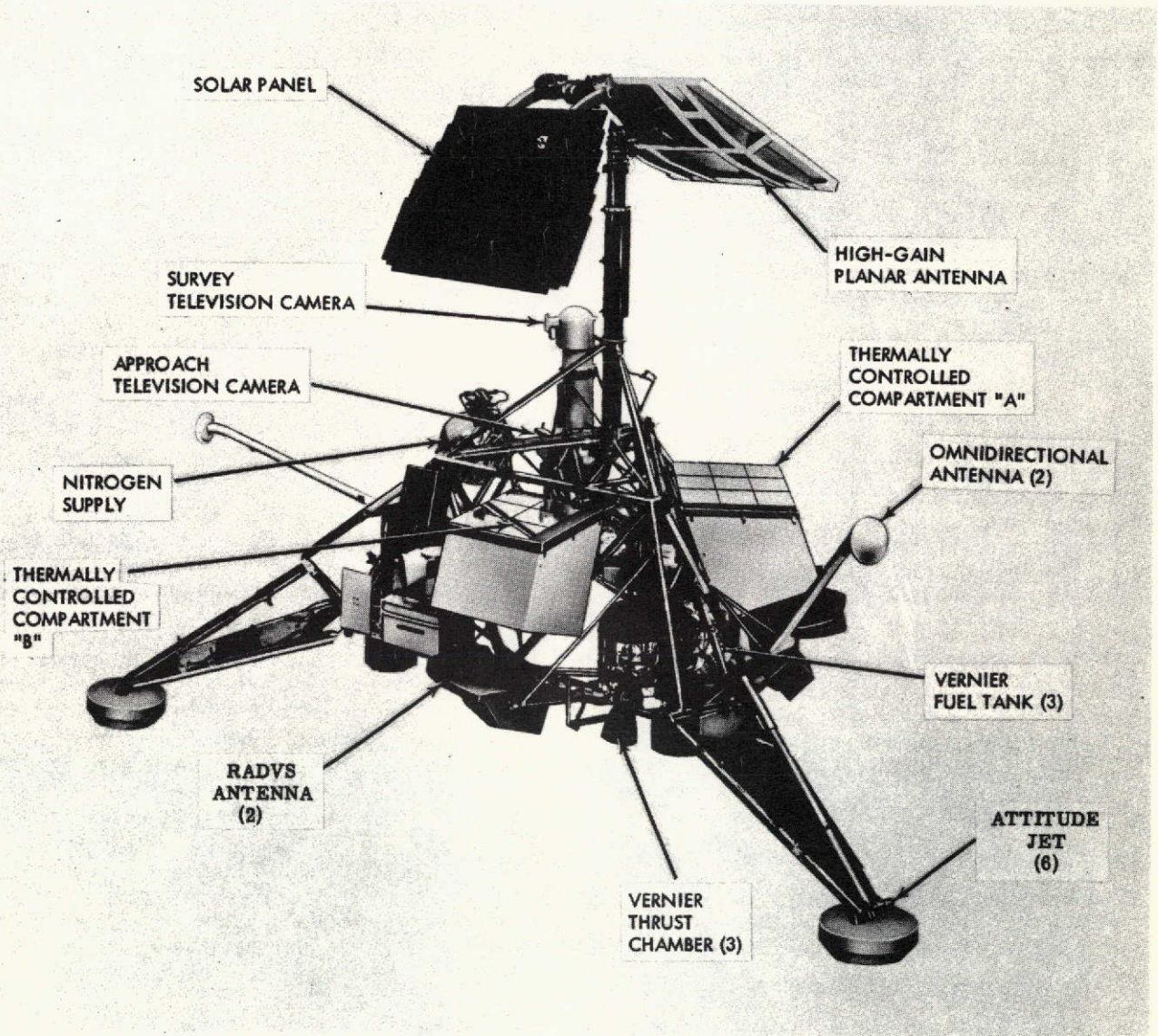
Figure 4.5.   Surveyor Spacecraft Showing high gain planar
array and antenna positioner.
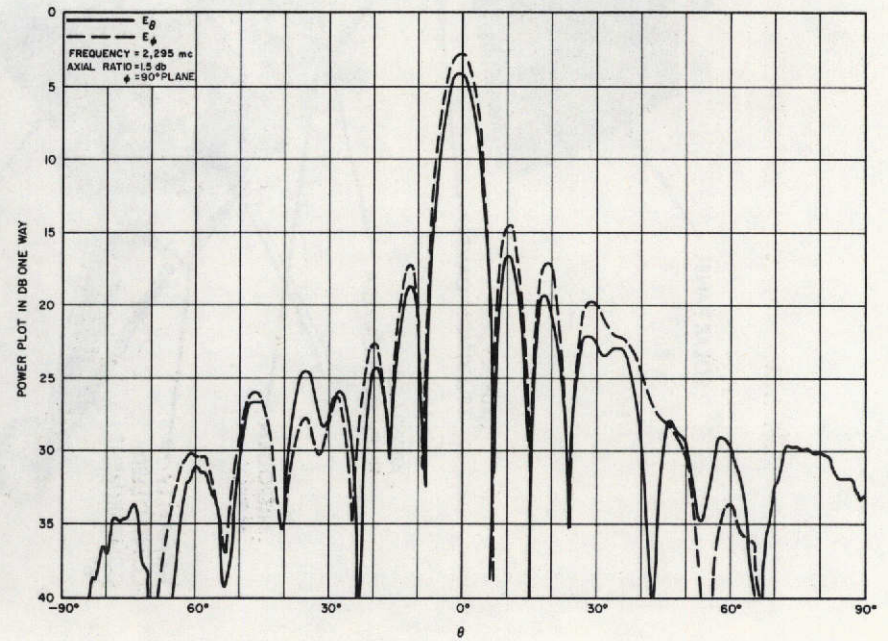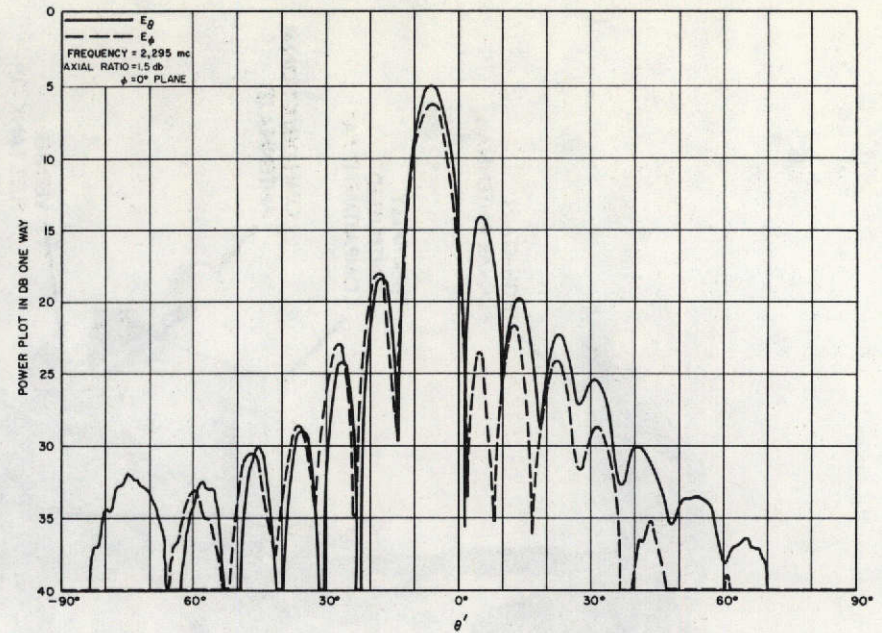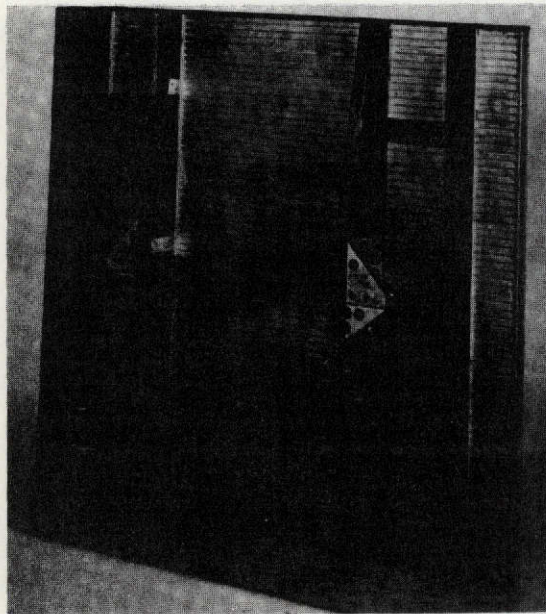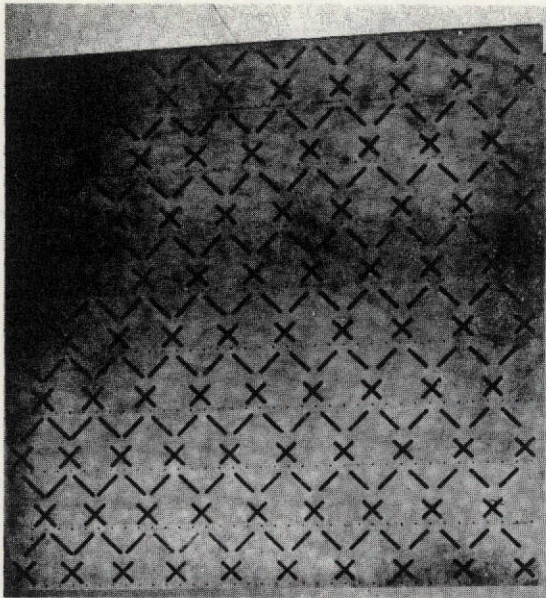
Figure 4.6.   Surveyor Planar Array and Antenna Patterns

4.3.3　Orbiting Solar Observatory (OSO) [18]

The OSO-I S-band antenna consists of a cavity backed circumferential slot radiator excited by 64 evenly spaced probes fed in phase. The slot radiator is covered with a fiberglass radome. A stripline corporate feed is associated with each quadrant; the outputs of the four corporate feeds connect to a 4-way power divider. The antenna is designed to provide approximately -6 dB gain over a nearly spherical coverage area. The predominant radiation is polarized in the plane of the spacecraft wheel spin axis. Elliptical polarization occurs in the region of the polar axis.

A schematic of a portion of the OSO "bellyband" antenna is shown in Figure 4.7. In addition to the probes and S-band cavities shown, two VHF whip antennas are integrated with and protrude from each quadrant of the slot array. The resulting S-band radiation patterns are shown in Figure 4.8. The characteristics and performance of the OSO-I antenna are given in Table 4.5.

Table 4.5　OSO-I S-Band Antenna Characteristics

Type	Annular ring slot array
Peak gain	-6 dB over 95% of the sphere
Beamwidth	n.a.
Dimensions	152 cm diameter x 1.9 cm high x 3.4 cm deep
Weight	31 kg
Mounting	"Bellyband" structure integrated with VHF whips into the spacecraft wheel
Materials	Aluminum, fiberglass, beryllium copper

CAVITY WALL

PROBE SUPPORT

STRIPLINE

PROBE
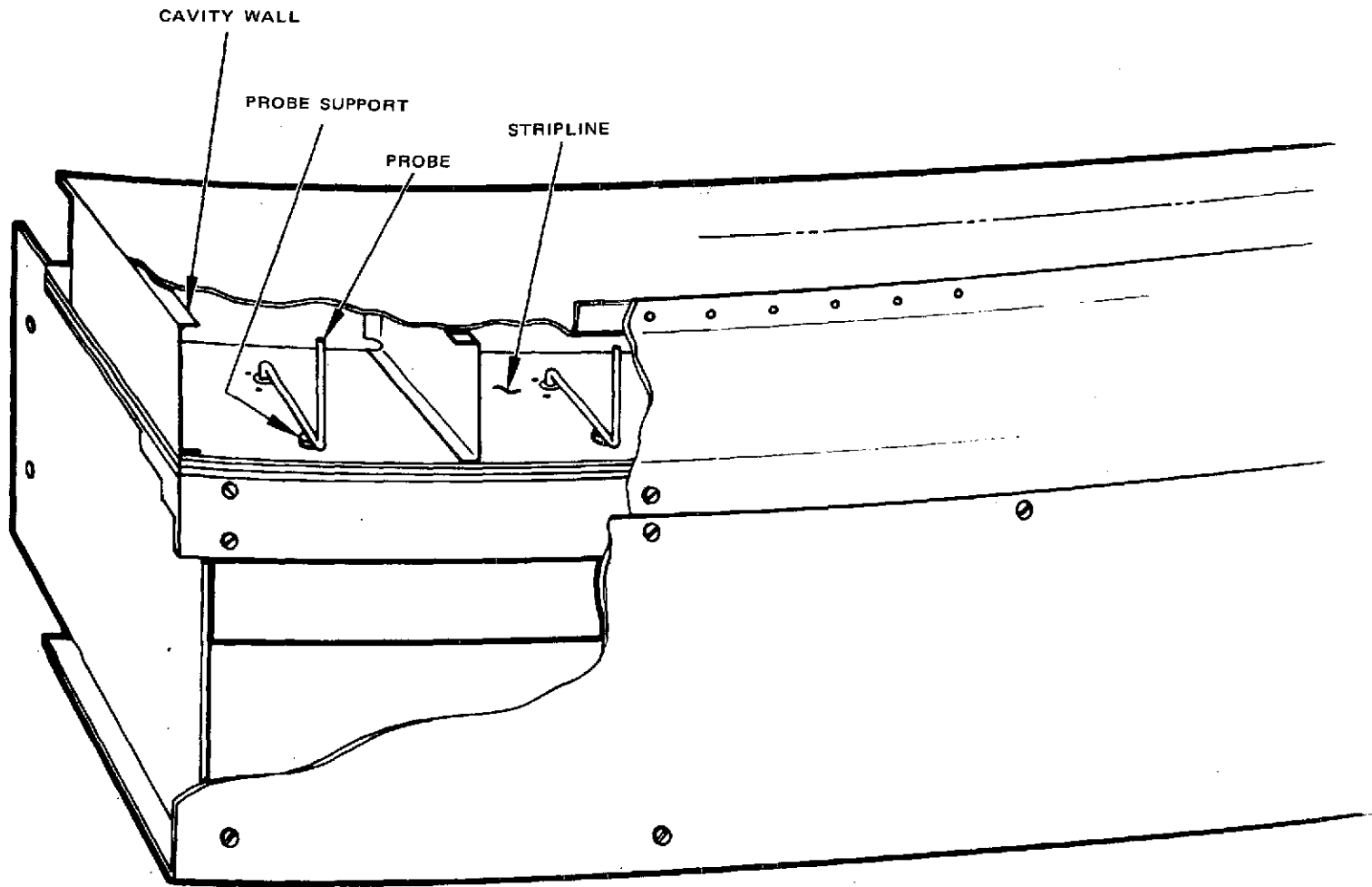
Figure 4.7.   OSO-I S-Band Annular Ring Slot Array Detail

A) AZIMUTH CUT

11/7/72

PAT. NO. 5 $\theta = 90^0$

ϕ OUT

B) ELEVATION CUT

POLAR ANGLE

$\theta \longrightarrow$

TOP

WHEEL

$\phi = 180$

BOTTOM

+2.40B
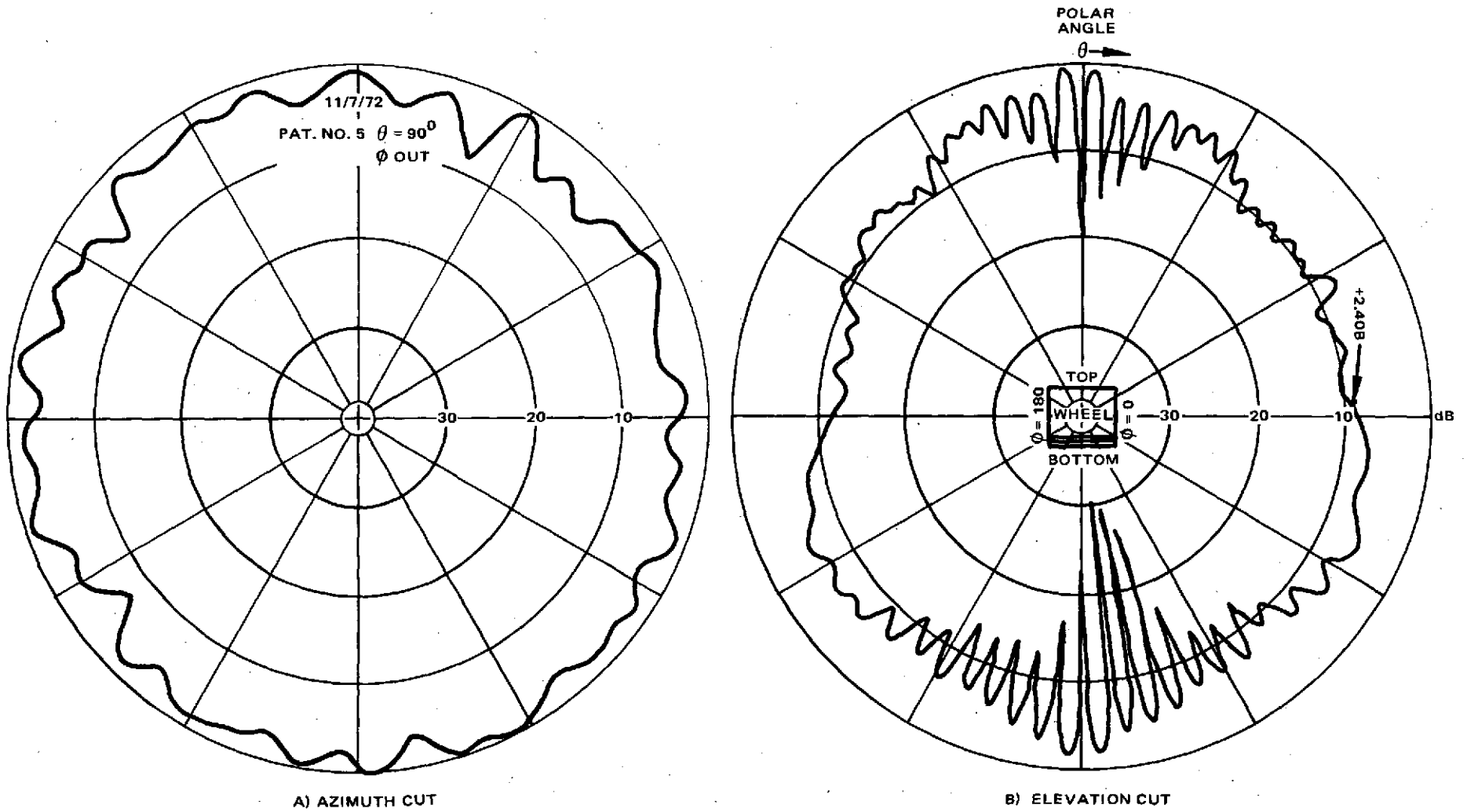
Figure 4.8. OSO S-Band Antenna Radiation Pattern
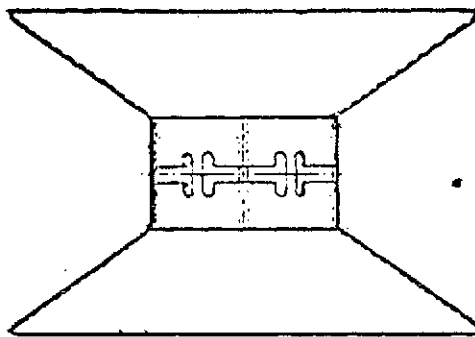
Figure 4.9. Bicone Antenna

4.3.4   Bicone Antennas

The Bicone antenna, by virtue of its omnidirectionality in the plane perpendicular to the spin axis of a spin-stabilized spacecraft, has been used on several Hughes-designed and launched spacecraft. These include the USAF Tactical Communications Satellite (TACSAT),[19] the INTELSAT IV, and the Canadian Domestic Satellite, ANIK. Of these, the TACSAT bicone operates at 2 GHz, whereas the commercial satellites operate at 4 GHz for telemetry.

The two cones which make up the aperture, shown in Figure 4.9, are usually spun out of sheet aluminum. The circular guide in the center is machined from aluminum stock, the slots are then machined, and the cones are then spot-welded to the circular guide. The bicones are then housed in a fiberglass thermal shield and mounted on top of the spacecraft.

A set of radiation patterns for the bicone antenna is shown in Figure 4.10. The characteristics and performance of the 2 GHz TACSAT antenna, which is representative of possible spin stabilized user satellite antennas, are given in Table 4.6.

Table 4.6   TACSAT Antenna Characteristics

Antenna type	Bicone
Peak gain	5 dB
Beamwidth	360 x 40 degrees
Polarization	Circular
Dimensions	61 cm diameter x 36 cm high
Weight	8.8 kg
Mounting	Mounted on mast at top of spacecraft concentric with spin axis
Materials	Aluminum, fiberglass
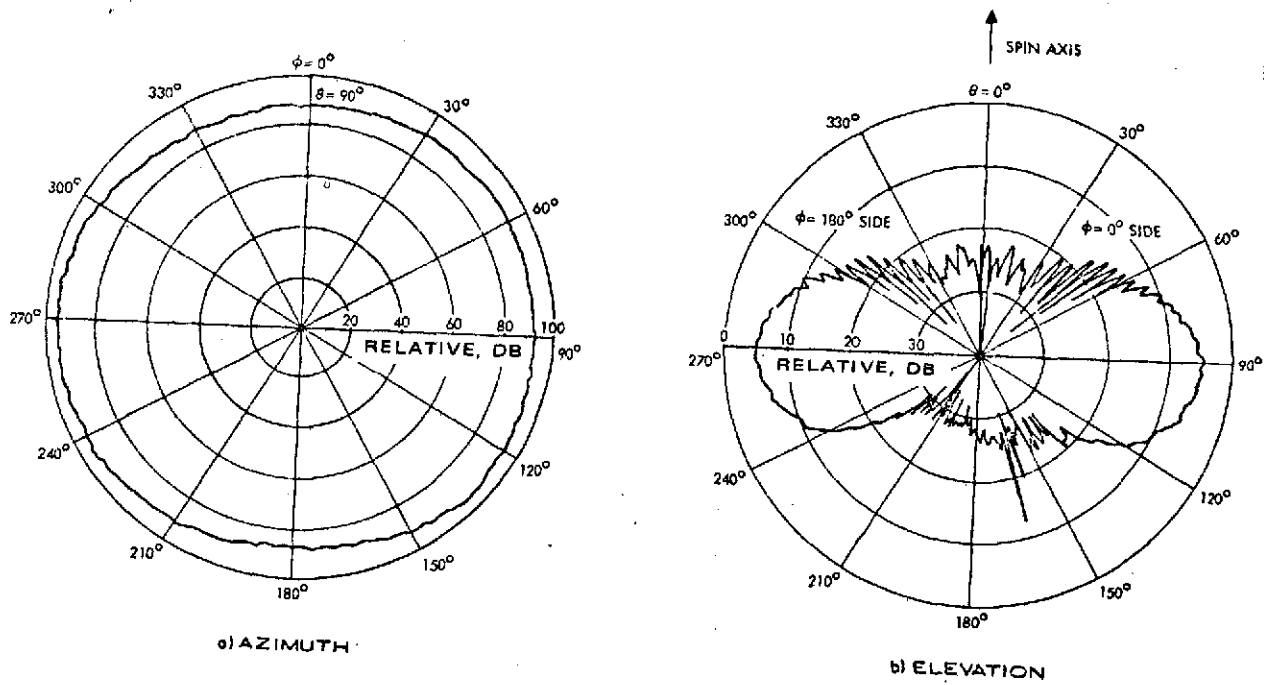
Figure 4.10. Bicone antenna radiation patterns

4.3.5 Short Backfire Antenna [20]

The short backfire antenna provides circular polarization by using a crossed dipole feed as shown in Figure 4.11, or linear polarization by using a single dipole. The antenna consists of two plane reflectors spaced approximately a half wavelength apart with the feed placed between them. The primary reflector is cupped to form a cavity. The antenna surfaces can be made from either perforated sheet metal or wire mesh with aluminum ribs. Stowage and deployment of this type of antenna will be necessary in most instances.

Typical radiation patterns for the backfire antenna are shown in Figure 4.12, and characteristics and performance are summarized in Table 4.7.

Table 4.7 Short Backfire Antenna Characteristics

Aperture diameter	26.7 cm
Peak gain	15.5 dB
Polarization	Linear or circular
Weight	1 kg
Materials	Perforated sheet metal or Chromel-R wire mesh with aluminum ribs

4.3.6 Quadrifilar Helix Antenna [21]

A potentially attractive user antenna is the fractional-turn quadrifilar helix. Such an antenna is theoretically capable of achieving approximately a 3 dB gain relative to an isotropic circularly polarized reference with less than 3 dB axial ratio over a beamwidth of 130 degrees. The configuration of such an antenna is shown in Figure 4.13. Typical dimensions for 2.25 GHz are also given in the figure. The radiation pattern of this antenna is ideally a cardioid with the null of the pattern along the axis of the antenna.
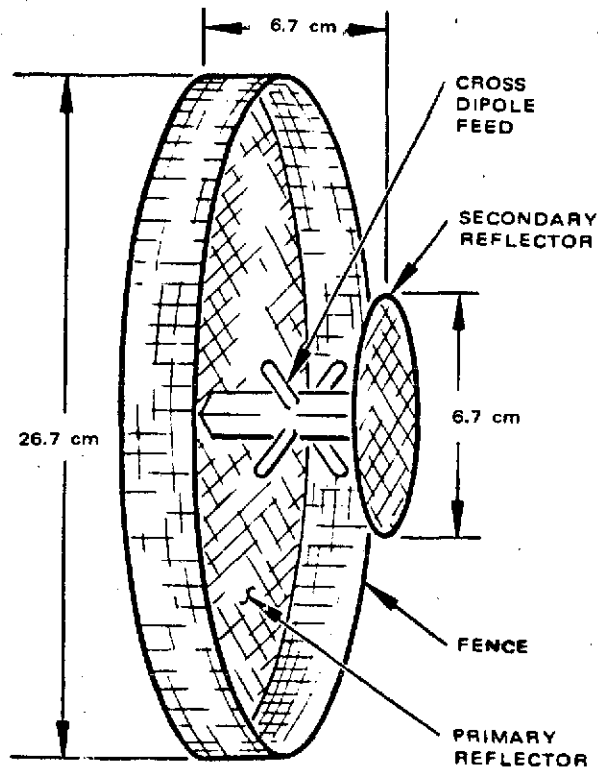
Figure 4.11. Short Backfire Antenna
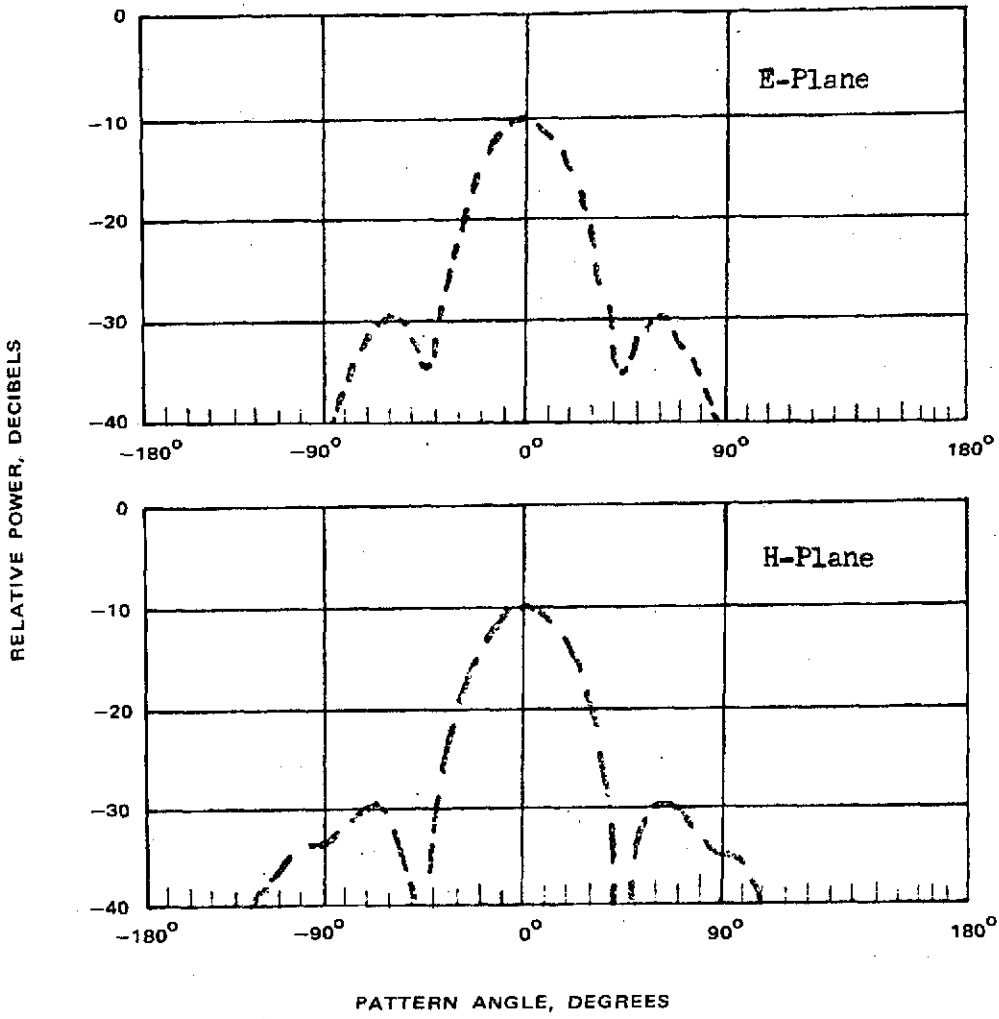
Figure 4.12. Typical Radiation Pattern of the Short Backfire Antenna.
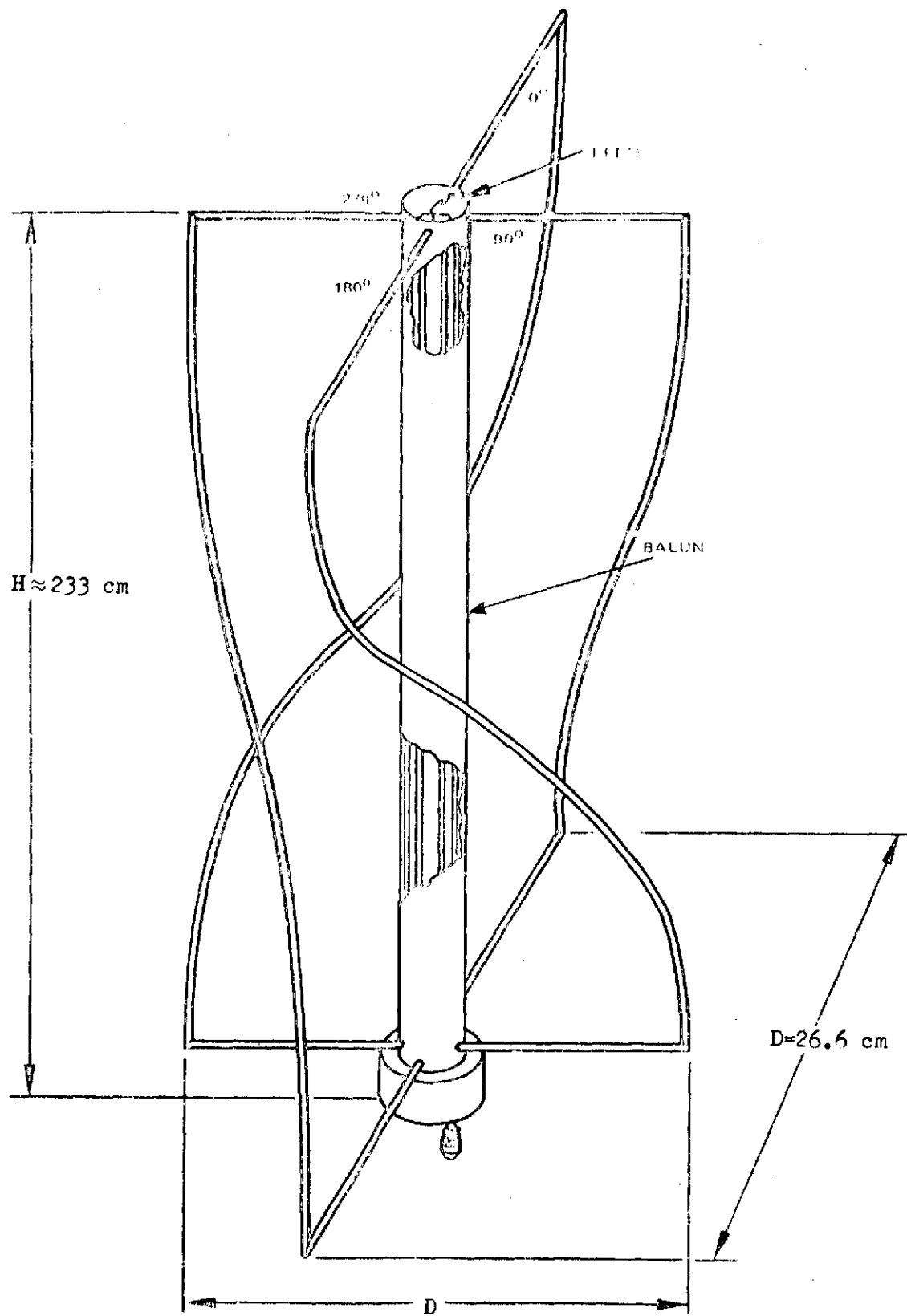
Figure 4.13. Quadrifilar Helical CP Element

$H \approx 233$ cm

$D \approx 26.6$ cm

D

BALUN

0"

90°

180°

270°

The quadrifilar helix antenna has the desirable property of reversing the direction of the pattern null, causing the beam to cover the opposite hemisphere, by reversing the phase of the feed between bifilar elements.[22] Consequently, a set of three such antennas orthogonally mounted on a user spacecraft could achieve the effect of six selectable elements if a dual-mode reversible feed network is implemented in the design. This type of antenna appears to lend itself well to stowage and deployment along its axis.

Typical characteristics of a 2.25 GHz quadrifilar helix antenna are given in Table 4.8.

Table 4.8 Quadrifilar Helix Antenna Characteristics

Element length	233 cm
Antenna diameter	26.6 cm
Peak gain	3 dB
Polarization	Circular
Beamwidth	130 degrees
Weight	660 gm
Materials	Beryllium copper tubing

4.3.7   Monofilar Helix Antenna [23]

The helical antenna has the advantage of being smaller in cross-section than other types of radiators with comparable gain and are less complex than dipoles and slot antennas. The axial mode helical radiator is formed by winding a wire in a helix with a pitch angle of from 11 to 16 degrees and a diameter of the order of $\lambda/3$. A metallic ground plane whose dimensions are of the order of λ is placed at one end of the helix. The helix is usually fed by a coaxial line whose outer conductor terminates on the ground plane and whose inner conductor passes through the ground plane to form the helix. The helix itself may be wound on a dielectric tube or supported by dielectric spokes extending from a tube along the longitudinal axis of the helix.

GROUND PLANE

HELICES (PLATED) AND ETCHED
ON THIN FIBERGLASS TUBE
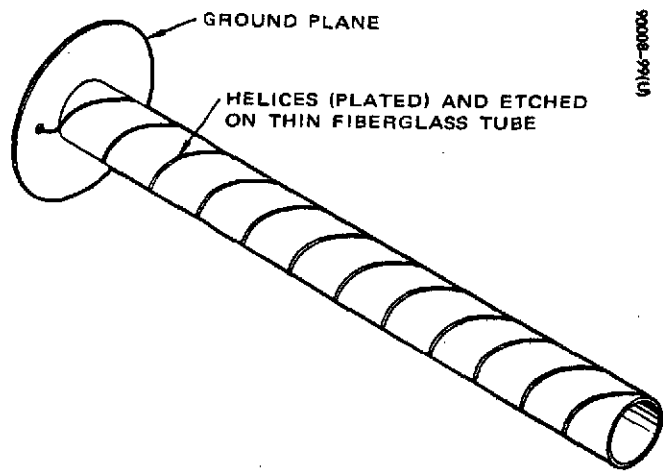
Figure 4.14.   Monofilar helix antenna

An example of a monofilar helical satellite antenna design
is the Hughes HS-350 antenna, shown in Figure 4.14. This helix, used
at S-band, achieves 13 dB gain, weighs 3.3 kg, and measures 30.5 cm
long by 5.34 cm in diameter.

4.3.8   Geostationary Meteorological Satellite Antenna [24]

The S-band antenna for the GMS consists of an array of cavity-
backed slot radiating elements integrated into the spinning spacecraft
solar panel. The beam is constantly despun by switching between adjacent
modules (four excited simultaneously) so that the angular rate approximately
equals the rate of the spinning satellite.

Each module of the antenna, shown in Figure 4.15, consists of an
array of three linearly polarized elements. An array of three elements
provides the required shaping in the elevation plane. Each element consists
of a pair of circumferential slots which couple to a waveguide that is
excited by a probe. There are a total of six slots in each module.
Performance characteristics of the GMS antenna are given in Table 4.9.

Table 4.9 GMS Antenna Performance and Characteristics

Type	Electronically despun array of cavity- backed slots
Peak gain	18.7 dB
Beamwidth	17.6 degrees
Polarization	Vertical linear
Weight	Approximately 180 kg
Dimensions	208 cm diameter annulus
Mounting	Structurally integrated with solar panel mounted peripherally around spacecraft
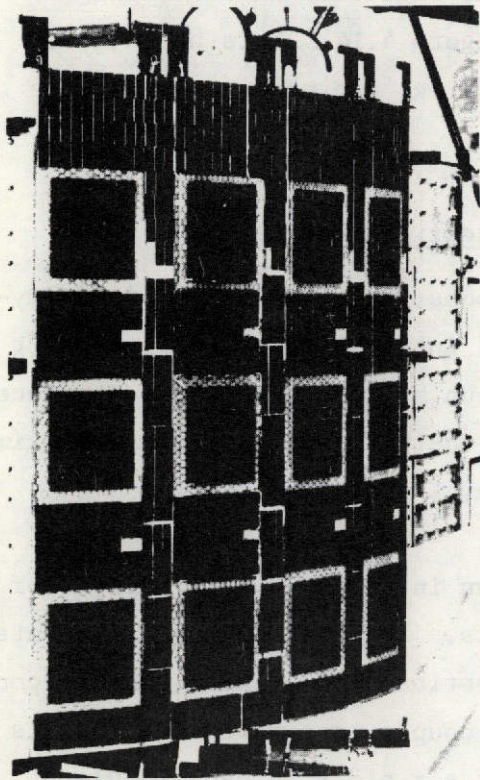
a) Structural engineering
   model
   (Photo 4R13975)
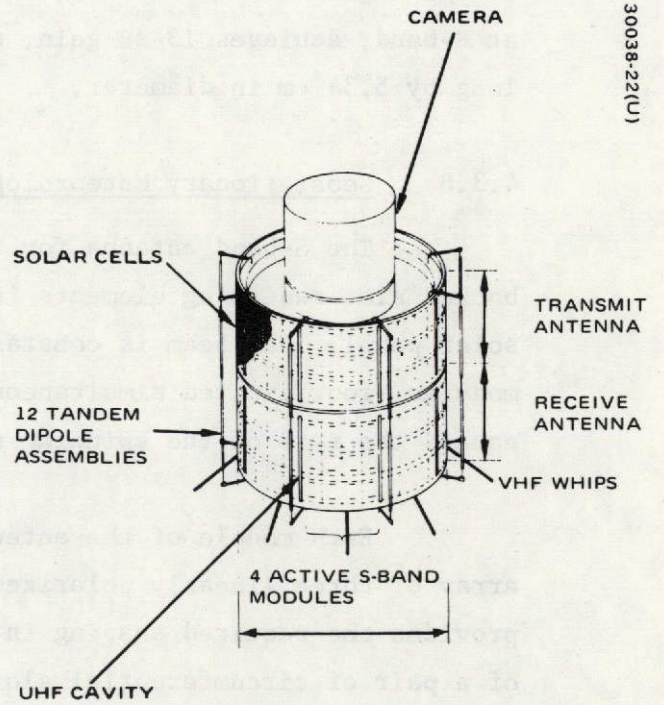
b) Spacecraft and antenna
   configuration

Figure 4.15.   GMS Electronically despun antenna

4.3.9   Conical Log Spiral Antenna[25]

The conical log spiral is being proposed for the Hughes HS-507 Pioneer Venus spacecraft. This antenna provides a gain greater than -6 dB over an angle of 140 degrees centered on the spacecraft forward spin axis. Figure 4.16 shows the configuration of the conical log spiral antenna and its corresponding radiation pattern. This particular antenna, which weighs approximately 1 kg, is most often used as a radiator for broadband frequency coverage, not necessarily a major requirement with TDRS usage.

FIBERGLASS
CONE

RIBBON
CONDUCTOR

MOUNTING PLATE/
GROUND PLANE

CONICAL LOG
SPIRAL RADIATOR
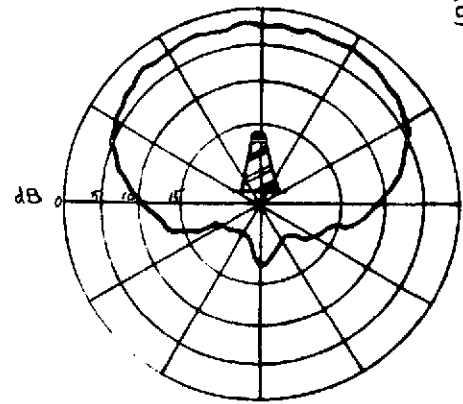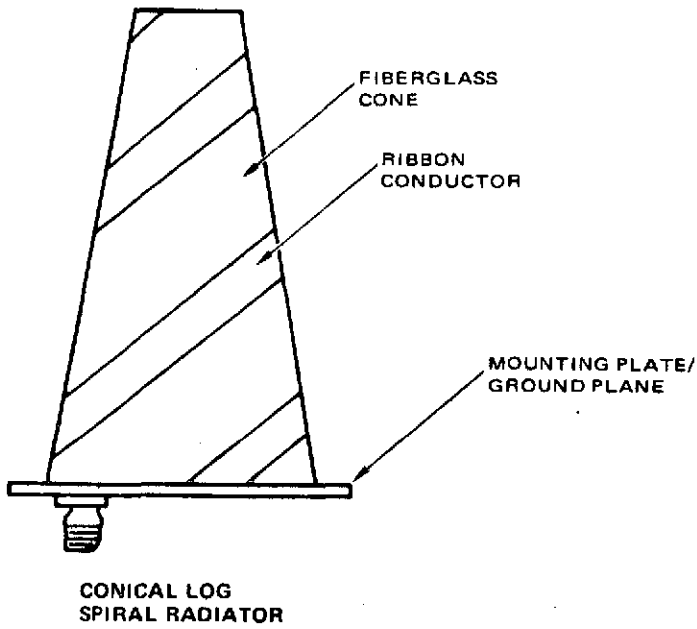
TYPICAL ⊖-PLANE RADIATION
PATTERN

30163-220(U)

Figure 4-16. HS-507 Conical Log Spiral Antenna and radiation pattern

4.4 Candidate Antennas and Their Characteristics

The antennas listed in Tables 4.1 and 4.2 are given in this section in greater detail. The weights and dimensions were originally developed for VHF and UHF and scaled to S-band. Where available, antenna radiation patterns are also given.

The antennas described in this section include:

Unfurlable turnstile

Conical spiral above a ground plane

Slotted dipole cone

Stripline turnstile

Cavity fed slot dipole

Discone

Cup dipole

Circular dipole array

Linear dipole array

Dipole planar array

Disc-on-rod endfire

Prime focus reflector

FIGURE 4.17. UNFURLABLE TURNSTILE ANTENNA
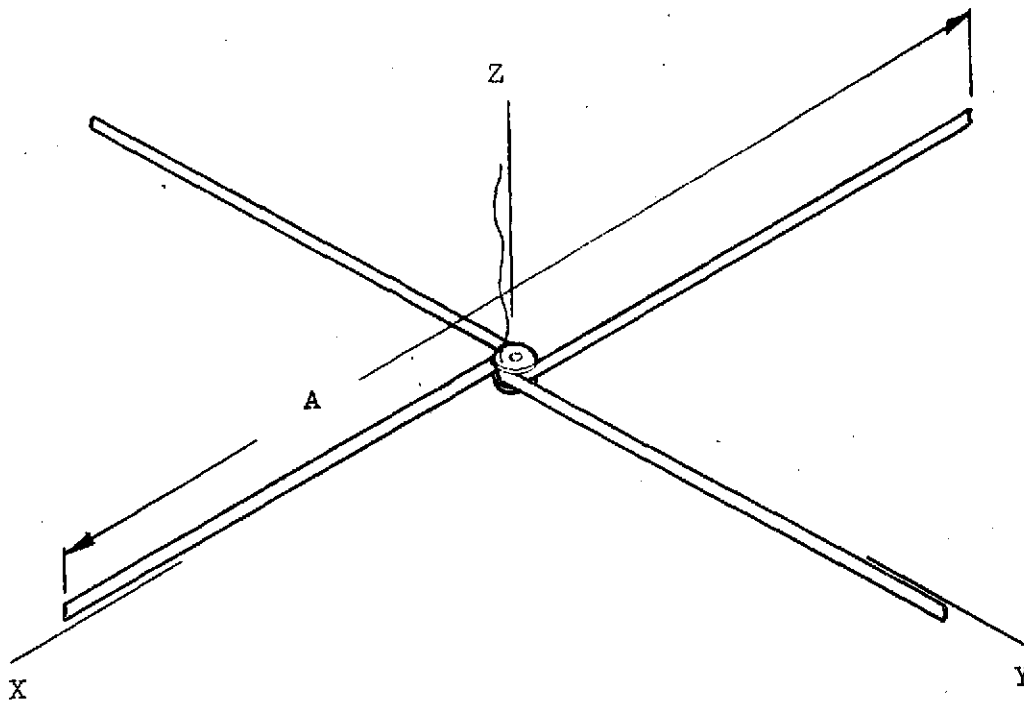
DESCRIPTION: TWO DIPOLES IN SPACE AND TIME QUADRATURE

GAIN: 2 dB
FRONT - BACK RATIO: 5 dB
FRONT - SIDE RATIO (90 DEG FROM PEAK): 3 dB
SPACECRAFT PERTURBATION - LARGE
 POLARIZATION - LINEAR AND CIRCULAR
WEIGHT - S-BAND   0.2 kg
          UHF   1.0 kg
          VHF   2.7 kg

FREQUENCY	A (Meters)
S	0.064
UHF	0.36
VHF	1.1

FIGURE 4.18.   UNFURLABLE TURNSTILE ANTENNA
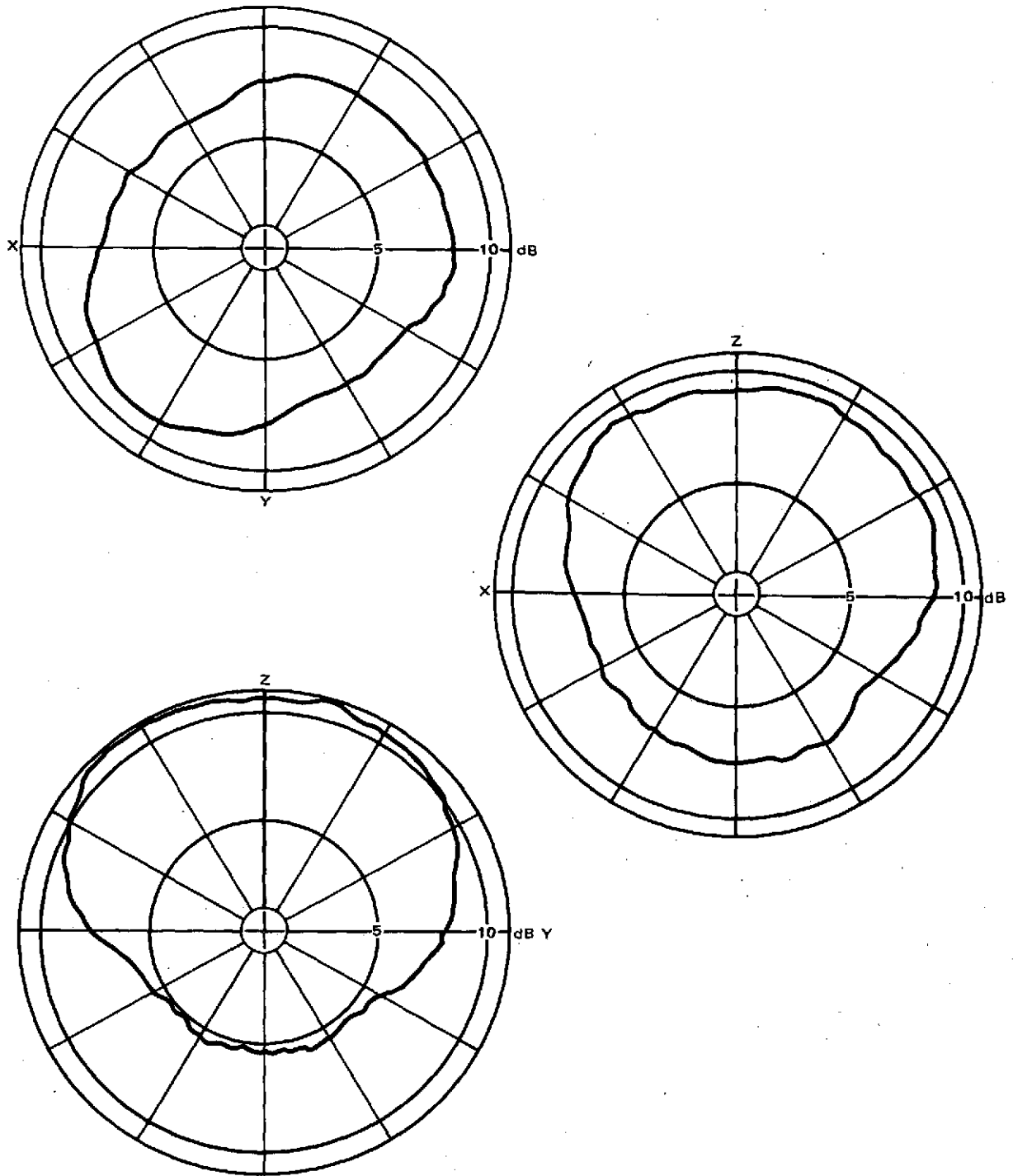
FIGURE 4.19.CONICAL SPIRAL ANTENNA ABOVE GROUND PLANE
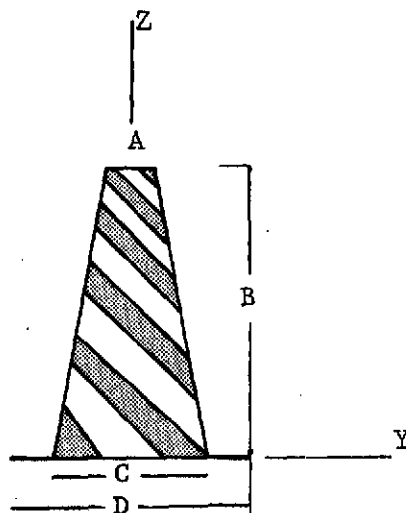
DESCRIPTION: TWO 2 ARM SPIRALS FED IN TIME QUADRATURE WRAPPED ON A
               CONE LOCATED ABOVE A GROUND PLANE.

GAIN: 2 dB
FRONT - BACK RATIO: 14 dB
FRONT - SIDE RATIO (90 DEG FROM PEAK): 14 dB
SPACECRAFT PERTURBATION: MEDIUM
POLARIZATION - CIRCULAR
WEIGHT - S-BAND   0.2 kg
         UHF   1.1 kg
         VHF   3.4 kg

FREQUENCY BAND	A	B	C	D	(Meters)
S	0.0125	0.076	0.041	0.059	
UHF	0.07	0.43	0.23	0.33	
VHF	0.18	1.1	0.58	0.91	

FIGURE 4.20. SLOTTED DIPOLE CONE
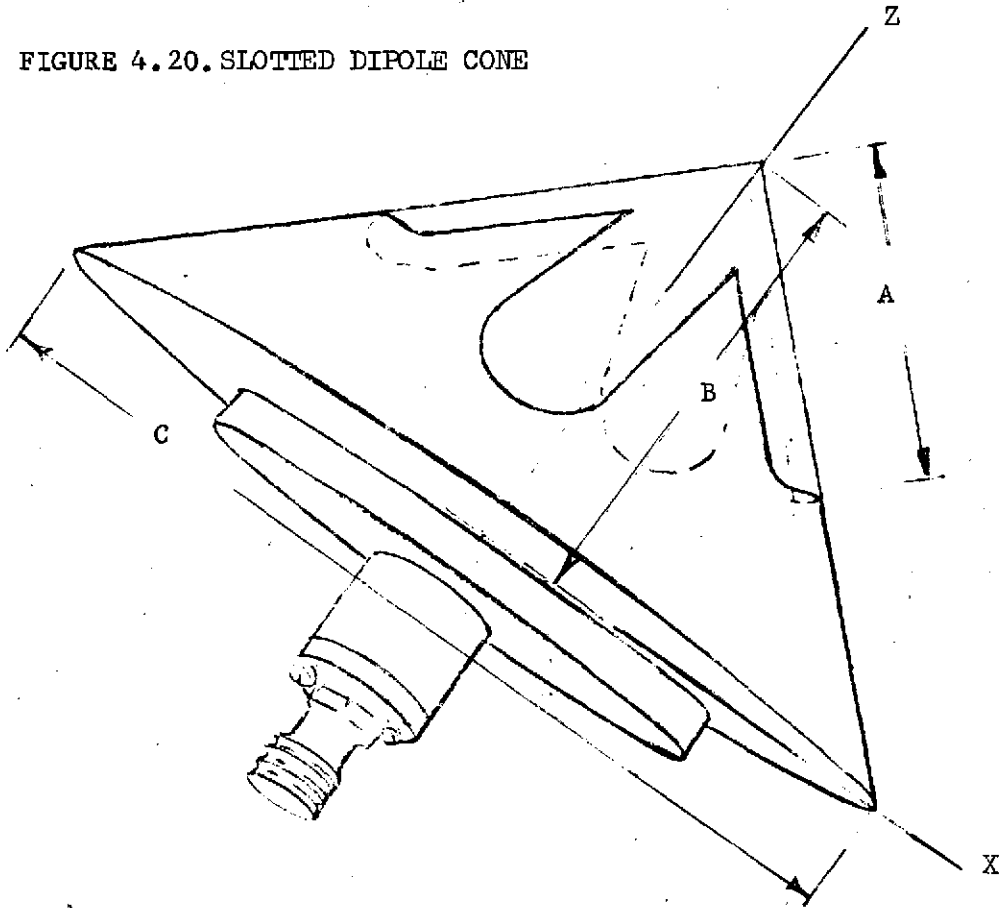
DESCRIPTION: CROSSED SLOT DIPOLE LOCATED AT APEX OF CONE
FED IN TIME QUADRATURE

GAIN: 2 dB
FRONT-BACK RATIO: 13 dB
FRONT-SIDE RATIO (90 DEG FROM PEAK): 0 dB
SPACECRAFT PERTURBATION: LARGE
POLARIZATION: LINEAR AND CIRCULAR
WEIGHT: S-BAND   0.2 kg
          UHF   1.1 kg
          VHF   3.4 kg

FREQUENCY BAND	A	B	C	(Meters)
S	0.059	0.071	0.142	
UHF	0.33	0.4	0.80	
VHF	0.98	1.2	2.4	

FIGURE 4.21. SLOTTED DIPOLE CONE
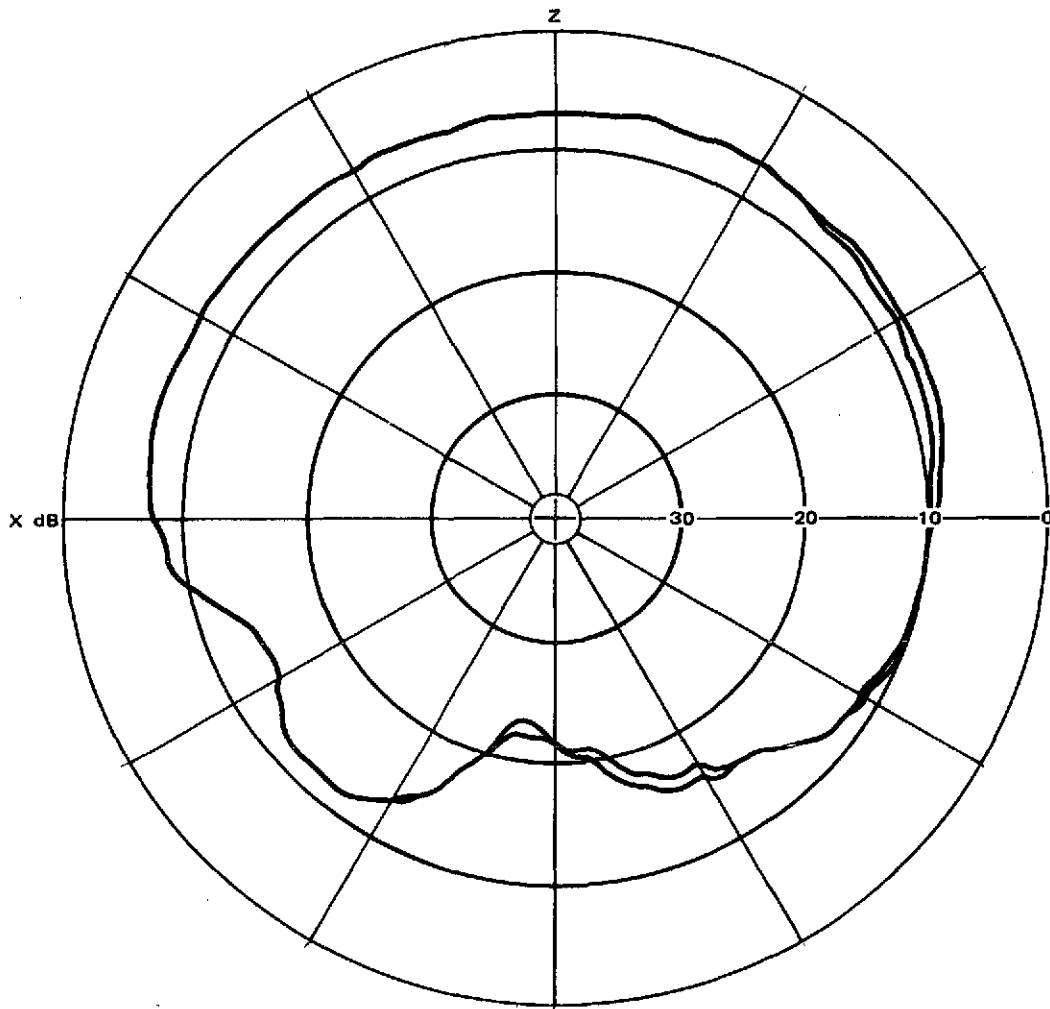
FIGURE 4.22.　SLOTTED DIPOLE CONE
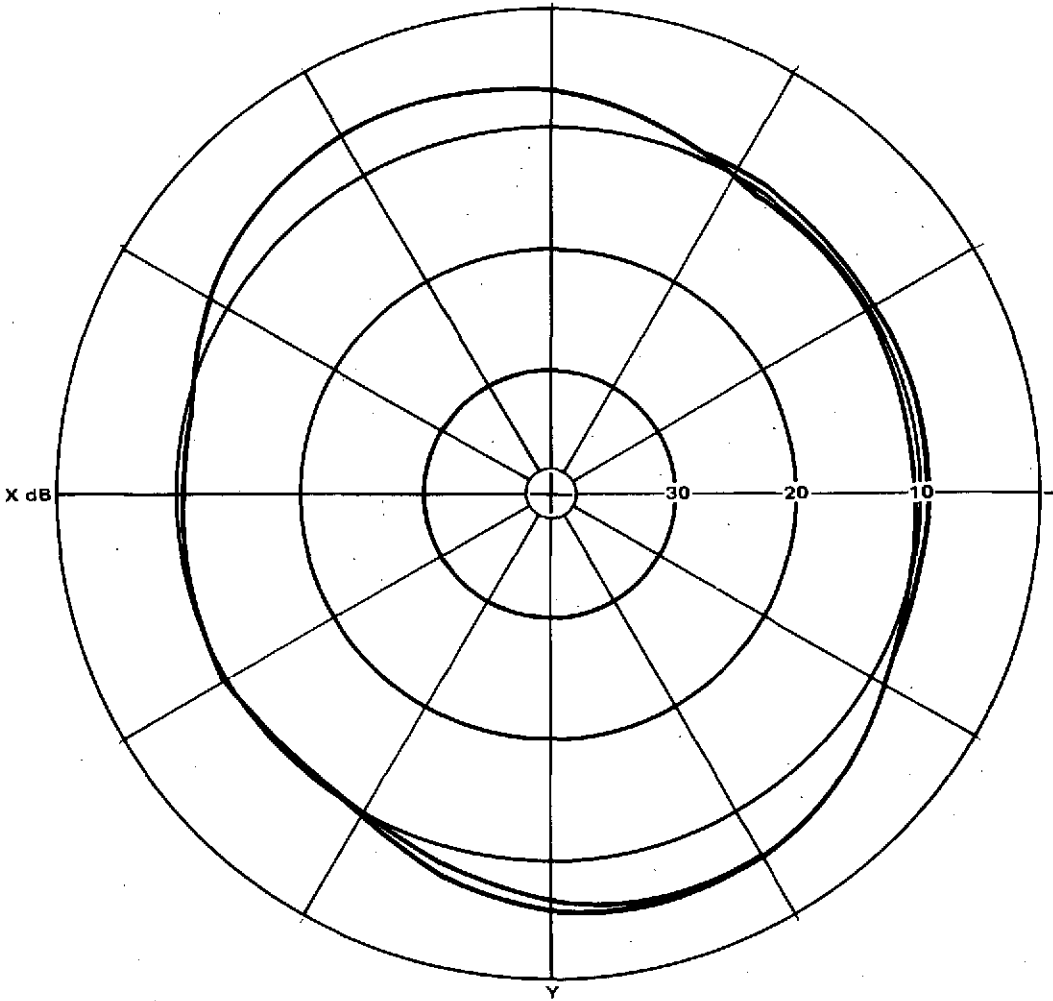
FIGURE 4.23. STRIPLINE TURNSTILE ANTENNA
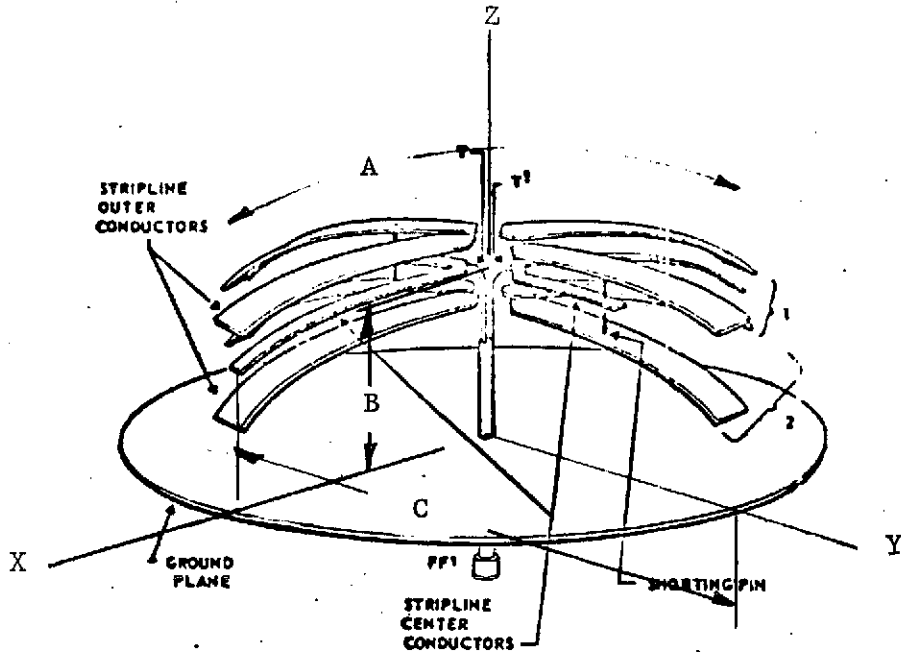
DESCRIPTION: TWO CURVED DIPOLES IN SPACE AND TIME QUADRATURE ABOVE A
FINITE GROUND PLANE

GAIN: 2.5 dB
FRONT - BACK RATIO: 25 dB
FRONT - SIDE RATIO (90 DEG FROM PEAK): 14 dB
SPACECRAFT PERTURBATION: MEDIUM

POLARIZATION - CIRCULAR
PATTERN:
WEIGHT: S-BAND   0.2 kg
           UHF   1.0 kg
           VHF   2.7 kg

FREQUENCY BAND	A	B	C	(Meters)
S	0.059	0.195	0.076	
UHF	0.33	0.11	0.43	
VHF	0.91	0.3	1.3	

4-48

FIGURE 4.24.   CAVITY FED SLOT DIPOLES
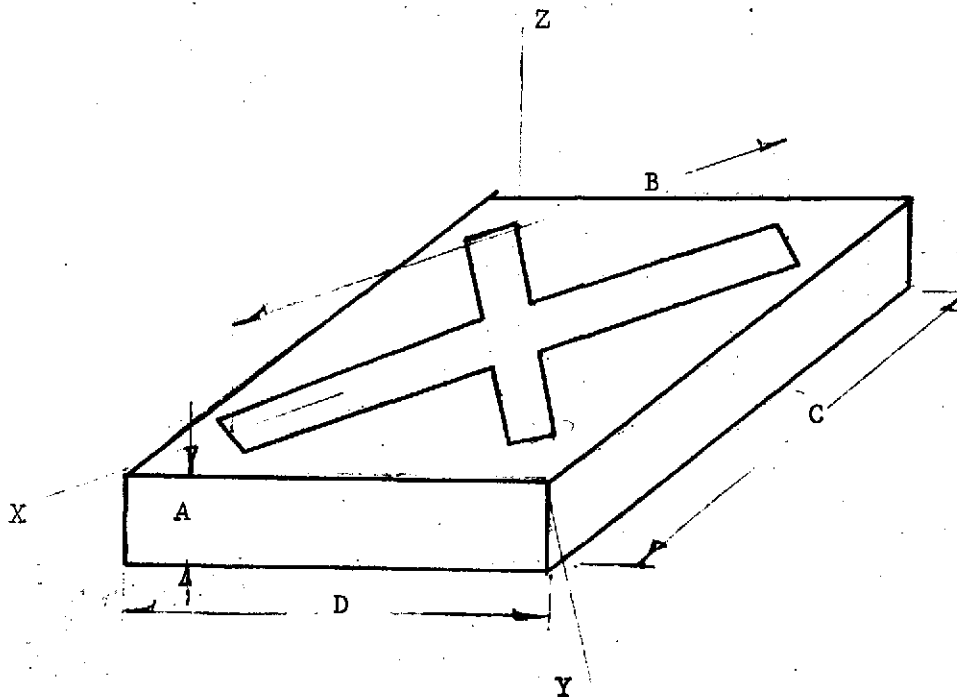
DESCRIPTION: CROSSED SLOT DIPOLES EXCITED BY A RESONANT CAVITY

GAIN: 2.5 dB
FRONT-BACK RATIO: 15 dB
FRONT-SIDE RATIO (90 DEG FROM PEAK): 15 dB
SPACECRAFT PERTURBATION: MEDIUM
POLARIZATION: LINEAR AND CIRCULAR
WEIGHT: S-BAND   0.2 kg
         UHF   1.1 kg
         VHF   3.4 kg

FREQUENCY BAND	A	B	C/D	(Meters)
S	0.0125	0.094	0.176	
UHF	0.176	0.53	0.99	
VHF	0.21	1.7	2.9	

FIGURE 4.25. CAVITY FEED SLOT DIPOLES

4-50
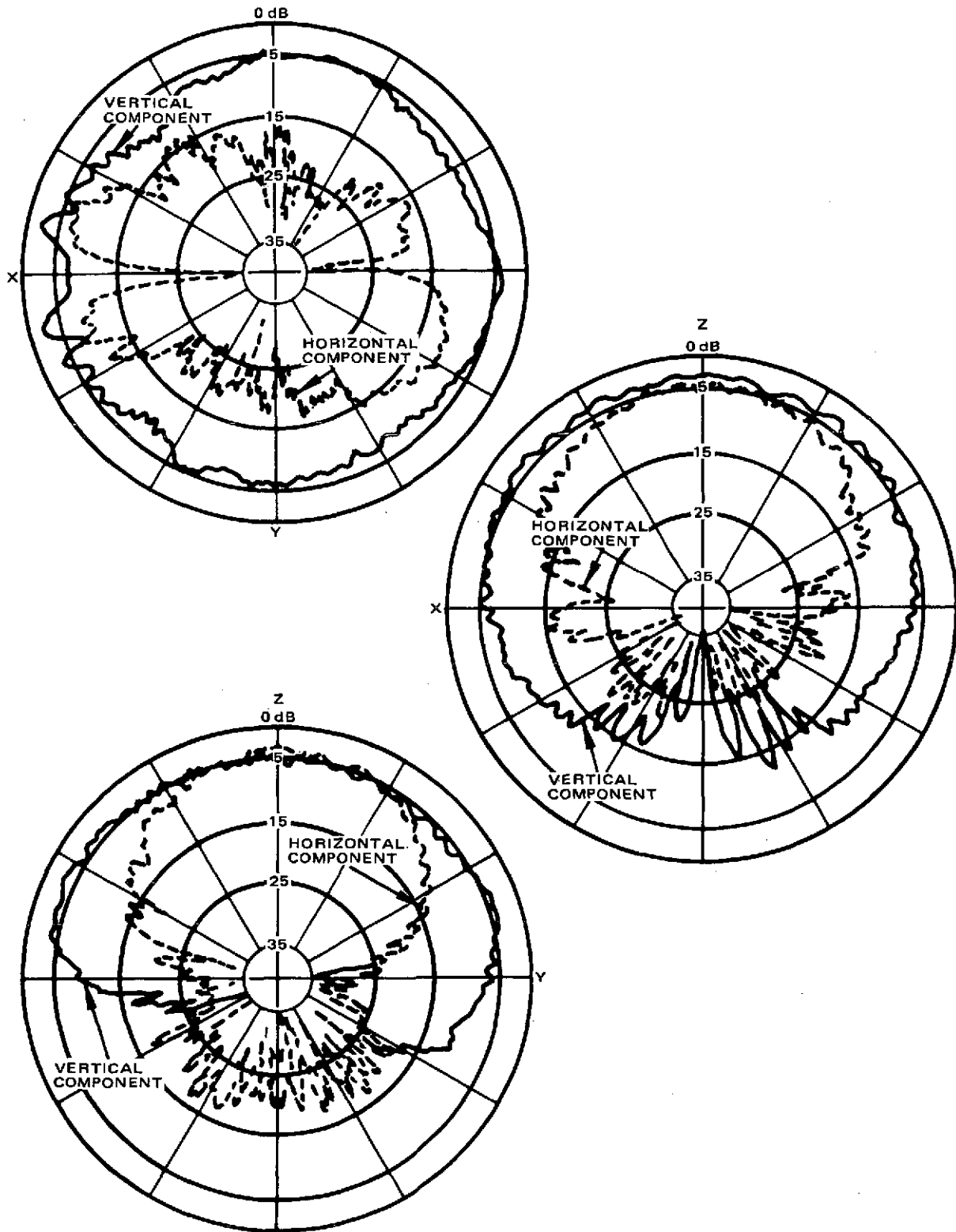
FIGURE 4.26. DISCONE
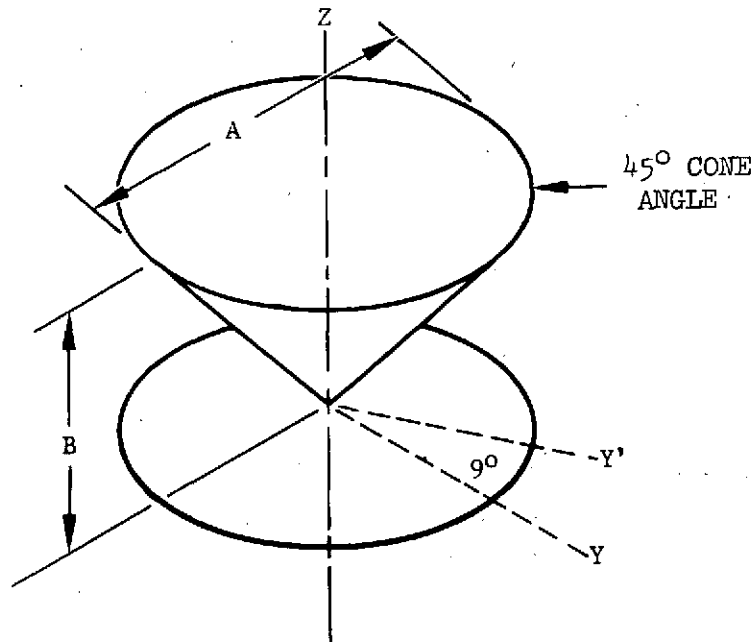
DESCRIPTION: ONE HALF OF A SINGLE CONE ABOVE A FINITE GROUND PLANE

GAIN: 3 dB
FRONT-BACK RATIO: 13 dB
FRONT-SIDE RATIO (90 DEG FROM PEAK): 5 dB
SPACECRAFT PERTURBATION: LARGE
POLARIZATION: LINEAR
WEIGHT: S-BAND   0.26 kg
        UHF   1.40 kg
        VHF   4.1 kg

FREQUENCY BAND	A	B	(Meters)
S	0.176	0.089	
UHF	0.99	0.5	
VHF	3.00	1.5	

Figure 4.27. DISCONE
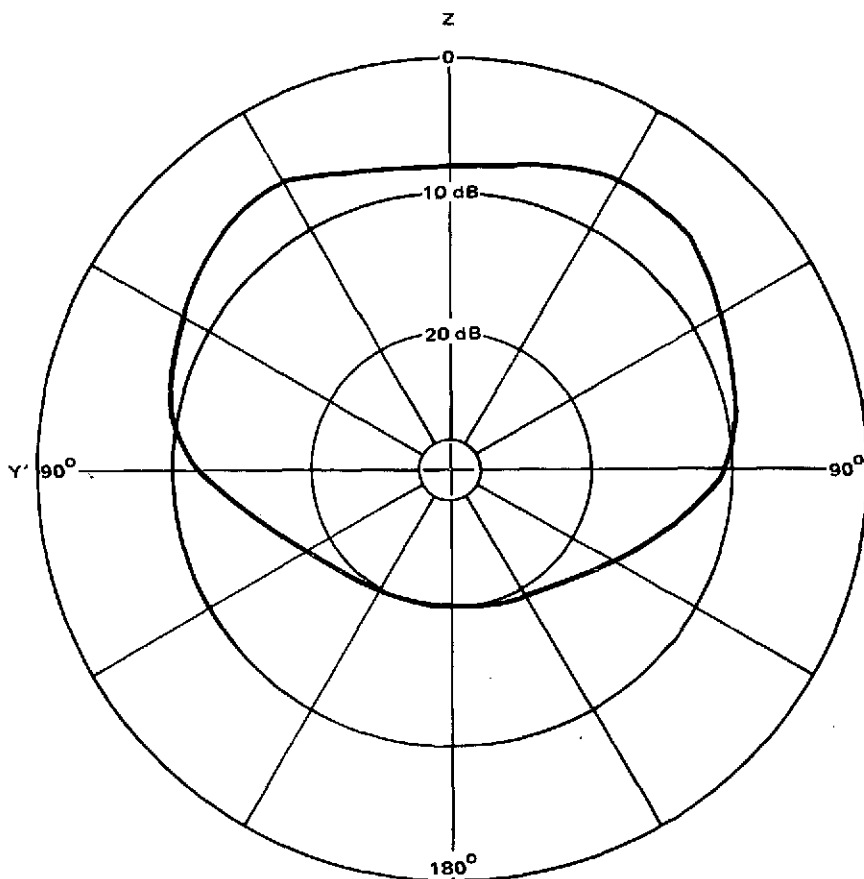
FIGURE 4.28. CUP DIPOLE
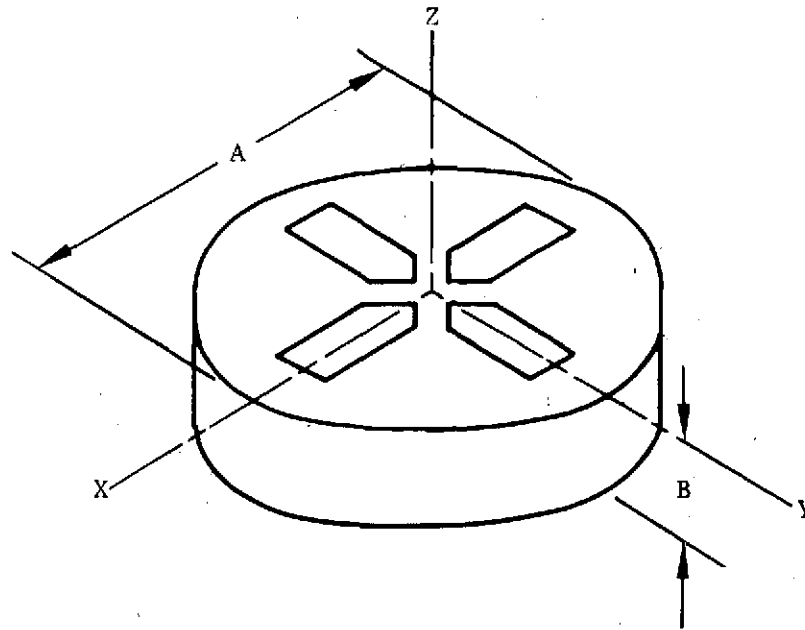
DESCRIPTION: TWO DIPOLES IN SPACE AND TIME QUADRATURE LOCATED IN A CUP
               CAVITY

GAIN: 3 dB
FRONT-BACK RATIO: 25 dB
FRONT-SIDE RATIO (90 DEG FROM PEAK): 17 dB
SPACECRAFT PERTURBATION: MEDIUM
POLARIZATION: LINEAR AND CIRCULAR
WEIGHT: S-BAND   0.26 kg
         UHF   1.40 kg
         VHF   6.1 kg

FREQUENCY BAND	A	B	(Meters)
S	0.117	0.048	
UHF	0.66	0.27	
VHF	1.80	0.55	

FIGURE 4.29. CUP DIPOLE
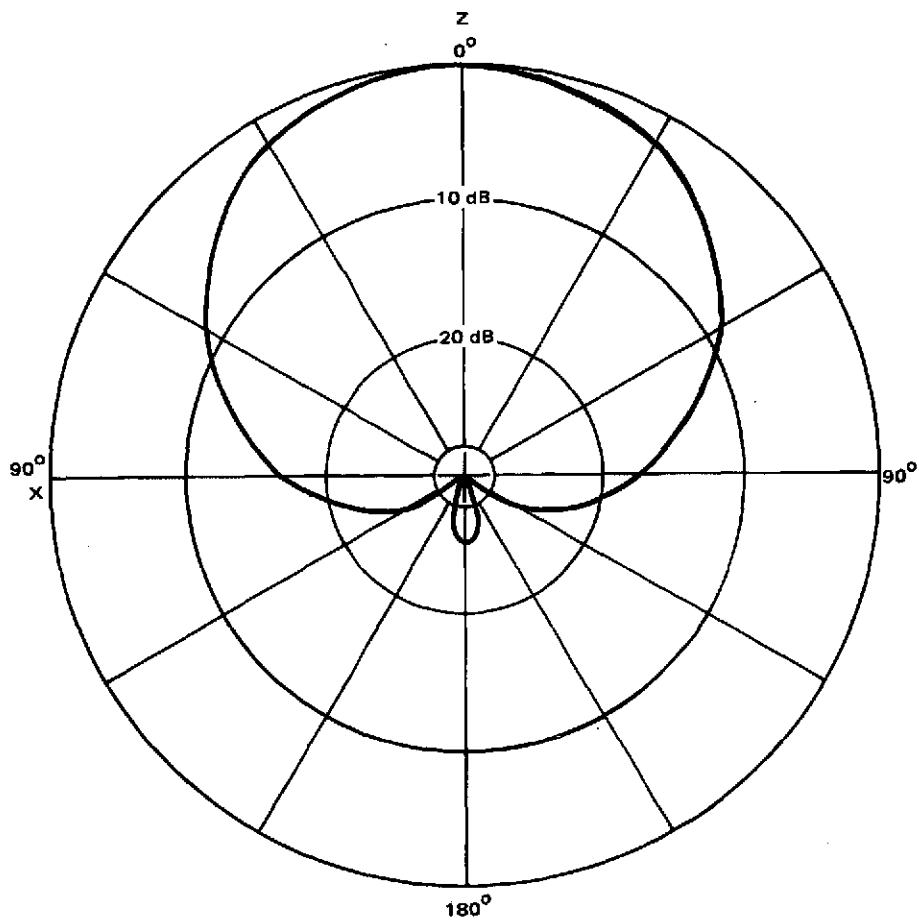
FIGURE 4.30. CIRCULAR DIPOLE ARRAY
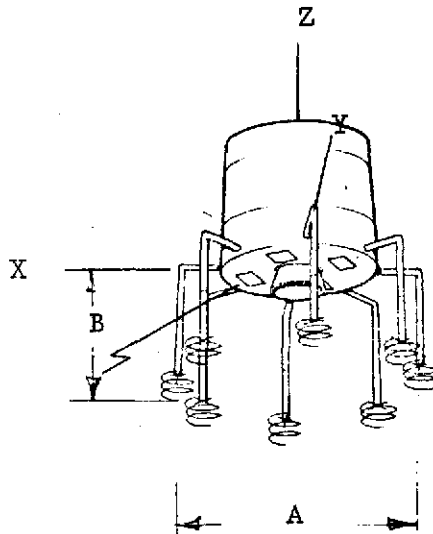
DESCRIPTION: 8 ELEMENT ARRAY CONSISTING OF CIRCULAR POLARIZED
              DIPOLES ELECTRONICALLY DESPUN (TYPICAL)

GAIN: 8 dB
FRONT-BACK RATIO: 10 dB
FRONT-SIDE RATIO (90 DEG FROM PEAK): 30 dB
SPACECRAFT PERTURBATION: MEDIUM
POLARIZATION: CIRCULAR
WEIGHT:* S-BAND   0.83 kg
        UHF   4.5 kg
        VHF   13.6 kg

*for 8-element design.

FREQUENCY BAND	A	B	(Meters)
VHF	2.2	0.91	
UHF	3.1	0.76	
S	0.57	0.14	

*(Array geometry and number of elements used dependent on
  spacecraft diameter and frequency.)

FIGURE 4.31.   CIRCULAR DIPOLE ARRAY

CUT THROUGH SPIN PLANE

HORIZONTAL PLARIZATION
VERTICAL POLARIZATION
−45° POLARIZATION

CUT THROUGH SPIN AXIS

4-56
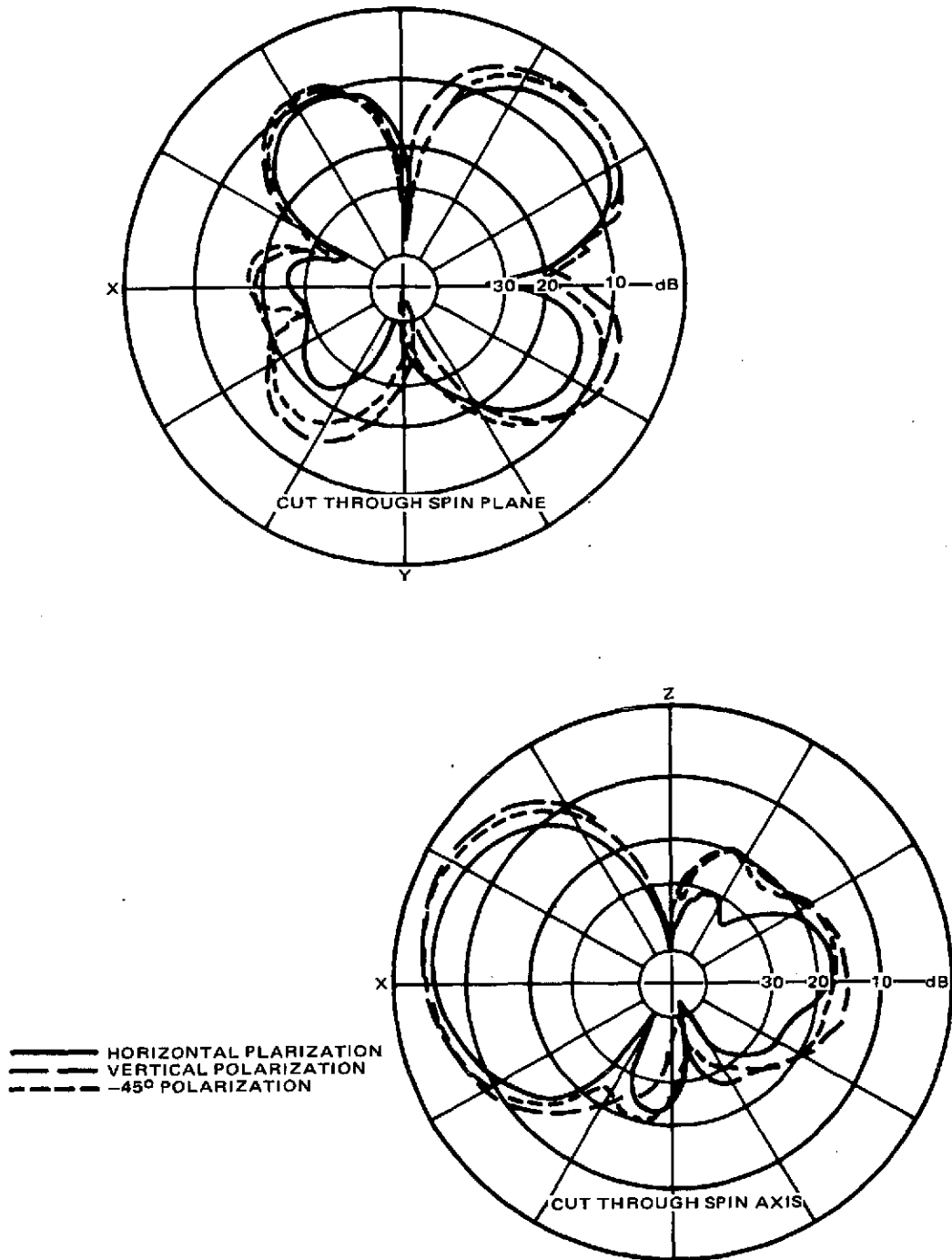
FIGURE 4.32. LINEAR DIPOLE ARRAY
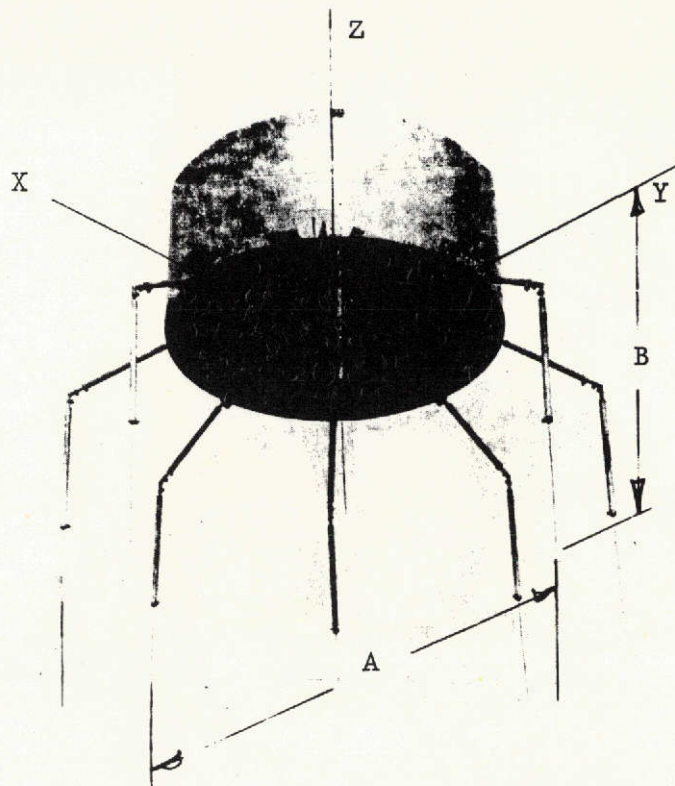
DESCRIPTION: 8 ELEMENT ARRAY CONSISTING OF LINEAR CENTER FED DIPOLES
ELECTRONICALLY DESPUN

GAIN: 8 dB
FRONT-BACK RATIO: 6 dB
FRONT-SIDE RATIO (90 DEG FROM PEAK): 15 dB
SPACECRAFT PERTURBATION: MEDIUM
POLARIZATION: LINEAR
WEIGHT: S-BAND   0.67 kg
         UHF   3.6 kg
         VHF   10.9 kg

for 8-element design

FREQUENCY BAND	A*	B	(Meters)
VHF	2.2	1.6	
UHF	0.76	0.53	
S	0.14	0.10	

*(Diameter variable, no. of elements variable, depend on s/c
 diameter and frequency.)

4-57

FIGURE 4.33. LINEAR DIPOLE ARRAY
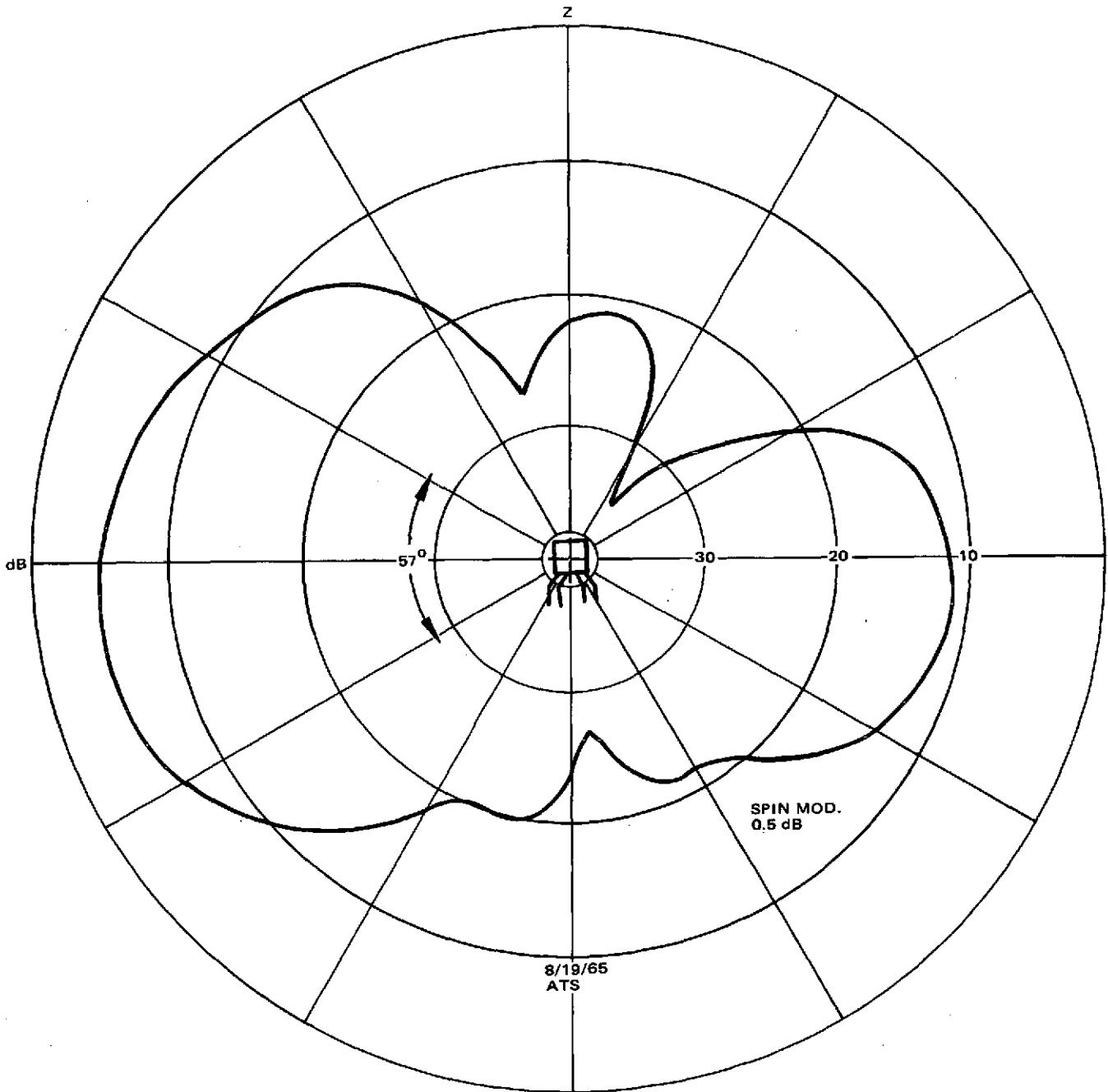
FIGURE 4.34. LINEAR DIPOLE ARRAY

SPIN MOD.
0.5 dB

47°

dB X

30   20   10

8/19/65
ATS

Y
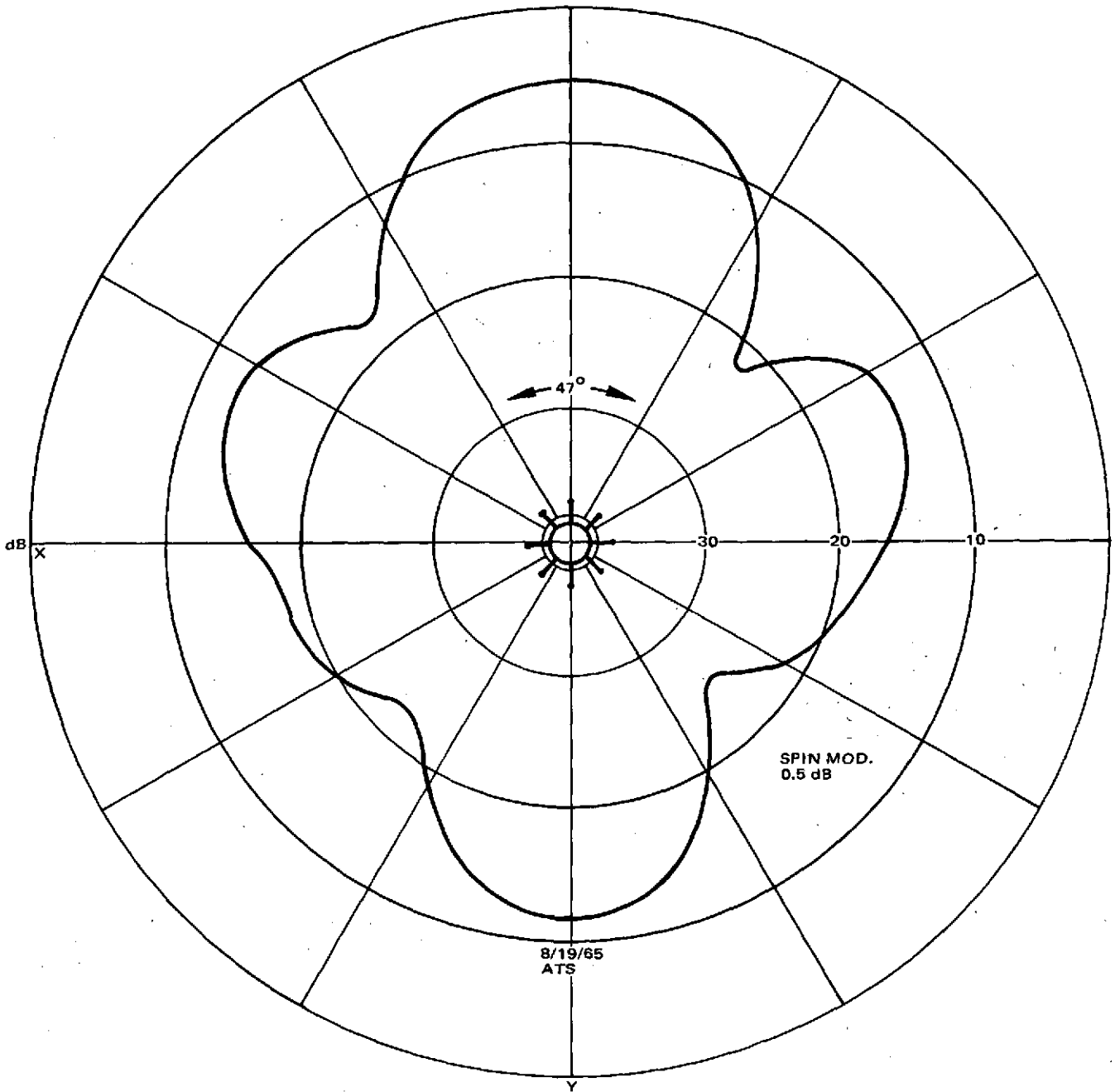
FIGURE 4.35. DIPOLE PLANAR ARRAY
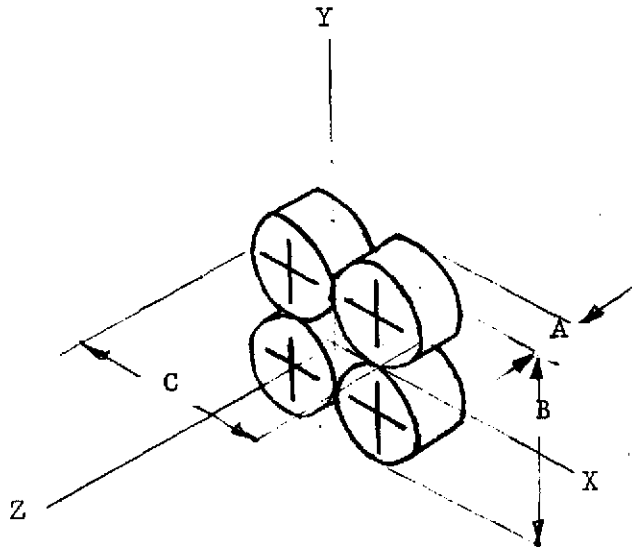
DESCRIPTION: 2 DIMENSIONAL ARRAY OF CUP-CAVITY DIPOLES

GAIN: 8 dB
FRONT-BACK RATIO: 30 dB
FRONT-SIDE RATIO (90 DEG FROM PEAK): 22 dB
SPACECRAFT PERTURBATION: SMALL
POLARIZATION: LINEAR OR CIRCULAR
WEIGHT: S-BAND 1.0 kg
        UHF 5.4 kg
        VHF 16.3 kg

FREQUENCY BAND	A	B	C	(Meters)
S	0.05	0.17	0.17	
UHF	0.27	0.93	0.93	
VHF	0.80	2.70	2.70	

FIGURE 4.36. DIPOLE PLANAR ARRAY
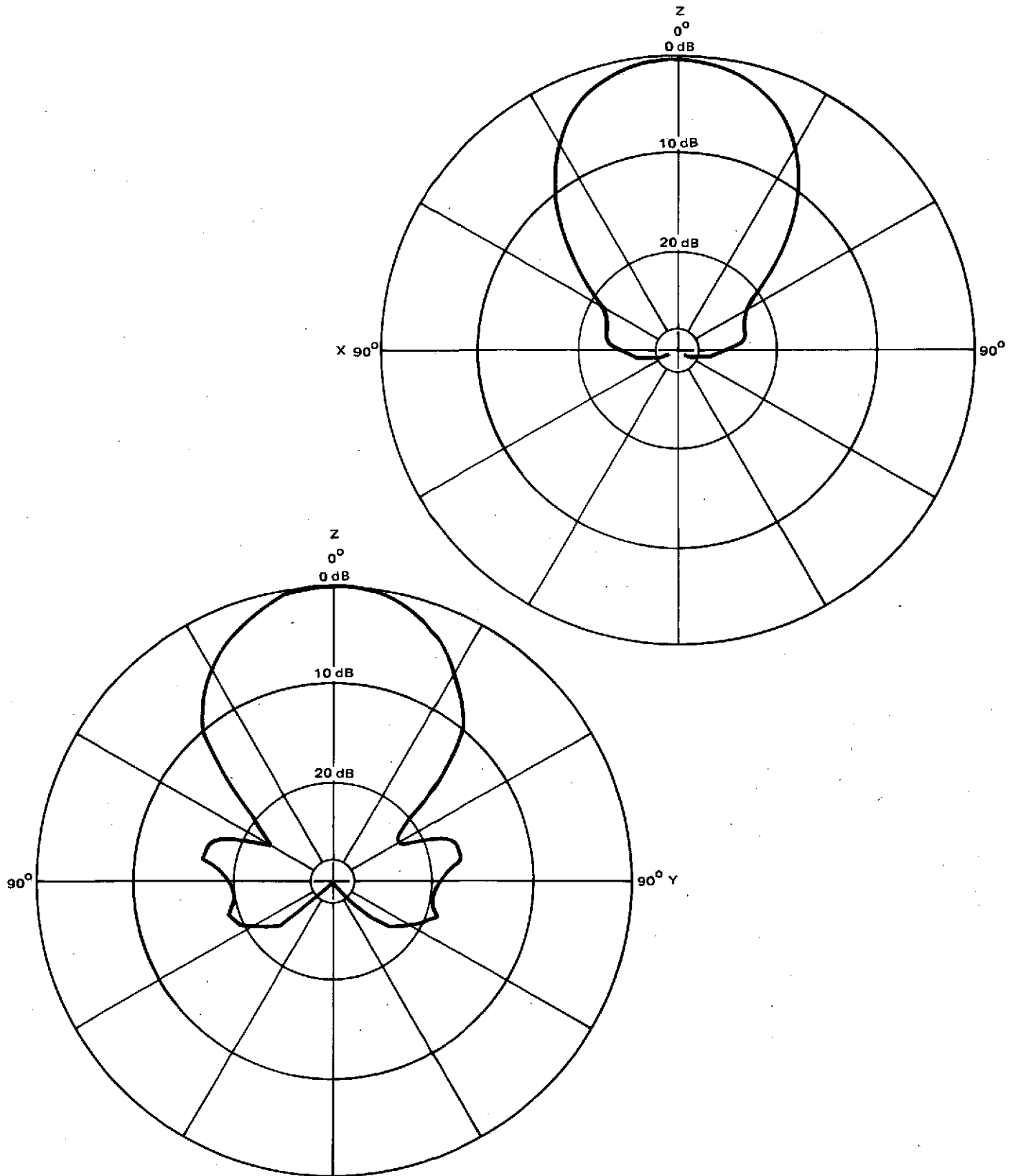
FIGURE 4.37. ; DISC-ON-ROD ENDFIRE
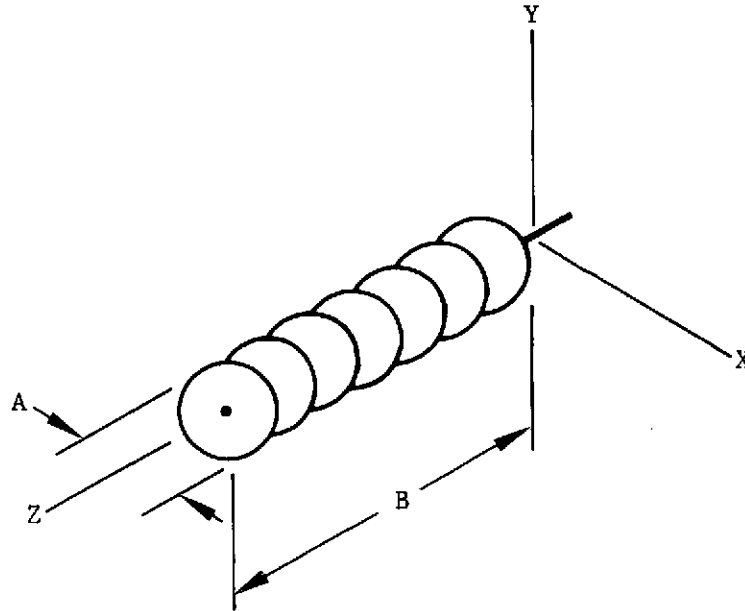
DESCRIPTION: ARTIFICIAL DIELECTRIC CIGAR ANTENNA CREATED BY CIRCULAR
DISC ON A ROD RADIATING ENDFIRE

GAIN: 9 dB
FRONT-BACK RATIO: 30 dB
FRONT-SIDE RATIO (90 DEG FROM PEAK): 30 dB
SPACECRAFT PERTURBATION: SMALL
POLARIZATION: LINEAR OR CIRCULAR
WEIGHT: S-BAND   0.43 kg
        UHF   2.3 kg
        VHF   6.8 kg

FREQUENCY BAND	A	B	(Meters)
S	0.053	0.2	
UHF	0.30	1.1	
VHF	0.88	3.0	

FIGURE 4.38. DISC-ON-ROD ENDFIRE
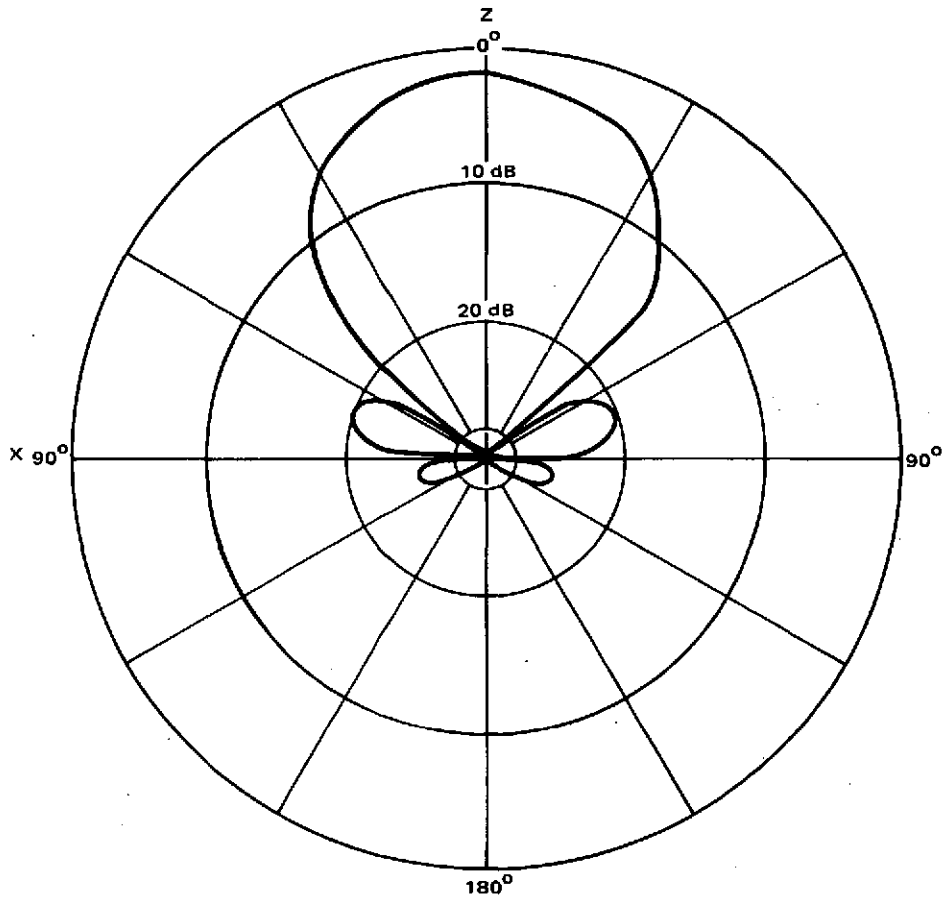
FIGURE 4.39.   PRIME FOCUS REFLECTOR ANTENNA
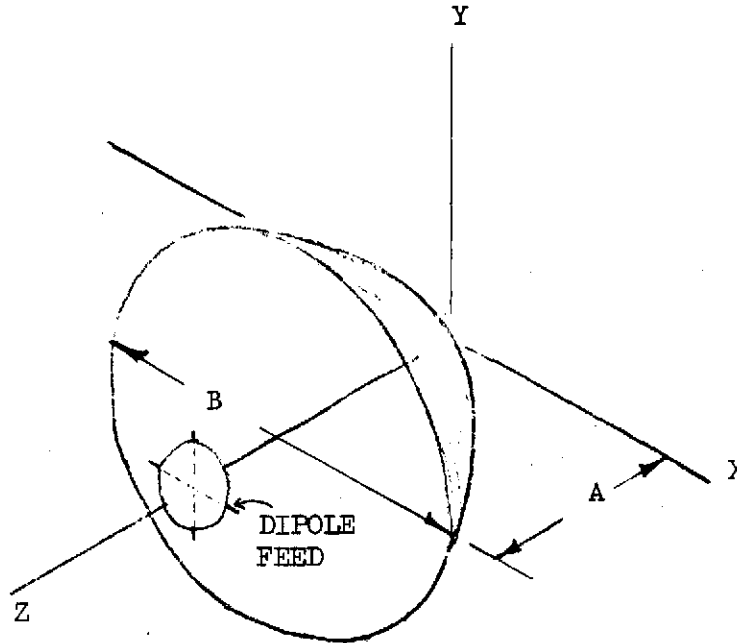
DESCRIPTION: DIPOLE FEEDING A PARABOLIC REFLECTOR

GAIN: 10.5 dB *
FRONT-BACK RATIO: 30 dB
FRONT-SIDE RATIO (90 DEG FROM PEAK):   11 dB
SPACECRAFT PERTURBATION: MEDIUM
POLARIZATION: LINEAR OR CIRCULAR
WEIGHT: S-BAND   1.2 kg
          UHF   6.8 kg
          VHF   20.0 kg

FREQUENCY BAND	A	B	(Meters)
S	0.089	0.23	
UHF	0.50	1.3	
VHF	1.50	3.90	

* Note the small size of the reflector. The gain given can be
  be considerably increased by increasing the dish size.

FIGURE 4.40. PRIME FOCUS REFLECTOR ANTENNA
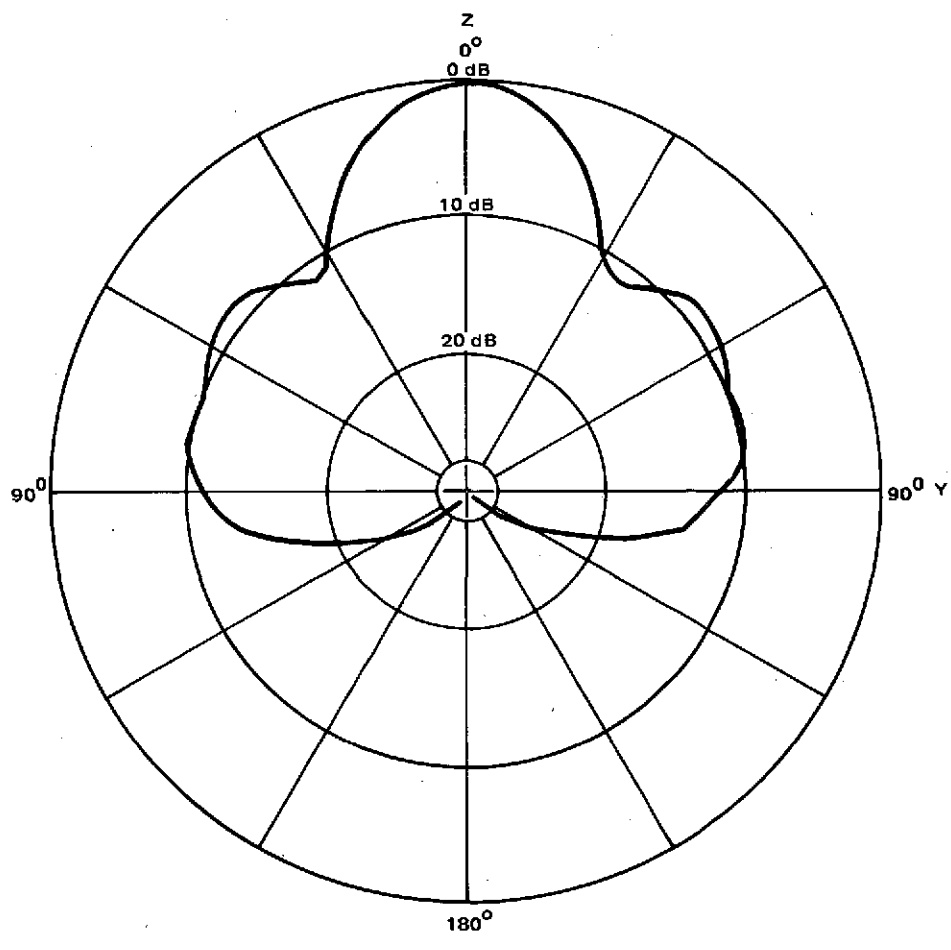
Table 4.10. SUMMARY OF ANTENNA CHARACTERISTICS

	Planar Array	Array of Helical Radiators	Paraboloidal Reflectors & Feeds	Rectangular Horns
Efficiency	70 - 80%	>90% have been achieved	55 - 60%	≈ 48% for horns designed to be the shortest possible for a given gain.
Sidelobes	20-22 db down, gains <25 db;25 db down, gains 25-30 db;25-30· db down, gains 35-50 db	10-15 db down	20-25 db down	8 db down
Bandwidth	12-15%	> 35%	Inherently very broad band; > 35%	> 35%
Power handling capbabilities	Not considered to be a limitation	>100 watts for < 10 GHz	Not considered to be a limitation	Not considered to be a limitation
Polarization	Slotted arrays are linearly polarized. Polarization converter required for circular polarization	Antenna radiates RHC or LHC depending on the screw sense of the windings. It becomes elliptical for angles off axis and approaches linear for angles much greater than the 3 db beamwidth	Reflector itself is insensitive to the polarization characteristics of the feed. Circular polarization is obtained by using a circular polarized feed	Determined by the polarization of the feed.
Effect of monopulse autotracking requirement	Radiating aperture must be able to be divided into four identical subapertures	The number of elements in the array must be an integral multiple of four	A cluster of four feed horns are necessary which requires careful design	A cluster of four horns would be required
Physical dimensions	Polarization converters are attached to the front face of the planar array and will add to the overall thickness	Arrays of end-fire radiators have the advantage of being smaller in cross section.	The depth of the antenna may equal or exceed its aperture dimension	The use of horns are not generally considered above 30 db gains because the horn length increases much more rapidly than the aperture dimensions, usually making poor use of available space

4.5   Antenna Weight Versus Gain Comparison

Several types of spacecraft antennas were examined for the purpose
of determining how their weights vary with gain.   In particular, four types
which were examined include slotted planar arrays, arrays of helices,
paraboloidal reflectors and feeds, and rectangular horns.   Table 4.10 pro-
vides a summary of the principal characteristics of each of these antennas.[26]

The relationships between the dimensions of the antennas and their
gains are shown in Figure 4.41 for an operating frequency of 2.25 GHz.   In
order to proceed to an estimation of the relationship between antenna weight
and gain, assumptions were made as to the materials best suited for their
fabrication.   For example, for an array of helices, lightweight, high-strength
materials such as beryllium and magnesium, and dielectric materials such as
fiberglass and teflon are used.   The weights of very large arrays are only
rough estimates and specific designs for these antenns in a space environment
have not been made.
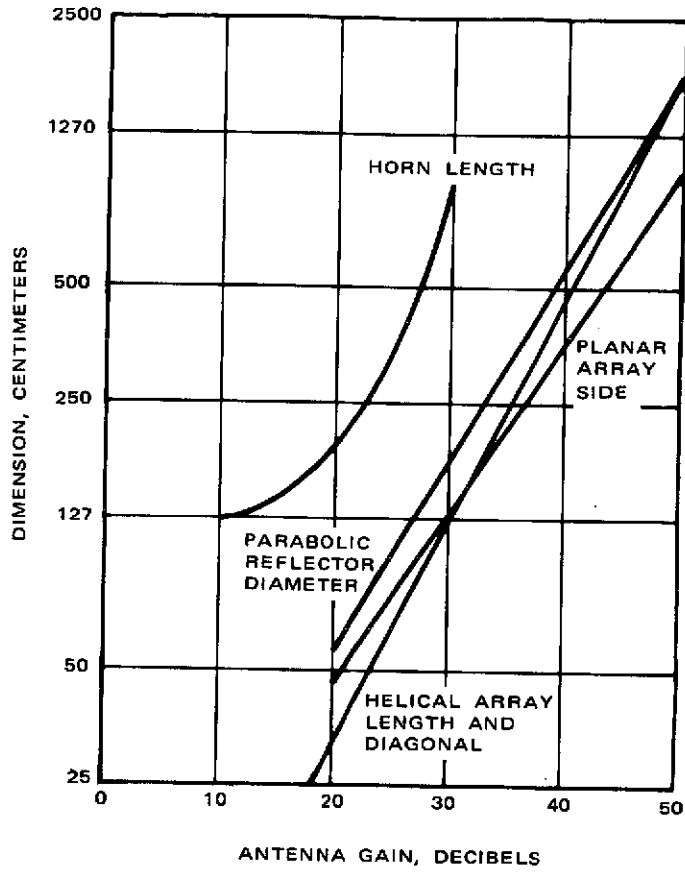
Figure 4.41. Comparison of Antenna Sizes

Figure 4.42 shows the results of the weight vs. gain comparison. In addition to the four antennas mentioned above, the data collected for two specific Hughes biconical horns are also plotted in the figure. It should be pointed out that there are several inherent limitations in the practicability of this kind of weight versus gain comparison. The data plotted are only for the antenna elements themselves and exclude such items as diplexers, antenna control electronics, gimbals, supporting structures, rotary joints, etc. This exclusion compensates in part for the fact that on a weight basis, directional antenna systems for spin-stabilized satellites suffer unfairly because of the requirement for despinning in comparison with antennas for 3-axis stabilized satellites. Alternatively, one could postulate a correction factor to even out this comparison. However, a single correction factor for spinners does not appear to be feasible.

It is further noted that in general electronically scanned antennas are desirable where mechanical motion of the antennas cannot be tolerated or the rapidity of the required beam steering exceeds the capabilities of mechanical mechanisms. For the user spacecraft and the TDRSS geometry under consideration, neither of the requirements for mechanical motion or rapidity of beam steering apply. Thus, based on this consideration alone, only mechanically steered or switched, or fixed antennas should be considered for application by the users.

It is for the above mentioned reasons that the weight versus gain comparison given here should be used only as a rough guide to give insight into the choice of user antenna selection, and not for the selection itself based on minimum weight.
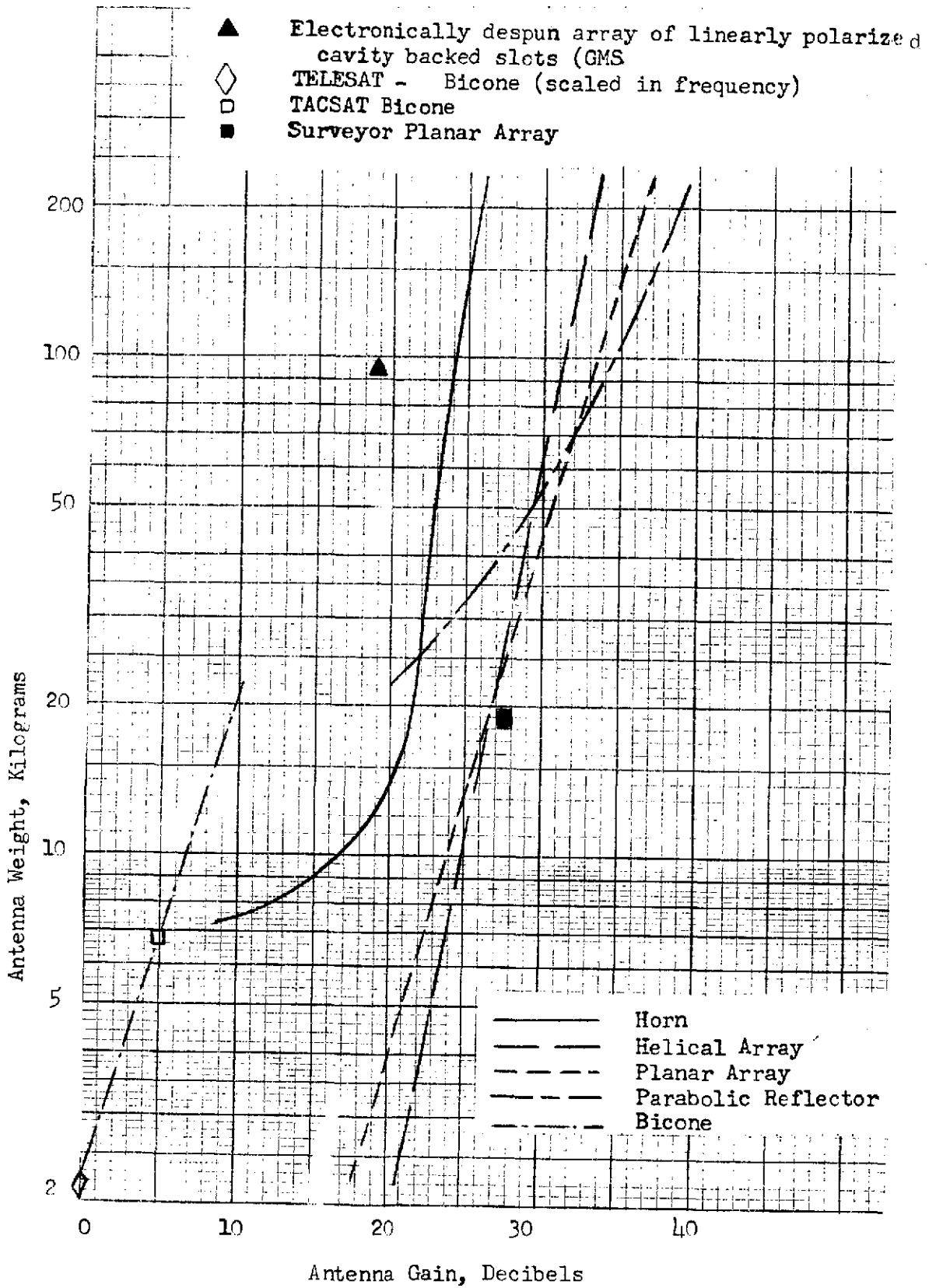
Figure 4.42. TDRS User Antenna Weight Comparison

5. SYSTEM CONSIDERATIONS

5.1 Telecommunication Link Budgets

This section presents an examination of the most recent TDRS system characteristics and performance parameters. The calculations of some parameters will be explained in detail and the sources of each of the assumptions will be clarified.

5.1.1 Free-Space Loss

The free-space loss is given by:

$$A_o \text{ (dB)} = 32.4 + 20 \log f \text{ (MHz)} + 20 \log d \text{ (km)}$$

Since the link frequencies are nominally 2.2 GHz, and using the maximum distance of 44,000 km from the user to the TDRS, the free-space loss is:

$$A_o = 192 \text{ dB}$$

5.1.2 User Transmitter Power and Antenna Gain

The values for user antenna gain and transmitter power will be left variable to be determined by the user mission, the needed data rate being the primary influencing factor. Two values of transmitter power will subsequently be assumed for purposes of illustrating antenna gain versus data rate: 1 watt and 5 watts delivered to the antenna terminals. Although the Statement of Work for the study specified a user transmitter power of 1 watt, it is not unreasonable to assume that some users can deliver 5 watts of RF power to the antenna terminals.

5.1.3 TDRS Antenna Gain and User Receiving System Noise Temperature

The TDRS S-band antenna gain over field of view of 26° is taken as 28 dB. This value was specified at a meeting with the User Impact Study Project Office. [3] The meeting also resulted in specification of the user receiving system noise temperature of 1500 K.

5.1.4 TDRS Receiving System Noise Temperature

A value of 540 K receiving system noise temperature for the TDRS has been assumed. This value is believed to be in consonance modern S-band receiver front-end technology using bipolar transistors. The resultant receiving noise power density at the TDRS is -201.3 dBw/Hz-K.

5.1.5 Bit Energy to Noise Density Ratio

For the forward link, with a probability of bit error of 10^{-5} and phase shift keying, a theoretical bit energy to noise density ratio of 9.6 dB is required. On the return link, convolutional encoding with an optimal decoder using soft decision (K=7, rate $\frac{1}{2}$) is assumed. The coding gain thus achievable is 5.5 dB. This results in a required bit energy to noise density ratio of 4.1 dB. [27]

5.1.6 Miscellaneous Losses

An overall miscellaneous loss of 3 dB is assumed to account for polarization mismatch, transponder loss, demodulation loss, and pseudo-noise (PN) loss.

5.1.7 System Margin

A margin of 3 dB over the threshold of bit energy to noise density ratio required to give a probability of bit error of 10^{-5} is considered necessary to assure confidence that the ultimate system performance is at least the specified value or better.

5.1.8 Link Budget Tables

Table 5.1 represents a summary of the forward link calculations taking into account the assumptions made above. The resulting forward link rate is given in terms of the user satellite antenna gain. A similar set of calculations is summarized for the return link in Table 5.2 in which the return link rate is given in terms of the available user satellite EIRP.

These link budget calculations were performed in the absence of RFI.

Table 5.1. S-Band/TDRSS Forward Link

TDRSS EIRP (FOV edge)	25 dBW
Space loss	-192
Misc. losses*	-3
Ant. gain G	G
Rec. carrier power, P_t	G-170 dBW

Rec. noise dens. (T=1500K)η -197 dBW/Hz

$$\frac{P_t}{\eta} \quad = \quad G + 27 \text{ dB/Hz}$$

$E/\eta = 9.6$ dB for 10^{-5} w/o coding

Margin** $= 3.0$ dB

$\underline{\text{Data rate} = R}$

$(P/\eta)_{req'd} = R + 12.6 \approx R + 13 \text{ dB/Hz}$

$$\boxed{R = G + 14 \text{ dB} \cdot \text{Hz}}$$

*   assumes circular polarization

**   includes multipath and cross-correlation

Table 5.2. S-Band/TDRSS Return Link

User power P_u ⎫
⎬   EIRP dBW
User gain G_u ⎭

Space loss -192

Misc. losses[*] -3

Ant. gain ($26°$ FOV) $\underline{+28}$

Rec. carrier power,   =   EIRP-167 dBW
  P'_u

Rec. noise density (T = 540 K) η = -201 dBW/Hz

   P'_u/η =   EIRP $+ 34$

   E_b/η = 4.1 dB; BER = 10^{-5} with coding

   Margin[**]   = 3.0 dB

   <u>Data Rate = R</u>

   $(P'/\eta)_{req'd}$ $\approx$ $R + 7.1$ $\approx$ $R + 7$ dB/Hz

R = EIRP $+ 27$ dB·Hz

*   assumes circular polarization

**   includes multipath and cross-correlation effects

Figure 5.1   INFLUENCE OF USER ANTENNA GAIN ON LDR

LINK RATE

USER ANTENNA GAIN — DECIBELS
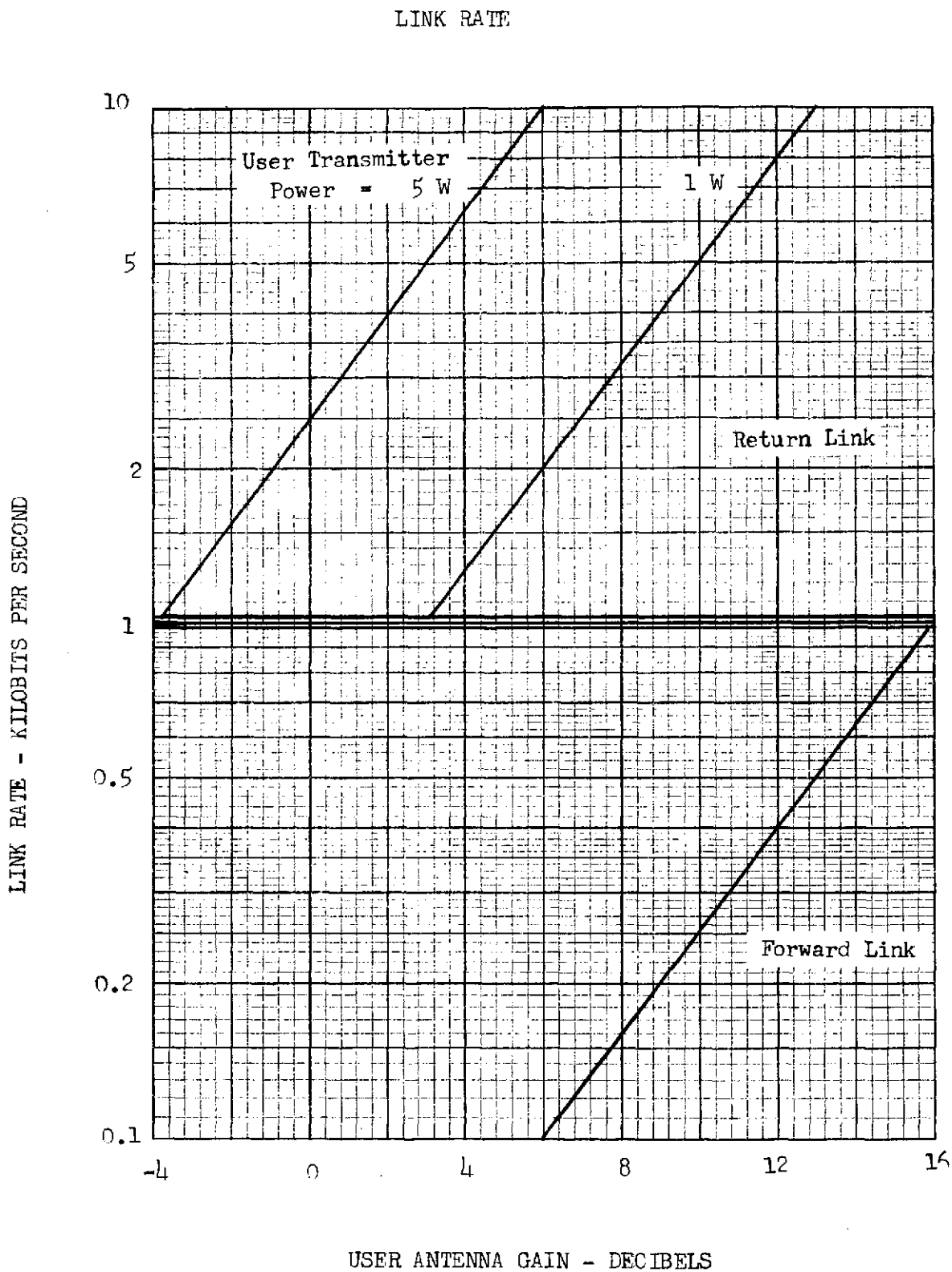
5.2 Data Rate Tradeoffs

For the forward link, the Statement of Work for the study requires a minimum command rate of 100 bits per second (20 dB-Hz) and a maximum rate of 1024 bps (30.1 dB-Hz). From Section 5.1, the forward link rate is given by

$$R = G_u + 14 \quad \text{dB-Hz}$$

where G_u is the antenna gain on the user satellite. Thus,

$$G_u = R - 14 = 30.1 - 14 = 16.1 \text{ dB maximum, and}$$
$$= 20 \quad - 14 = -6 \text{ dB minimum.}$$

The bottom half of Figure 5.1 shows the relationship between the forward link rate and user antenna gain. It is seen , for example, that a 500 bps command rate can be achieved with a user antenna gain of 13 dB.

For the return link, the Statement of Work requires a minimum telemetry rate of 1 kbps and a maximum of 10 kbps. Again, from Section 5.1, the return link rate is given by

$$R = EIRP + 27 \quad \text{dB-Hz}$$

where EIRP is the user equivalent isotropically radiated power. Thus,

$$EIRP = R - 27 = 40 - 27 = 13 \text{ dBW maximum, and}$$
$$= 30 - 27 = 3 \text{ dBW minimum.}$$

For the two different levels of user RF power, 1 watt and 5 watts, the top half of Figure 5.1 shows the influence of user antenna gain on the return link bit rate. A modest 5 dB user antenna gain is seen to produce either a 1.6 kilobit or an 8 kilobits per second return link rate, depending on the user's RF power level.

A number of conclusions can be drawn from the data rate tradeoffs shown in Figure 5.1. First, the return link appears to be adequately sized to bracket the user data rates specified in the study Statement of Work. Needless to say, the 7 dB difference between the 5 watt and 1 watt user critically affects the type of antenna required aboard the user satellite. The significance of this dB-for-dB coupling between antenna gain and transmitter power can be illustrated by taking a 2.5 kbps return link rate as an example. The curves show that the 5 watt user requires only a 0 dB antenna gain, whereas the 1 watt user needs 7 dB. Along with the 0 dB antenna gain comes the inherent quality of omni-directionality, whereas the 7 dB gain antenna requires either orientation, or switching between multiple 7 dB gain antennas, or accepting reduced user orbital coverage by the TDRS if only a single fixed 7 dB antenna gain can be afforded. Thus, wherever possible, to avoid the requirement of oriented or steered antennas, the user should provide about 5 watts of RF power into a low gain antenna.

Given the parameters previously assumed, the forward link is not as well matched to the required data rates as the return link. For the ranges of bit rates required by the Statement of Work, that is 100 bps to 1024 bps, user antenna gains in the range of 6 to 16 dB are required. In order to reduce these gains to more modest levels, it is recommended that either the user's receiving system noise temperature be reduced or the TDRS transmit power be increased, or some combination of both. With respect to the former, the current Hughes TDRS baseline makes use of bipolar silicon transistors which provide an overall noise temperature of 540 K, a reduction of 4.5 dB below the assumed 1500 K user noise temperature. It is hoped that such a reduction in noise temperature can also be achieved by the users.

6. REFERENCES

1. *Tracking and Data Relay Satellite System Configuration and Tradeoff Study - Part II*, Final Report, Hughes Aircraft Company SCG 30096R, April 1973.

2. National Aeronautics and Space Administration, Request for Proposal 5-93920-334, Statement of Work, Tracking and Data Relay Satellite System User Impact and Network Compatibility Study, 14 March 1972.

3. K. Stern, "TDRSS User Impact Study Meeting Notes, April 12, 1973", HS337/0102-10A, Letter to Mr. Frank Shelton, GSFC, dated 18 April 1973.

4. D. D. Williams, "Dynamic Analysis and Design of the Synchronous Communication Satellite", Hughes Aircraft Company, Report TM-649, May 1960.

5. J. Jenny and P. Shaft, *The Effects of Multipath and RFI on the TDRSS Command and Telemetry Links - A Final Report*, Electromagnetic Systems Laboratories for NASA/GSFC, Contract NAS5-20228, March 1972.

6. S. Nichols, *Satellite Turnstile Antennas*, U. S. Naval Research Laboratories Report 6907, August 6, 1969, AD 694003.

7. J. B. Keller, "The Geometrical Theory of Diffraction", *1953 Proc. Symp. on Microwave Optics*, Eaton Electronics Research Lab., McGill Univ., Montreal, Canada.

8. R. W. P. King, and T. T. Wa, *The Scattering and Diffraction of Waves*, Cambridge, Mass., Harvard University Press, 1959, p. 4.

9. A. R. Lopez, "The Geometrical Theory of Diffraction Applied to Antenna Pattern and Impedance Calculations", *IEEE Trans. on Antennas and Propagation*, Vol. AP-14, No. 1, January 1966, pp. 40-45.

10. J. H. Richmond, "A Wire-Grid Model for Scattering by Conducting Bodies", *IEEE Trans. on Antennas and Propagation*, Vol. AP-14, 1966, pp. 782-786.

11. N. C. Albertsen, J. E. Hansen, and N. E. Jensen, "Numerical Prediction of Radiation Patterns for Antennas Mounted on Spacecrafts", *IEEE Conference on Aerospace Antennas*, June 8-10, 1971, pp. 219-228.

12. J. Goldhirsh, et al, "Radiation from a Short Dipole Mounted on a Monopole Near a Thick Conducting Cylinder of Resonant Length", *IEEE Trans. on Antennas and Propagation*, Vol. AP-19, March 1971, pp. 219-228.

13. J. Goldhirsh, et al, "Radiation from a Dipole Near a Conducting Cylinder of Finite Length", *IEEE Trans. on EMC*, EMC-R, No. 3, August 1970, pp. 96-105.

14. W. Korvin and R. B. Jackson, "Antennas for Space Vehicles," *Space/ Aeronautics*, November, 1964, pp. 60-67.

15. Proposal for Advanced Study of an Applications Technology Satellite (ATS-4) Mission, Appendix A - Antenna Weight-Spacecraft Weight Ratio Optimization, Hughes Aircraft Company SSD 50033P, November 1965.

16. Project SYNCOM, Syncom I System Summary, Hughes Aircraft Company, SSD 3337R, June 1963.

17. A. F. Seaton, and G. A. Carnegis, "A Novel Circularly Polarized Planar Array for Surveyor", *AIEE Convention Record*, No. 1, 1963, pp. 1-9.

18. Orbiting Solar Observatory, OSO-I Pre-Proto Design Review, Hughes Aircraft Company, SCG 36003V, Contract NAS 5-11400, January 1973.

19. R. D. Brandes, "The Tactical Communications Satellite", *IEEE Trans. on Aerospace and Electronic Systems*, Vol. AES-6, No. 4, July 1970, pp. 432-441.

20. D. C. Patel, "Directivity of Short Backfire Antenne", *Proc. IEEE*, Vol. 118, No. 11, November 1971, pp. 1550-1552.

21. C. C. Kilgus, "Resonant Quadrifilar Helix Design", *Microwave Journal*, December 1970, pp. 49-54.

22. C. C. Kilgus, "Multielement, Fractional Turn Helices", *IEEE Trans. on Antennas and Propagation*, July 1968, pp. 499-500.

23. H. Jasik, *Antenna Engineering Handbook*, New York, McGraw-Hill, 1961, p. 7-2.

24. *Proposal for Geostationary Meterological Satellite*, Hughes Aircraft Company, Executive Summary, SCG 30036P, February 1973.

25. J. D. Dyson, "The Characteristics and Design of the Conical Log-Spiral Antenna", *IEEE Trans. on Antennas and Propagation*, July 1965, pp. 488-499.

26. *Study of Low Altitude Satellite Utilizing a Data Relay Satellite System*, Phase I Final Report, Hughes Aircraft Company, SSD 90008R, Section 5, Contract NAS 5-11602, 21 January 1969.

27. *Tracking and Data Relay Satellite System Configuration and Tradeoff Study - Part I Final Report*, Hughes Aircraft Company, Volume 4, 29 September 1972, p. 3-48.

APPENDIX A

Preliminary 1978, 1979 and 1980 NASA Mission Models

NOTES ON PRELIMINARY
1978, 1979 and 1980 MISSION MODELS

I. IN ITEM A, B AND C A SPECIFIC MISSION IS DEFINED, IN ITEM D A CLASS OF MISSIONS IS DEFINED

II. MINIMUM CONTACT HOURS COLUMN GIVES THE MINIMUM, REQUIRED, CONTACT HRS PER QUARTER ASSUMING NO TDRSS

III. RF FREQUENCIES COLUMNS GIVE THE NUMBER OF LINKS IN EACH FREQUENCY BAND (TLM) AND THE REQUIRED CONTACT HOURS IN THAT BAND. AN (X) IN THE COMMAND COLUMNS INDICATES THE COMMAND FREQUENCY (VHF - 148 MHz OR S-BAND - 2100 MHz)

IV. TRACKING SYSTEM - INDICATES REQUIRED TRACKING SYSTEM
      SRARR = S-BAND RANGE AND RANGE RATE
      VRARR = VHF (148/136) RANGE AND RANGE RATE
      MT = MINITRACK

V. MISSION PLANNING STATUS
      A - APPROVED MISSION - DATA RELATIVELY FIRM
      U - UNAPPROVED MISSION - DATA NOT FIRM - PLANNING DATA
      E - EXTRAPOLATED MISSION - ALL DATE EXTRAPOLATED
      IF BOTH U AND E BOXES ARE CHECKED THEN SOME PARAMETERS ARE EXTRAPOLATED

VI. BIT RATES COLUMNS - DATA RATES GIVEN IN kbs UNLESS AN L, M, OR H IS ENTERED
      L - <10 kbs
      M ->10 to 1000 kbs
      H - >1000 kbs

VII. STAB. SYSTEM
      O → AN ORIENTED SPACECRAFT (3 AXIS, GRAV. GRAD., ORIENTED PLATFORM)
      S → SPINNING SPACECRAFT
      FULL X IMPLIES A HIGH PROBABILITY
        \ IMPLIES A POSSIBILITY

VIII. TRANSMIT ERP IN dbw
      FULL X INDICATES PROBABLE
        \ INDICATES POSSIBLE

A-4

1978 PLANNING MISSION MODEL, 8/72 UPDATE

SPACECRAFT NAME OR CLASS	MIN. CONTACT HRS PER QUARTER	RF FREQUENCIES MHz — TELEMETRY 136	250	400	1700	>2200	CMD	TRACKING SYSTEM SRARR V	SRARR S	VRARR	MT	MISSION PLANNING STATUS A	U	E	ORBIT APOGEE x PERIGEE @ INC (KM) x (KM) @ DEG	BIT RATES (kbs) TLM RT	TLM PB	CMD	STAB. SYSTEM O	S	TRANSMIT ERP (DBW) <4	4-10	>10	SUPPORT SYSTEM TDRSS	T+G	G ONLY
A. EARTH ORBITS																										
1. OSO-5	230	1/230	--	--	--	1/105	X	--	--	--	X	--	X	--	550 x 550 @ 33°	6.4	128	<1	X	--	X	\	--	X	--	--
2. HEAO-B	170	--	--	--	--	2/170	--	X	X	--	--	X	--	--	460 x 460 @ 28°	26	512	1	X	X	--	\	--	X	--	--
3. OSO-K	230	1/230	--	--	--	1/105	X	--	--	X	--	--	X	--	550 x 550 @ 33°	6.4	128	<1	X	--	X	\	--	X	--	--
4. IMP-J	2100	2/2100	--	--	--	--	X	--	--	X	--	X	--	--	250K x 200K @ 28°	3.2	1.6	<1	--	X	--	X	--	--	--	X
5. ERTS-C	425	-- BU	--	--	--	3/425	--	X	X	--	--	--	X	--	925 x 925 @ 99°	1/24	3.5K/150K	1	X	--	--	--	X	X	X	--
6. BIOS-D	140	1/140	--	--	--	--	X	--	--	X	--	X	--	--	370 x 370 @ 33°	--	22	<1	\	--	\	--	--	X	--	--
7. EOS-A	425	--	--	--	--	3/425	--	X	X	--	--	--	X	--	980 x 980 @ 99°	12/1200	30K	1	X	--	--	--	X	--	X	X
8. IMP-K (NEMD)	2100	--	--	--	--	2/2100	--	X	X	--	--	--	X	--	153K x 1240 @ 30°	32 θ_{max}	--	<1	--	X	\	X	--	--	X	--
9. IMP-K' (NEMD)	2100	--	--	--	--	2/2100	--	X	X	--	--	--	X	--	153K x 240 @ 30°	32 θ_{max}	--	<1	--	X	\	X	--	--	X	--
10. SSS-C	400	1/400	--	--	--	--	X	--	--	X	--	X	--	--	25.5K x 230 @ 30°	.4	1.4	<1	--	X	\	--	--	--	X	X
11. RAE-D	1700	2/1700	--	--	1/500	--	X	--	--	X	--	X	X	--	15K x 15K @ 29°	--	10/50	<1	\	--	\	\	--	--	--	X
12. RAE-D'	1700	2/1700	--	--	1/500	--	X	--	--	X	--	X	X	--	15K x 15K @ 29°	--	10/50	<1	\	--	\	\	--	--	--	X
13. TIROS-N	200	BU	--	--	1/200	--	--	X	X	--	--	--	X	--	1680 x 1680 @ 103°	2.4	1.5K	1	X	--	X	\	--	X	--	--
14. EPS-B	370	1/370	--	--	--	--	X	--	--	X	--	X	X	--	900 x 900 @ 90°	1	L	<1	--	X	\	--	--	X	--	--
15. NIMBUS-G	370	1/230	--	--	1/230	2/370	X	X	X	X	--	--	X	--	1020 x 1020 @ 100°	4	128	1	X	--	X	\	--	X	--	--
16. SATS-C	400	1/400	--	--	--	1/400	X	--	X	X	--	--	X	--	930 x 930 @ 50°	1/20	40	1	X	--	X	\	--	X	--	--
17. SATS-E	250	1/250	--	--	--	1/250	X	--	--	X	--	--	--	--	500 x 500 @ 99°	L	LM	<1	--	\	X	\	--	X	--	--
18. SHUTTLE	A	--	B	--	--	2/A	--	X	X	--	--	--	X	X	VARIABLE-C	L	H	2	X	--	--	\	--	--	X	--

*A = APPROVED
U = UNAPPROVED
E = EXTRAPOLATED

#L = 10 kbs
M = 10-1000 kbs, H>1000 kbs

** O = ORIENTED PLATFORM θ = MAXIMUM RATE OF FOUR X2 STEPS
S = SPIN

Sheet 1 of 2

1978 PLANNING MISSION MODEL, 8/72 UPDATE

SPACECRAFT NAME OR CLASS	MIN. CONTACT HRS PER QUARTER	RF FREQUENCIES MHz — TELEMETRY 136	250	400	1700	>2200	CMD V	CMD S	TRACKING SYSTEM SRARR	VRARR	MT	MISSION PLANNING *STATUS A	U	E	ORBIT APOGEE x PERIGEE @ INC (KM) x (KM) @ DEG	BIT RATES TLM (kbs) RT	PB	CMD	STAB. SYS ** O	S	TRANSMIT ERP (DBW) 4	4-10	>10	SUPPORT SYSTEM TDRSS	T+G	G ONLY
B. SYNCHRONOUS																										
1. GOES(A)	25	1/25	--	1/0	1/0	1/0	--	--	--	--	--	X	--	--	SYNC	--	--	<1	--	\	\	--	--	--	--	X
2. ATS G	2160	2/2160		ATS	UNIQUE		X	--	--	--	--	X	--	--	SYNC	2	--	<1	X	--	--	X	--	--	--	X
3. SAS D	1680	--	--	--	--	1/1680	--	X	X	--	--	--	X	--	SYNC	41	--	1	X	--	\	X	--	--	--	X
4. ATS-H	1800	1/1800		ATS	UNIQUE		X	--	--	--	--	--	--	X	SYNC	--	--	<1	\	--	--	--	--	--	--	X
5. SATS D	1680	--	--	--	--	1/1680	--	X	X	--	--	--	X	X	SYNC	1/20	40	1	--	X	X	--	--	--	--	X
6. SAS-E	1680	--	--	--	--	1/1680	--	X	X	--	--	--	--	X	SYNC	41	--	1	X	--	\	X	--	--	--	X
C. LUNAR – DEEP SPACE																										
1. IMP-L(NII)	2160	--	--	--	--	2/2160	--	X	X	--	--	--	X	--	L_{1E} (b) ORBIT	4.1 max (Θ)	--	1	--	\	X	\	--	--	--	X
D. EXTRAPOLATED MISSION CLASSES																										
1. SATS F	400	--	--	--	--	1/400	--	X	X	--	--	--	--	X	350 x 350 @ 99°	L	LM	1	--	\	X	\	--	X	--	--
2. GEOS 76	500	--	--	--	--	1/500	--	X	X	--	--	--	--	X	900 x 900 @ 45°	L	M	1	\	--	X	\	--	X	--	--
3. LST A	200	--	--	--	--	2/200	--	X	X	--	--	--	--	X	450 x 450 @ 30°	L	MH	1	X	--		X	--	X	--	--
4. EPS C	400	1/400	--	--	--	1/400	--	X	X	--	--	--	--	X	900 x 900 @ 80°	L	M	<1	--	\	X	\	--	X	--	--
5. EPS D	400	--	--	--	--	1/400	--	X	X	--	--	--	--	X	600 x 600 @ 90°	L	M	<1	--	\	X	\	--	X	--	--

*A = APPROVED
B = UNAPPROVED
E = EXTRAPOLATED

#L = <10 kbs
M = 10-1000 kbs, H >1000 kbs

**O = ORIENTED PLATFORM
S = SPIN

Θ = MAXIMUM RATE OF FOUR X2 STEPS
(b) = EARTH INNER LIBRATION POINT ORBIT

1979 PLANNING MISSION MODEL, 8/72 UPDATE

SPACECRAFT NAME OR CLASS	MIN. CONTACT HRS PER QUARTER	RF FREQUENCIES MHz TELEMETRY 136	250	400	1700	>2200	CMD V	CMD S	TRACKING STATION SRARR	VRARR	MT	MISSION PLANNING STATUS A	U	E	ORBIT APOGEE x PERIGEE @ INC (KM) x (KM) @ DEG	BIT RATES TLM # (kb) RT	TLM PB	CMD	STAB SYSTEM O	S	TRANSMIT ERP (DBW) <4	4-10	>10	SUPPORT SYSTEM TDRSS	T&C	O ONLY
A. EARTH ORBITS																										
1. OSO-K																										
2. RAE-D																										
3. RAE-D'																										
4. SATS-E																										
5. IMP-K																										
6. IMP-K'																										
7. HEAO-D																										
8. EOS-A																										
9. SATS-C																										
10. EOS-B'	425	-	-	-	-	3/425	-	X	X	-	-		X	-	980 x 980 @ 99°	12/1200	30K	1	X	-	-	-	X	X	-	-
11. BIO-E	140	1/140	-	-	-	-	X	-	-	X	-		X	X	370 x 370 @ 33°	-	22	1	\	-	\	-	-	X	-	-
12. SHUTTLE																										
13. NIMBUS-G																										
14. SATS-F	250	-	-	-	-	1/250	-	X	X	-	-		X	-	350 x 300 @ 99°	1/20	40	1	-	\	\	-	-	X	-	-
15. SATS-G	250	-	-	-	-	1/200	-	X	X	-	-		X	-	650 x 560 @ 99°	1/20	40	1	-	\	\	-	-	X	-	-
16. HEAO-C	225	-	-	-	-	2/225	-	X	X	-	-		X	-	460 x 460 @ 28°	2G	512	1	X	X	-	\	-	X	-	-

*A = APPROVED
B = UNAPPROVED
E = EXTRAPOLATED

# L = <10 kbs
M = 10-1000 kbs, H >1000 kbs

* O = ORIENTED PLATFORM
S = SPIN

1979 PLANNING MISSION MODEL, 8/72 UPDATE

A-7

SPACECRAFT NAME OR CLASS	MIN. CONTACT HRS PER QUARTER	RF FREQUENCIES MHz — TELEMETRY 136	250	400	1700	>2200	CMD V	S	TRACKING SYSTEM SRARR	VRARR	MT	MISSION PLANNING STATUS A	U	E	ORBIT APOGEE x PERIGEE @ INC (KM) x (KM) @ DEG	BIT RATES TLM (kbs) RT	PB	CMD	STAB. SYSTEM O	S	TRANSMIT ERP (DBW) <4	4-10	>10	SUPPORT TDRSS	T&G	G ONLY
B. SYNCHRONOUS																										
1. GOES-A																										
2. ATS-G																										
3. SATS-D																										
4. SAS-E	1680	-	-	-	-	1/1630	-	X	X	-	-	-	X	X	SYNC	41		1	X		\	X	-	-	-	X
5. SAS-D																										
6. ATS-H																										
7. ATS-I	1600	1/1800 ATS UNIQUE					X	-	-	X	-	-	X		SYNC	-	-	<1	X			-	-	-	-	X
C. LUNAR DEEP SPACE																										
1. IMP-L																										
D. EXTRAPOLATED MISSION CLASSES (Some maybe shuttle payloads and/or sortie experiments.)																										
1. BIO MED-A	2100	1/2100 UNIQUE					X	-	-	X	-	-	X	X	SYNC	L	L	<1	-	\	\	-	-	-	-	X
2. LST-A																										
3. REL. EXP.-A	200	1/200	-	-	-	-	X	-	-	X	-	-	-	X	400 x 400 @ 30°	L	L	<1	-	X	X	-	-	X	-	-
4. EPS-C	400	1/400	-	-	-	1/400	X	-	-	X	-	-	-	X	900 x 900 @ 80°	L	M	<1	-	\	\	-	-	X	-	-
5. EPS-E	460	1/460	-	-	-	1/460	X	-	-	X	-	-	-	X	750 x 750 @ 35°	L	M	<1	\	-	\	-	-	X	-	-
6. SATS-H	1680	-	-	-	-	1/1680	-	X	X	-	-	-	X	X	SYNC	L	M	1	\	-	\	-	-	-	-	X
7. EPS-D	400	-	-	-	-	2/400	-	X	X	-	-	-	-	X	200 x 5000 @ 65°	M	M	1	\	X	\	-	-	X	-	-
8. ERS-A	200	1/200	-	-	-	-	X	-	-	X	-	-	-	X	550 x 550 @ 3°	L	M	<1	-	\	\	-	-	X	-	-
9. ERS-B	425	-	-	-	-	1/425	-	X	X	-	-	-	-	X	550 x 550 @ 30°	L	M	1	-	\	\	-	-	X	-	-
10. GEOS-76																										

*A = APPROVED
B = UNAPPROVED
E = EXTRAPOLATED

#L = <10 kbs
M = 10-1000 kbs, H >1000 kbs

**O = ORIENTED
S = SPIN

1980 PLANNING MISSION MODEL, 8/72 UPDATE

SPACECRAFT NAME OR CLASS	MIN. CONTACT HRS PER QUARTER	RF FREQUENCIES MHz TELEMETRY 136	250	400	1700	2200	CMD V	S	TRACKING SYSTEM SRARR	VRARR	MT	MISSION PLANNING STATUS A	U	E	ORBIT APOGEE x PERIGEE @ INC (KM) x (KM) @ DEG	BIT RATES TLM (kbs) RT	PB	CMD	STAB. SYS. O	S	TRANSMIT ERP (DBW) <4	4-10	>10	SUPPORT SYSTEM TDRSS	T&G	G ONLY
A. EARTH ORBITS																										
1. OSO-K																										
2. RAE-D																										
3. RAE-D'																										
4. EOS-C	600	-	-	-	-	3/500	-	X	X	-	-	-	X	-	980 x 980 @ 99°	12/1200	30K	1	X	-	-	-	X	X	-	-
5. IMP-K																										
6. IMP-K'																										
7. EOS-B	425	-	-	-	-	3/425	-	X	X	-	-	-	X	-	980 x 980 @ 99°	12/1200	30K	1	X	-	-	-	X	X	-	-
8. BIO-F	140	1/140	-	-	-	-	X	-	-	X	-	-	X	X	370 x 370 @ 33°	--	22	<1	\	-	\	-	-	X	-	-
9. SHUTTLE																										
10. NIMBUS-G																										
11. SATS-F	250	-	-	-	-	1/250	-	X	X	-	-	-	X	-	350 x 300 @ 99°	1/20	40	1	-	\	\	-	-	X	-	-
12. SATS-G	250	-	-	-	-	1/250	-	X	X	-	-	-	X	-	650 x 560 @ 99°	1/20	40	1	-	\	\	-	-	X	-	-
13. HEAO-C	225	-	-	-	-	2/225	-	X	X	-	-	-	X	-	460 x 460 @ 28°	28	512	1	X	X	-	\	-	X	-	-

1980 PLANNING MISSION MODEL, 8/72 UPDATE

Spacecraft Name or Class	Min. Contract Hrs per Quarter	136	250	400	1700	>2200	CMD V	CMD S	Track SRARR	Track VRARR	Track MT	Status A	Status U	Status E	Orbit Apogee x Perigee @ Inc (KM)x(KM)@DEG	BIT TLM RT	BIT TLM PB	CMD	Stab O	Stab S	ERP <4	ERP 4-10	ERP >10	TDRSS	T&G	G ONLY
B. SYNCHRONOUS																										
1. SAS-E	1680	-	-	-	-	1/1690	-	X	X	-	-	-	X	X	SYNC	41	-	1	X	-	\	X	-	-	-	X
2. SAS-D	1690	-	-	-	-	1/1680	-	X	X	-	-	-	X	-	SYNC	41	-	1	X	-	\	X	-	-	-	X
3. ATS-H															SYNC	-										
4. ATS-I	1800	1/1800 ATS UNIQUE					X	-	-	X	-				SYNC	-	-	<1	X	-	X	-	-	-	-	X
C. LUNAR DEEP SPACE																										
1. IMP L																										
D. EXTRAPOLATED MISSION CLASSES (Some may be shuttle payloads and/or sortie experiments.)																										
1. BIO MED-A	2100	1/2100	UNIQUE				X	-	-	X	-	-	X	X	SYNC	L	L	<1	-		-	-	-	-	-	X
2. LST-A																										
3. REL. EXP. A	200	1/200	-	-	-	-	X	-	-	X	-	-	-	X	400 x 400 @ 30°	L	L	<1	-	\	\	-	-	X	-	-
4. EPS-D	400	-	-	-	-	1/400	-	X	X	-	-	-	-	X	200 x 5000 @ 65°	M	M	1	\	X	\	-	-	X	-	-
5. EPS-E	460	1/460	-	-	-	1/460	X	-	-	X	-	-	-	X	770 x 770 @ 35°	M	M	1	\	-	\	-	-	X	-	-
6. EPS-F	520		-	1/520	-		X	-	-	X	-	-	-	X	LUNAR	L	L	<1	\	-	\	-	-	-	-	X
7. SATS-H	1680	-	-	-	-	1/1680	-	X	X	-	-	-	X	X	SYNC	L	M	1	\	-	\	\	-	-	-	X
8. SATS-I	400	-	-	-	-	1/400	-	X	X	-	-	-	-	X	1000 x 1000 @ 100°	L	M	1	\	-	\	\	-	-	X	-
9. SATS-J	400	1/400	-	-	-	1/400	X	X	X	X	-	-	-	X	1000 x 1000 @ 45°	L	M	1	\	-	\	-	-	-	X	-
10. HEAO-D	225	-	-	-	-	2/225	-	X	X	-	-	-	-	X	450 x 450 @ 28°	26	512	1	X	X	-	-	X	X	-	-
11. ERS-A	200	1/200	-	-	-	-	X	-	-	X	-	-	-	X	550 x 550 @ 3°	L	M	<1	-	\	\	-	-	X	-	-
12. ERS-B	425	-	-	-	-	1/425	-	X	X	-	-	-	-	X	550 x 550 @ 80°	L	M	1	-	\	\	-	-	X	-	-
13. ERS-C	425	1/200	-	-	-	1/425	-	X	X	-	-	-	-	X	1000 x 1000 @ 30°	L	M	1	-	\	\	-	-	X	-	-
14. ERS-D	425	-	-	-	-	1/425	-	X	X	-	-	-	-	X	1000 x 1000 @ 20°	L	M	1	-	\	\	-	-	X	-	-

*A = APPROVED
U = UNAPPROVED
E = EXTRAPOLATED

# L = 10 kbs
M = 10-1000 kbs, H >1000 kbs

** O = ORIENTED
S = SPIN